NASA

SPACE VEHICLE
DESIGN CRITERIA
(CHEMICAL PROPULSION)

CASE FILE
COPY

LIQUID ROCKET ENGINE NOZZLES

JULY 1976

NATIONAL AERONAUTICS AND SPACE ADMINISTRATION

FOREWORD

NASA experience has indicated a need for uniform criteria for the design of space vehicles. Accordingly, criteria are being developed in the following areas of technology:

> Environment
> Structures
> Guidance and Control
> Chemical Propulsion

Individual components of this work will be issued as separate monographs as soon as they are completed. This document, part of the series on Chemical Propulsion, is one such monograph. A list of all monographs issued prior to this one can be found on the final pages of this document.

These monographs are to be regarded as guides to design and not as NASA requirements, except as may be specified in formal project specifications. It is expected, however, that these documents, revised as experience may indicate to be desirable, eventually will provide uniform design practices for NASA space vehicles.

This monograph, "Liquid Rocket Engine Nozzles," was prepared under the direction of Howard W. Douglass, Chief, Design Criteria Office, Lewis Research Center; project management was by Harold Schmidt. The monograph was written by J. C. Hyde and G. S. Gill,* Rocketdyne Division, Rockwell International Corporation and was edited by Russell B. Keller, Jr. of Lewis. Significant contributions to the text were made by A. T. Sutor, Rocketdyne Division, Rockwell International Corporation. To assure technical accuracy of this document, scientists and engineers throughout the technical community participated in interviews, consultations, and critical review of the text. In particular, E. M. McWhorter of Aerojet Liquid Rocket Company; M. T. Schilling of Pratt & Whitney Aircraft Group, United Technologies Corporation; and J. M. Kazaroff of the Lewis Research Center individually and collectively reviewed the monograph in detail.

Comments concerning the technical content of this monograph will be welcomed by the National Aeronautics and Space Administration, Lewis Research Center (Design Criteria Office), Cleveland, Ohio 44135.

July 1976

*Currently with Societe d' Etude de la Propulsion Par Reaction, France.

i

GUIDE TO THE USE OF THIS MONOGRAPH

The purpose of this monograph is to organize and present, for effective use in design, the significant experience and knowledge accumulated in development and operational programs to date. It reviews and assesses current design practices, and from them establishes firm guidance for achieving greater consistency in design, increased reliability in the end product, and greater efficiency in the design effort. The monograph is organized into two major sections that are preceded by a brief introduction and complemented by a set of references.

The State of the Art, section 2, reviews and discusses the total design problem, and identifies which design elements are involved in successful design. It describes succinctly the current technology pertaining to these elements. When detailed information is required, the best available references are cited. This section serves as a survey of the subject that provides background material and prepares a proper technological base for the *Design Criteria* and Recommended Practices.

The *Design Criteria*, shown in italics in section 3, state clearly and briefly what rule, guide, limitation, or standard must be imposed on each essential design element to assure successful design. The *Design Criteria* can serve effectively as a checklist of rules for the project manager to use in guiding a design or in assessing its adequacy.

The Recommended Practices, also in section 3, state how to satisfy each of the criteria. Whenever possible, the best procedure is described; when this cannot be done concisely, appropriate references are provided. The Recommended Practices, in conjunction with the *Design Criteria*, provide positive guidance to the practicing designer on how to achieve successful design.

Both sections have been organized into decimally numbered subsections so that the subjects within similarly numbered subsections correspond from section to section. The format for the Contents displays this continuity of subject in such a way that a particular aspect of design can be followed through both sections as a discrete subject.

The design criteria monograph is not intended to be a design handbook, a set of specifications, or a design manual. It is a summary and a systematic ordering of the large and loosely organized body of existing successful design techniques and practices. Its value and its merit should be judged on how effectively it makes that material available to and useful to the designer.

iii

CONTENTS

LIST OF FIGURES

LIST OF TABLES

xi

LIQUID ROCKET ENGINE NOZZLES

1. INTRODUCTION

The nozzle of a rocket engine is a carefully shaped aft portion of the thrust chamber that controls the expansion of the exhaust gas so that the thermal energy of combustion is effectively converted into kinetic energy of combustion products, thereby propelling the rocket vehicle. The nozzle is a major component of a rocket engine, having a significant influence on the overall engine performance and representing a large fraction of the engine structure. The design of the nozzle consists of solving simultaneously two different problems: the definition of the shape of the wall that forms the expansion surface, and the delineation of the nozzle structure and hydraulic system. This monograph deals with both of these problems. The shape of the wall is considered from immediately upstream of the throat to the nozzle exit for both bell and annular (or plug) nozzles. Important aspects of the methods used to generate nozzle wall shapes are covered for maximum-performance shapes and for nozzle contours based on criteria other than performance. The discussion of structure and hydraulics covers problem areas of regeneratively cooled tube-wall nozzles and extensions; it treats also nozzle extensions cooled by turbine exhaust gas, ablation-cooled extensions, and radiation-cooled extensions. Treatment of materials and structures for ablation-cooled and radiation-cooled nozzles and extensions is limited herein because these subjects are treated in detail in references 1 and 2. Drilled-wall and channel-wall nozzles are not treated in the monograph because these nozzles have seen limited service, if any, in operational engines.

In general, the nozzle shape is selected to maximize performance within the constraints placed on the system. This goal is relatively easy to achieve with the tools presently available. Problems arise when unusual requirements introduce additional constraints that are not readily handled. A typical example is the desire to maximize expansion area ratio to obtain high vacuum performance from an upper-stage engine and still be able to ground test the engine without the added expense of using an altitude facility. Techniques for developing nozzle contours that strike the best compromise between performance and nonperformance considerations (e.g., testing expense or cooling method) are not well defined; however, cut-and-try optimizations are possible with the present technology.

The nozzle structure of a large rocket must provide strength and rigidity to a system wherein weight is at a high premium and the loads are not readily predictable. The maximum loads on the nozzle structure often occur during the start transients before full flow is established. The side loads on the nozzle during separated flow cannot be predicted

1

accurately in magnitude, direction, or frequency and therefore present a difficult problem to the designer trying to build a minimum-weight structure that will withstand these loads. The structure often is designed overly strong, on the basis of experience with similar nozzles, with provisions for later weight reduction incorporated in the original design. This monograph describes the techniques that best enable the designer to develop the nozzle structure with as little difficulty as possible and at the lowest cost consistent with minimum weight and specified performance.

2. STATE OF THE ART

The nozzles used on liquid rocket engines inherently are very efficient components and are highly refined at the present state of development. The efficiency of these nozzles has been improved less than 1 percent in recent years. The quest for higher performance has, however, led to very large increases in area ratios. For example, the nozzle on the J-2 engine used on the Saturn V second and third stages has an area ratio of 27, whereas the nozzle planned for the Space Shuttle Orbiter Engine has an area ratio of over 77. With increasing area ratio, the nozzle becomes a proportionally larger part of the engine with some corresponding increase in importance. Because there is little to be gained by increasing nozzle efficiency, most of the work in nozzle development has been directed toward obtaining the same efficiency from a shorter package through the use of short bell* nozzles and annular nozzles such as expansion-deflection (E-D) and plug (aerospike). Figure 1 shows the various types of nozzles used on liquid rocket engines; the bell and conical are standard operational configuraitons, while the annular bell, E-D, and plug are advanced-development configurations. Tables I* and II* display the major features of the nozzles that have been used on most of the operational liquid rocket engines. Nearly all of these engines have bell nozzles. Most of the large engines have tube walls and are regeneratively cooled, whereas the small engines usually are radiation- or ablation-cooled.

There is a recent trend away from tube-wall nozzles toward channel construction. Channel walls provide better cooling in regions of high heat transfer of the nozzle by decreasing the surface area exposed to the hot gas and increasing the thermal conduction from the exposed surface area. The Space Shuttle Main Engine (SSME) has been designed for milled axial coolant channels in the main combustion chamber and throat up to an expansion area ratio of 5 and tube walls from an expansion area ratio of 5 to 77.5.
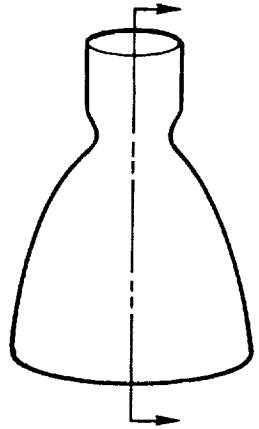
Considerable development work has been done on the plug nozzle; less has been done on the E-D nozzle. These advanced configurations provide the same performance as the bell but from a markedly smaller package. An annular bell nozzle was used on the Lance booster. Plug and E-D nozzles have not been used on an operational engine system; however, the probability of their use on future engines is high. It is not the purpose of this monograph to cover advanced concepts, but because a large amount of work has been done on the plug nozzle, this design is covered briefly; the E-D nozzle is less important and is not treated.

2.1 NOZZLE CONFIGURATION
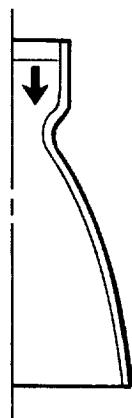
The nozzle configuration best suited to a particular application depends on a variety of factors, including the altitude regime in which the nozzle will be used, the diversity of stages in which the same nozzle will be employed, and limitations on development time or funding.

*Terms, symbols, and materials are defined or identified in Appendix A.
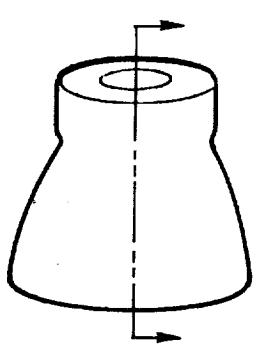
Factors for converting U.S. customary units to the International System of Units (SI units) are given in Appendix B.

3
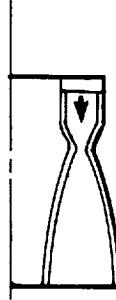
(a)   Bell
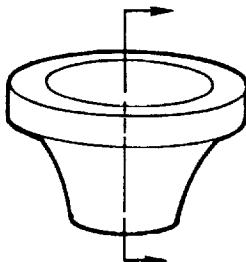
(b)   Conical

(c)   Annular bell

(d)   Expansion-deflection (E-D)

(e)   Plug (truncated aerospike)
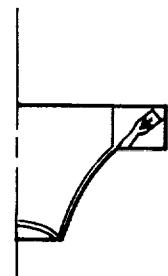
Figure 1. — Basic types of nozzles used in liquid rocket engines.

4

Table I. – Chief Features of Nozzles Used in Operational High-Thrust Liquid Rocket Engines

Engine	System application	Thrust, lbf	Chamber pressure, psia	Specific impulse, lbf-sec/lbm	Propellants			A_c/A_t	Chamber/ nozzle joint	Entrance half-angle, deg
					Oxidizer	Fuel	MR			
RS-1801	Lunar Excursion Module ascent engine	3500 vac	120 vac	310 vac	N_2O_4	50:50	1.60	2.9	Integral	30.0
AJ 10-118	Delta second stage	7575 alt	206 alt	267 alt	IRFNA	UDMH	2.8	3.27	Welded	25
AJ 10-138	Titan III transtage	8000 alt	105 alt	302 alt	N_2O_4	50:50	2.0	2.54	Integral	7.5
VTR-10	Lunar Excursion Module descent engine	9850 vac	104 vac	305 vac	N_2O_4	50:50	1.6	2.52	–	–
RL10A-3-3	Centaur upper stage	15 000 alt	400 alt	444 alt	LOX	LH_2	5.0	4	Integral	10.5
YLR81-BA-11	Agena upper stage	15 800 vac	506 vac	298 vac	IRFNA	UDMH	2.57	5.335	Welded	–
AJ10-137	Apollo Service Module	20 500 vac	97 vac	310 vac	N_2O_4	50:50	1.6	2.00	Bolted	7.5
YLR99-RM-1	X-15 aircraft; Pioneer spacecraft	49 390 alt	600 alt	236 alt	LOX	NH_3	1.25	4.10	Integral	31.5
YLR113-AJ-1	Rocket sled	50 000 to 150 000 sl	235 to 595 sl	195 to 240 sl	N_2O_4	UDMH	2.1	2.04	Integral	25
LR91-AJ-5	Titan II second stage	100 000 alt	827 alt	321 alt	N_2O_4	50:50	1.80	2.51	Integral	30
LR89-NA-7	Atlas MA-5 booster engine	330 000 sl (2 thrust chambers)	578 sl	254 sl	LOX	RP-1	2.28	1.67	Integral	–
LR79-NA-11	Thor MB-3	169 500 sl	588 sl	256 sl	LOX	RP-1	2.15	1.67	Integral	10
H-1C and H-1D	S-1 stage of Saturn 1B launch vehicle	204 300 sl 228 800 alt	705 sl 707 alt	269 sl 301 alt	LOX	RP-1	2.23	1.62	Integral	–
LR87-AJ-5	Titan II first stage	214 400 sl 236 400 alt	783 sl 783 alt	263 sl 289 alt	N_2O_4	50:50	1.93	2.04	Integral	25
J-2	S-II and S-IV stages of Saturn V	230 000 alt	725 (nozzle stagnation)	423 alt 294 sl	LOX	LH_2	5.5	1.58	Integral	13.73
F-1	S-1C stage of Saturn V	1 522 000 sl 1 748 000 alt	1126 injector 983 throat	274 sl 315 alt	LOX	RP-1	2.27	1.307	Integral	13

(continued)

5

Table 1. – Chief Features of Nozzles Used in Operational High-Thrust Liquid Rocket Engines (concluded)

Engine	D_t, in.	A_t, in.^{2}	Length, throat to exit, in.	Exit type	Divergence half-angle, deg	D_e, in.	A_e, in.^{2}	A_e/A_t	Nozzle extension	Extension/ nozzle joint	Method of cooling nozzle and extension
RS-1801	4.578	16.5	35.27	72% bell	—	30.9	750	45.6	None	NA	Film and ablation
AJ10-118	5.25	21.64	23.1	Complex contour	—	23.5	432.8	20	Optional	Clamped flange	Regenerative to 20:1; radiation to 30:1 or 40:1
AJ10-138	7.48	43.9	49.61	Bell	—	47.33	1758.5	40	Yes	Bolted flange	Ablation to extension; radiation thereafter
VTR-10	8.320	54.34	62.11	72.3% bell, round entrance	—	57.26	2574.0	47.5	Yes	—	Ablation to 16:1; radiation to 47.5:1
RL10A-3-3	5.14	20.75	46.3	Bell	32.5	38.8	1182.75	57	None	NA	Regenerative
YLR81-BA-11	4.670	17.13	39.8	Bell	25.7	31.326	770.32	45	Yes	Bolted flange	Regenerative to 13:1; radiation to 45:1
AJ10-137	12.447	121.675	111.8	Bell	—	98.40	7605	62.5	Yes	Bolted flange	Ablation to 6:1; radiation to 62.5:1
YLR99-RM-1	8.64	58.6	—	Conical	20	27.20	574.3	9.8	None	NA	Regenerative
YLR113-AJ-1	15.25	182.56	35.41	Conical	17	36.41	1040.66	5.7	None	NA	Film
LR91-AJ-5	9.12	65.41	72	Bell	17	64.0	3217	49.2	Yes	Bolted flange	Regenerative to 13:1; ablation to 49.2:1
LR89-NA-7	16.2	206.0	58	100% bell	—	45.83	1648.8	8	None	NA	Regenerative
LR79-NA-11	16.2	206.0	58	100% bell	—	45.8	1646.6	8	None	NA	Regenerative
H-1C and H-1D	16.16	205	55	Bell	—	45.49	1630	8	Yes	Bolted flange	Regenerative
LR87-AJ-5	15.25	182.56	42.46	Bell	23	43.14	1461.6	8	None	NA	Film and regenerative
J-2	14.7	169.6	90	Bell	4.226 min 27.5 max	77	4656.6	27.5	None	NA	Combined fluid and regenerative
F-1	35	961.4	158	Bell	—	140	15 400	16	Yes	Bolted flange	Regenerative to 10:1; turbine exhaust to 16:1

NA = not applicable

6

Table II. – Chief Features of Nozzles Used in Operational Low-Thrust Liquid Rocket Engines

Engine	System application	Thrust, lbf	Chamber pressure, psia	Specific impulse, lbf-sec/lbm	Propellants Oxidizer	Propellants Fuel	MR	A_c/A_t	Chamber/ nozzle joint	Entrance half-angle, deg
Model 8093	Centaur ACS and ullage orientation	1.5 vac	198 vac	155 vac	90% H_2O_2 (mono)		–	17.4	Welded	(0.06 in. radius)
M2A	Comsat positioning and orientation	1.9 to 3.0 vac	117 to 185 vac	225 vac	N_2H_4 (mono)		–	44.8	Integral	60
Model 8250 Unit 1	Agena-Gemini target vehicle SPS	16 vac	78 vac	252 vac	MON	UDMH	1.1	15.8	Integral	40
SE-7	Gemini attitude control	23 vac	132 vac	258 vac	N_2O_4	MMH	0.7	3.8	Integral	31.5
PD6000179	Titan III transtage ACS	16.0 vac / 26.7 vac	120 vac / 200 vac	221 vac / 225 vac	N_2H_4 (mono)		–	33.7	Welded	50
Model TD-339	Surveyor vernier propulsion system	30 to 104 vac	70 to 250 vac	287 vac	MON	MMH:H_2O (72:28)	1.5	10	Welded	47
MC-4-610	Ranger and Mariner propulsion	50 vac	190 vac	235 vac	N_2H_4 (mono)		–	37	Welded	60
R-4D	Apollo Service Module RCS	60 sl / 100 vac	96.5 sl / 96.5 vac	168 sl / 280 vac	N_2O_4	50:50	2.03	4.2	Integral	53
SE-7-1	Saturn SIV-B ullage	72 vac	101 vac	274 vac	N_2O_4	MMH	1.27	3.1	Integral	31.5
SE-8	Apollo Command Module ACS	93 vac	137 vac	274 vac	N_2O_4	MMH	2.0	3.1	Integral	26.1
Model 700800	Saturn SI-B and SIV-B ACS	147 vac	101 vac	292 vac	N_2O_4	MMH	1.64	5.8	Integral	45
Model 8250 Unit II	Agena-Gemini target vehicle SPS	200 vac	94 vac	257 vac	MON	UDMH	1.15	7.9	Integral	40
RS-2101	Mariner Mars 1971 spacecraft	300 vac	117 vac	283 vac	N_2O_4	MMH	1.55	4.9	Clamp	44.7
Model 7161 (500 lbf)	Lunar landing training vehicle ACS	500 sl	325 sl	122 sl	90% H_2O_2 (mono)		–	12.7	Integral	45
LR101-NA-15 Mod. 2	Atlas MA-5 vernier engine	913 sl	337 sl	205 sl	LOX	RP-1	1.8	3.0	Integral	10

(continued)

7

Table II. – Chief Features of Nozzles Used in Operational Low-Thrust Liquid Rocket Engines (concluded)

Engine	D_t, in.	A_t, in.^{2}	Length, throat to exit, in.	Exit type	Divergence half-angle, deg	D_e, in.	A_e, in.^{2}	A_e/A_t	Nozzle extension	Extension/ nozzle joint	Method of cooling nozzle and extension
Model 8093	0.075	0.0044	0.344	Conical	18	0.293	0.0674	15	None	NA	Radiation
M2A	0.105	0.0086	0.9	Conical	15	0.662	0.34	40	None	NA	Radiation
Model 8250 Unit I	0.377	0.1118	3.715	80% bell	29	2.832	6.28	56.2	None	NA	Radiation
SE-7	0.358	0.1008	2.599	80% bell (scarfed)	31.6	2.27	4.05	40.2	None	NA	Ablation
PD6000179	0.313	0.0772	3.	Optimized bell	15	2.20	3.8	49	None	NA	Radiation
Model TD-339	0.54	0.23	6.5	Overturned bell	37	5.09	19.7	86	Yes	Welded	Regen. to extension; radiation thereafter
MC-4-610	0.437	0.15	4.05	Bell	23.6	2.904	6.623	44	None	NA	Radiation
R-4D	0.868	0.592	6.98	Bell	8	5.46	23.41	40	Yes	Bolted flange	Radiation
SE-7.1	0.710	0.3959	—	80% bell (scarfed)	—	4.49	15.85	40	None	NA	Ablation
SE-8	0.710	0.3959	2.190	82% bell	36 entrance 10.6 exit	2.13	3.563	9	Yes	Bolted flange	Ablation
Model 700800	1.040	0.849	6.350	Bell	32	6.06	28.84	33.9	None	NA	Ablation
Model 8250 Unit II	1.423	1.59	—	80% bell	27	4.9	18.85	11.86	None	NA	Radiation
RS-2101	1.354	1.44	—	80% bell	44.75	8.56	57.5	40	Yes	Clamp	Film and radiation
Model 7161 (500 lbf)	1.195	1.121	1.640	80% bell	15	2.078	3.39	3	None	NA	Radiation
LR101-NA-15 Mod. 2	1.63	2.09	4.75	Conical	15	3.86	11.70	5.6	None	NA	Regenerative

ACS = attitude control system   SPS = secondary propulsion system
RCS = reaction control system   NA = not applicable

8

The propellant combination, chamber pressure, mixture ratio, and thrust level will, in most cases, be determined on the basis of factors other than the nozzle configuration and therefore will be inputs to the nozzle-selection study. These parameters have a minor effect on selection of configuration, but a significant effect on the selection of nozzle cooling method.

Payload from a given propulsion system is nearly constant over a wide range of any independent variable (e.g., chamber pressure) in the vicinity of the optimum value for that variable. Nozzle parameters therefore can be selected on the basis of preliminary optimization studies. Iteration is not essential unless gross changes to the preliminary data are made.

Figure 2 presents a sketch of a typical bell-nozzle configuration and illustrates basic nozzle nomenclature that will be employed in the monograph.
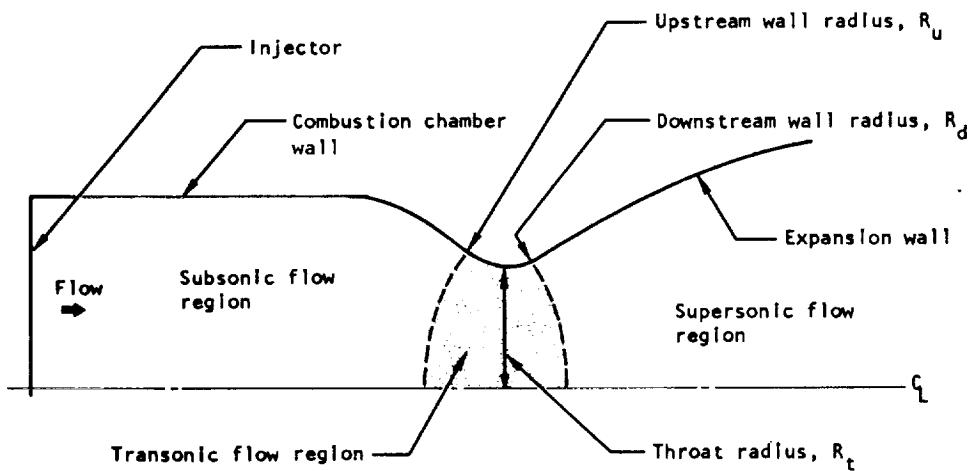
Figure 2. — Sketch illustrating basic nozzle configuration and nomenclature.

2.1.1 Throat Geometry

The throat of the nozzle is the region of transition from subsonic to supersonic flow. For typical rocket nozzles, local mass flux and hence the rate of heat transfer to the wall are highest in this area. The shape of the nozzle wall in the vicinity of the throat dictates the distribution of exhaust-gas flow across the nozzle at the throat. For the geometries used in most rocket nozzles, this throat flowfield is independent of the nozzle geometry downstream of the throat and for a distance of about one throat radius upstream of the throat; the effect on nozzle performance of inlet flow to the throat is treated in reference 3. The nozzle wall in the neighborhood of the throat usually consists of an upstream circular

9

arc that is tangent to a downstream circular arc at the geometric throat. The radii of these arcs are selected on the basis of a rough trade of performance and fabrication considerations against cooling difficulty and weight.

2.1.1.1 UPSTREAM WALL

The nozzle wall geometry immediately upstream of the throat determines the distribution of gas properties at the throat. Constant-radius arcs are used for the shape of the throat-approach wall. A small radius is desirable both for minimum overall length and for minimum wall area exposed to the high heat fluxes associated with flow near Mach 1. However, as the radius decreases, the difficulty in obtaining an accurate solution of the transonic flowfield increases. Existing transonic methods (e.g., ref. 4) are limited to radius ratios of about 1.0 for accurate results. A computer solution (ref. 5) can generate accurate results for radius ratios of 0.6 (ref. 6). Computer calculations using a power-series expansion of the parabolic partial differential equations for transonic flow showed that the nozzle aerodynamic efficiency remained constant for R_u/R_t values from 1.5 down to 0.6. A nozzle inlet of relatively large radius (R_u/R_t = 1.4), however, has been shown to be effective in boundary-layer film cooling through the nozzle throat.

In an annular nozzle, the throat is an annulus, not a circular opening of radius R_t. The width of the annular throat is referred to as the throat gap G_t. This parameter has the same significance in design as R_t. For annular nozzles with both walls convex relative to the gas and with equal radii, ratios of upstream wall radius to throat gap (R_u/G_t) of 1.0 or more are used. When both walls are convex to the flow but unequal in radius, the minimum solvable radius ratio is larger than that for the equal-radius case.

Nozzle flowrate is directly proportional to the aerodynamic flow area at the nozzle throat. This flow area, designated A_t^*, is the geometric flow area A_t corrected for the effects of nonuniform transonic flow. As shown in figure 3, the ratio A_t^*/A_t (which is equivalent to the discharge coefficient for potential flow) and thus nozzle flowrate decrease with decreasing radius ratio. This effect can be predicted accurately with existing transonic programs. Reference 7 presents information on flow coefficients in nozzles with throats of comparatively small radius of curvature, at throat Reynolds numbers larger than 1×10^6; for these nozzles, boundary-layer effects are not believed to be significant.

Most transonic solutions in current use are based on reference 8. The velocity distribution along some reference streamline is assumed, the power-series form of the compressible-flow equation is integrated numerically, and the wall is located by summing the flow in each streamline until the desired mass flow is attained. The number of terms in the series required to obtain an accurate solution depends on the wall geometry.

10
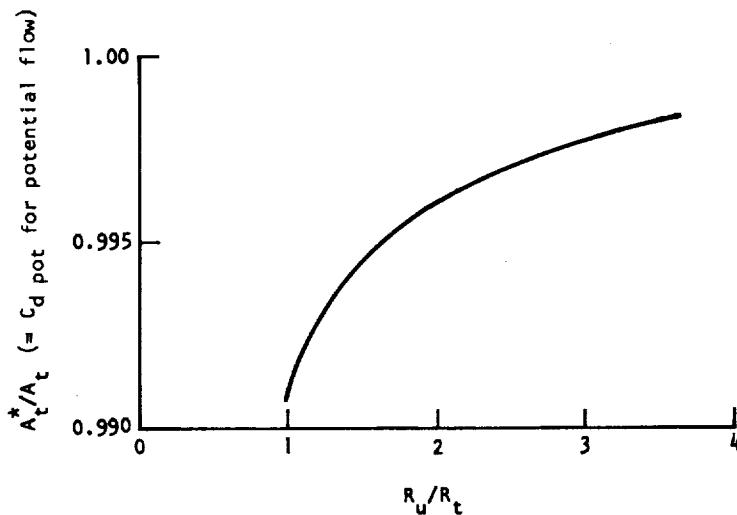
Figure 3. — Variation of A_t^*/A_t with R_u/R_t.

The first solutions for transonic flow (e.g., the solution incorporated in ref. 4) were developed for a thermally perfect gas. Later programs included the variation of specific heat with temperature (ref. 9).

2.1.1.2 DOWNSTREAM WALL

For a given area ratio, maximum nozzle efficiency within a given length is obtained by using a sharp-corner (zero-radius) transition between the upstream radius and the supersonic contour. For tube-wall nozzles, however, the minimum-radius wall that can be fabricated is limited by the radius to which the tubes can be bent. Similar limits to wall radius exist for other methods of fabrication.

A downstream wall radius 0.4 times the throat radius usually is a good compromise between fabrication difficulty and minimum nozzle length for tube-wall construction. A minimum bend radius of twice the tube outside diameter is required for round tubes of relatively ductile materials such as stainless steel, nickel, or copper. Difficult-to-work materials must be limited to larger bend radii. For elliptical cross sections, the tube bend radius should be greater than twice the major outside dimension of the tube cross section. For ablative materials, the radius must be large enough to avoid shearing of the material during firing.

When the gas density is relatively low (low chamber pressure) or the nozzle is relatively small, the downstream-wall radius ratio R_d/R_t must be large enough to provide expansion slow enough to maintain chemical composition near equilibrium. If the expansion is too rapid and a significant deviation from equilibrium composition occurs near the throat, important losses in performance result for certain energetic propellant combinations. The downstream wall geometry is selected primarily from a trade between chemical (kinetic) performance, which increases with radius ratio, and aerodynamic performance, which decreases with radius ratio.

An additional design consideration for nozzles with a circular arc throat and a conical divergence section is that the nozzle wall geometry just downstream of the throat can have a significant bearing on the heat transfer to the downstream wall because the geometry can subject the boundary layer to an adverse pressure gradient (ref. 10). Available experimental information (refs. 10 and 11) for nozzles with a conical half-angle of 15° indicates that R_d/R_t probably should not be made smaller than about 0.75. Detection of oblique shock waves arising from the downstream tangency region is discussed in reference 12. The influence of nozzle wall geometry on methods to reduce heat transfer to the wall is discussed in reference 13.

2.1.2 Expansion Geometry

The expansion geometry extends from the throat to the nozzle exit. The function of this part of the nozzle is to accelerate the exhaust gases to a high velocity in a short distance while providing near-ideal performance. Both engine length and specific impulse strongly influence the payload capability of rocket vehicles. Considerable care is given to the design of the nozzle expansion geometry in order to obtain the maximum performance from a length commensurate with optimum vehicle payload. When this requirement is not critical, a simple straight-wall (i.e., conical) nozzle of desired length and half-angle greatly facilitates tooling and fabrication and thus reduces cost. The conical nozzle generally is found on small rockets. As noted earlier and as shown in table I, bell nozzles are used on all of the larger systems currently flying. The expansion surface of this type of nozzle is contoured for optimum performance within a restrictive length and gives the nozzle a characteristic bell shape. The length of a bell nozzle is generally specified as a percent (e.g., an "80% bell"). This expression designates the length of the bell nozzle as a percent of the length of a 15°-half-angle conical nozzle having the same expansion area ratio.

The plug nozzle (spike nozzle) and the inverse plug nozzle such as the forced-deflection or reverse-flow nozzle have not been operational; however, these nozzles are of general interest because they can be made to flow full at large area ratios at sea level.

2.1.2.1 BELL NOZZLE

2.1.2.1.1 Optimum Contour

The supersonic region of a bell nozzle is designed with the use of one of the many available computer programs (e.g., ref. 14). The nozzle shape obtained is a mathematical optimum based on a variational-calculus maximization technique described in references 6, 15, and 16. Although the optimization is mathematically accurate, the initial conditions (obtained from the transonic solution) and the gas properties in the nozzle are approximate. However, the shape of the nozzle is not sensitive to these parameters, and performance of a bell nozzle is not sensitive to small variations from the optimum contour.

The availability of computer programs makes it possible to economically generate optimum nozzle expansion geometries for rocket engines. Equilibrium gas properties are used in the calculation of optimum wall contour. Programs for nonequilibrium gas composition have been developed (ref. 17), but the extent of their application in rocket nozzle design is uncertain.

Programs for calculation of the three-dimensional supersonic flowfield are available (ref. 18); these programs allow a cut-and-try design optimization within the geometric limitations of the programs. A simplified analytical procedure is to approximate three-dimensional flowfields with axisymmetric and plane flow sections. Cold-flow model testing is used extensively to examine the performance of three-dimensional nozzles.

The loss in nozzle performance due to the viscous interaction of the expanding gas and the nozzle wall is considered in the selection of the nozzle length and area ratio. The results obtained from the various boundary-layer programs in use vary considerably (ref. 19). Most of the current solutions for the boundary-layer thickness and drag in an accelerating flow are based on the method given in reference 20. Details of the numerical procedure vary from program to program, and this variation accounts for many of the differences in results. Methods for boundary-layer analysis rely heavily on empirically derived coefficients for friction and heat transfer. Figure 4 shows typical viscous-drag losses computed for rocket nozzles. The nozzle drag loss was calculated by solving the boundary-layer integral-momentum and -energy equations; the calculated loss was expressed as a percentage of the nozzle thrust and plotted against a parameter that is roughly proportional to Reynolds number.

For accurate performance prediction, boundary-layer displacement thickness is computed. Under conditions where the boundary layer is unusually thick relative to the nozzle size, the boundary-layer displacement thickness is computed and the wall is moved outward by the displacement thickness point by point.

13
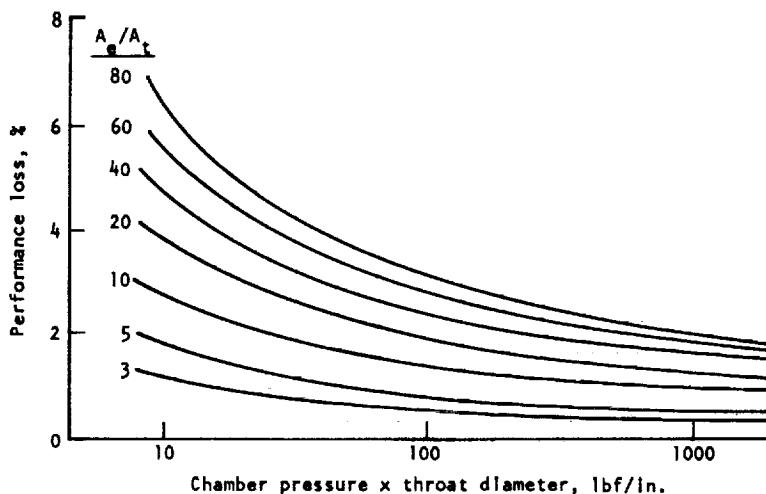
Figure 4. — Computed performance loss due to viscous-drag effects in
bell nozzles (storable propellants).
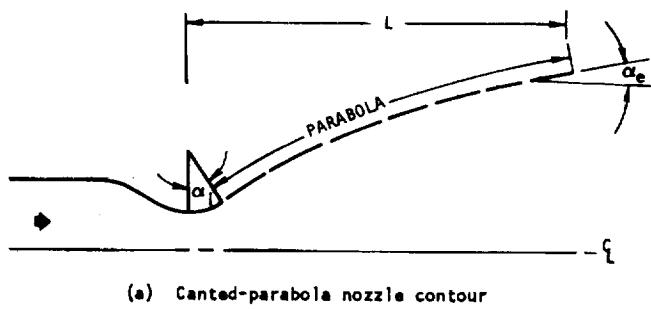
Propellant combinations with very high combustion temperatures (e.g., fluorine/hydrogen) in some cases exhibit performance losses of 5 to 10 percent unless the wall just downstream of the throat is designed to provide an expansion rate slow enough to maintain composition near equilibrium up to an area ratio of 2 to 5. A technique for direct optimization of the nozzle contour for a reacting gas (nonequilibrium process) has been developed (ref. 17), but it is very complex and not generally used. The method used for high-energy propellants is to select a downstream wall geometry that provides a much slower expansion than the minimum-radius configuration; then, at some specific point, terminate the controlled-expansion wall, and design the remainder of the nozzle from the equilibrium method. The performances of several configurations are computed, and the results are used to select new configurations for further study or to settle on one of the geometries examined.

The configuration resulting from this approach has a downstream throat curvature longer than that required for a gas expanding at equilibrium conditions. The kinetic performance is higher, but the possible aerodynamic performance is reduced because less of the given length of nozzle from throat to exit is used for an optimum aerodynamic contour. If the designer selects a number of controlled-expansion geometries and termination points, then repeats the process, the final design can be based on comparative kinetic-plus-aerodynamic performance. Actually, the flow composition "freezes" (remains constant) near the end of the controlled section; however, a nozzle designed by this method will produce

14
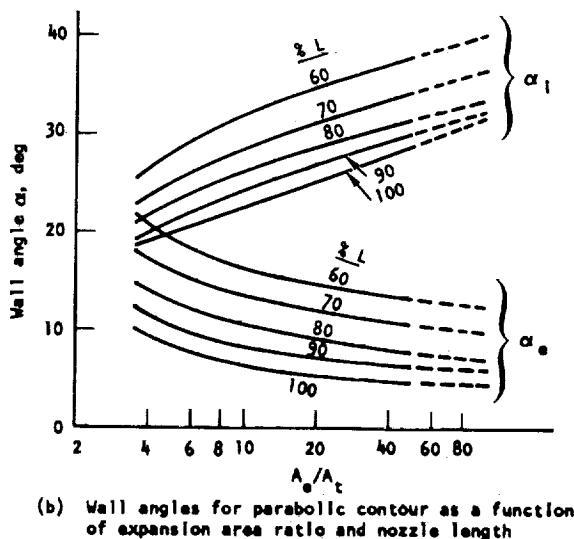
near-optimum performance for the actual flow conditions. Experimental programs have shown that these nozzles do produce high performance under the conditions investigated (ref. 21).

2.1.2.1.2 Nonoptimum Contour

The available optimization methods are based on assumptions that often only roughly approximate the actual conditions. Bell-nozzle contours obtained by the mathematical-optimum design method vary only slightly with gas properties. For a given area ratio and length, a single canted parabola will very closely approximate the variety of optimum contours corresponding to the various chamber conditions that may occur in rocket engines. For engineering purposes, near-optimum parabolic contours are suitable for many applications and can be generated without using a computer. Figure 5 illustrates the canted-parabola contour and shows initial and final wall angles for a range of area ratios and lengths.

(a) Canted-parabola nozzle contour

(b) Wall angles for parabolic contour as a function of expansion area ratio and nozzle length

Figure 5. — Canted-parabola contour as an approximation of optimum bell contour.

15

Mathematical-optimum nozzles cannot be designed for all conditions. The design method fails for nozzle lengths less than some minimum value, and this minimum length increases with increasing area ratio. Figure 6 shows the range of local flow angles and Mach numbers over which the mathematical-optimum design method of reference 16 will produce an acceptable design.
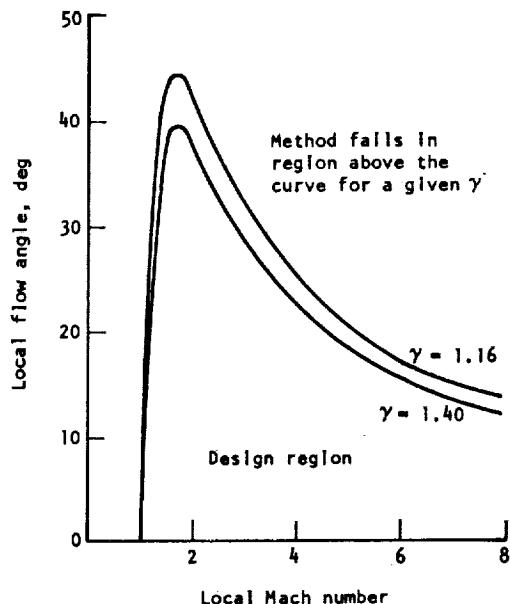
Figure 6. — Graphic display of region over which the mathematical-optimum method for contour design can be used.

The contour of a high-performance nozzle can be obtained by designing an ideal nozzle to a higher area ratio than required, so that when the ideal nozzle is truncated to the desired area ratio the correct nozzle length is obtained (ref. 14). This type of nozzle is sometimes referred to as an "optimum" nozzle; however, it can only approach the performance of the mathematical-optimum design. Performance differences between these types of nozzles are small. Unlike the optimum-design method, the truncated-ideal method can be used to design a nozzle as short as desired.

As noted earlier, conical nozzles are used when performance and length are not critical and minimum fabrication time and cost are desired. For low area ratios, cones can be used with no measurable loss in performance. The performance of a straight-wall nozzle approaches the results obtained from one-dimensional point-source flow analysis as area ratio increases,

16

but at low area ratios, the oscillation of divergence efficiency with area ratio, as shown by the solid curves in figure 7, affects the selection of area ratio or wall half-angle. Shocks emanating from the beginning of the straight-wall portion of the nozzle can occur in cones (ref. 22).

2.1.2.1.3 Overexpanded Nozzle

Nozzles designed for vacuum operation have large expansion area ratios in order to achieve high specific impulse. It is desirable to ground test engines in the course of the development program. During ground testing, most altitude engines are overexpanded, often to the extent that the exhaust gas separates from the nozzle wall. This flow separation can result in serious problems. For example, a nonoptimum (parabolic) contour was selected for the nozzle of the J-2 engine in order to raise the exit wall pressure. The high-exit-pressure nozzle was supposed to run unseparated at an area ratio of 27 with a chamber pressure of 700 psi. A wall-pressure minimum that occurred between area ratio of 14 and the nozzle exit produced an unstable condition that caused unsteady asymmetric separation, especially during the startup. The large loads that occurred caused various thrust-chamber structural failures. A short bolt-on diffuser was developed to eliminate separation during mainstage operation of the J-2 (ref. 23). Restraining arms were attached from the test stand to the nozzle skirt to absorb the separation loads at startup.

Separation of flow occurs when the gas in the boundary layer is unable to negotiate the rise to ambient pressure at the end of the nozzle. The exact atmospheric pressure at which flow will separate from the wall of a nozzle cannot be predicted accurately. Various rules of thumb to predict separation have been suggested; however, general agreement on one of these methods has not been reached. An early rule stated that a danger of separation existed when the ratio of exit pressure to ambient pressure was equal to 0.4. Later methods based on fitting of experimental results accounted for the increase in overexpansion that can be obtained with increasing Mach number. A fit of experimental data for short contoured nozzles over a broad range of nozzle area ratios (ref. 24) indicates that separation will occur when

$$P_{wall}/P_{amb} = 0.583 \, (P_{amb}/P_c)^{0.195}$$

where

P_{wall} = exhaust-gas static pressure on the wall at separation

P_{amb} = ambient pressure

P_c = chamber pressure = exhaust-gas total pressure
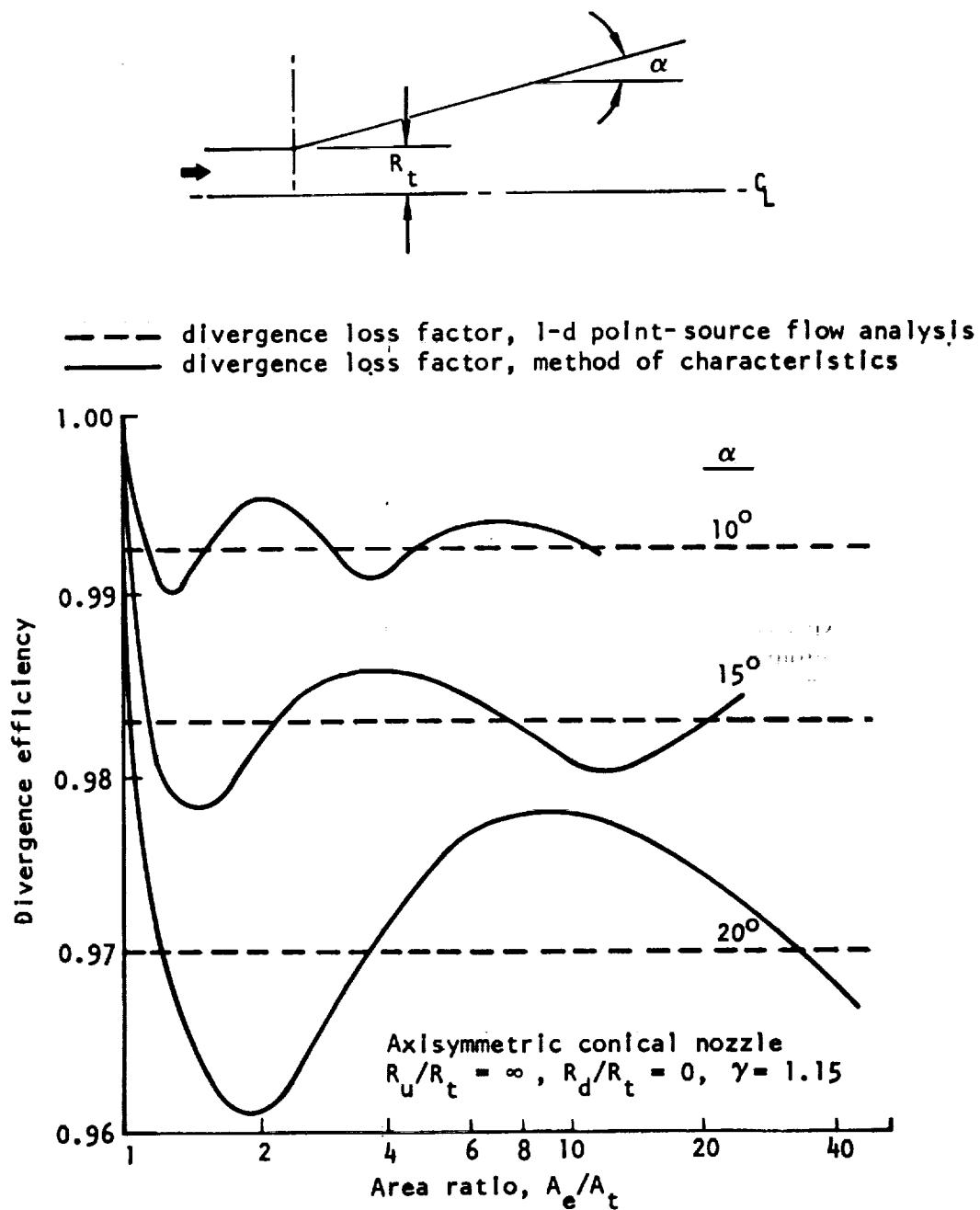
Figure 7. — Variation of theoretical nozzle divergence efficiency with area ratio and divergence half-angle.

The method of reference 25 was the basis for a separation-prediction criterion that includes the effects of gas properties and nozzle shape on separation. A recent and fairly complete treatment of flow separation in nozzles is presented in reference 26. The results of the various prediction methods have shown agreement with experimental data in many cases, but in general predictions are used only as a guide.

2.1.2.1.4 Nozzle Extension

Two types of nozzle extensions are used on rocket nozzles. In the most widely used type, the nozzle contour from the throat to the exit is designed for maximum performance. The purpose of the extension is to provide a means of breaking the nozzle into two parts between the throat and the exit. The break generally is made at the point where the method of cooling the wall is changed; for example, an active cooling method (regenerative) is used in the high-heat-load region from the injector to the break, and a passive method (e.g., radiation) from the break to the exit. The extension also is used to (1) allow different fabrication techniques for the combustion chamber and nozzle, (2) minimize weight, (3) ease handling, and (4) reduce the total heat input to the active coolant.

The second type of extension is used to increase altitude performance of existing engines by increasing the expansion area ratio without changing the existing engine nozzle. The extension wall contour can be optimized to a specified end point for the basic flowfield at the nozzle exit. The method is a routine application of the same technique used for optimum bell-contour design. The flow properties across the exit of the basic nozzle are used as a starting line for the calculation. For area ratios larger than 15, straight-wall extensions produce nearly the same performance as optimized contoured extensions.

2.1.2.1.5 Small Nozzle

As rocket size decreases, viscous-flow effects become increasingly important, and the techniques used to design and analyze conventional-size nozzles become less accurate. Thus, low-thrust small-nozzle rockets developed for applications such as satellite attitude and orbit control require special methods for nozzle design and analysis because of the relatively large effects of viscosity on perforamnce.

Velocity slip and temperature jump at the wall as well as the effects of boundary-layer curvature are included in the flow analysis of nozzles with a Reynolds number (Re) of less than 500 (ref. 27). For low-Re nozzles, the throat boundary layer increases and therefore the discharge coefficient decreases with increasing radius ratio as shown in figure 8. The discharge coefficient C_d in figure 8 is the ratio of actual mass flow in the nozzle to the mass flow of the nozzle for one-dimensional inviscid flow; figure 3 shows the variation of discharge coefficient $C_{d\,pot}$ with throat geometry for inviscid flow, i.e., Re = ∞. Reference
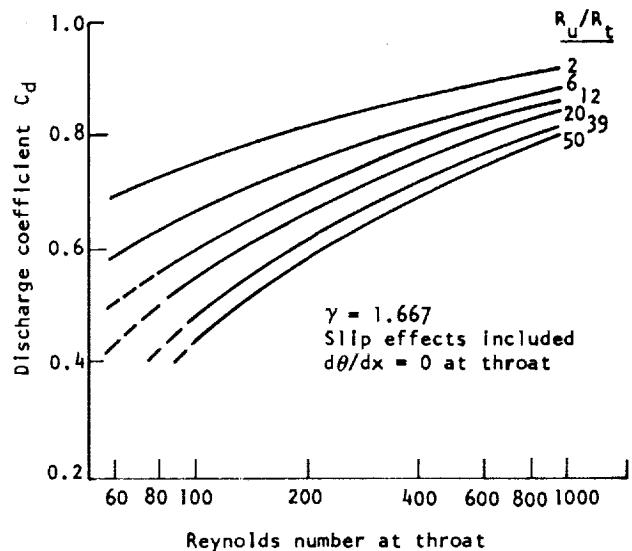
Figure 8. — Nozzle discharge coefficient as a function of Reynolds number at throat for various values of R_u/R_t.

28 contains information on the flow coefficient (i.e., discharge coefficient) over a range of throat Reynolds numbers between 650 and 350 000 (for which there is virtually no information in the literature). For throat Re values of less than 100, the method of boundary-layer correction to an inviscid core breaks down; i.e., the boundary-layer thickness at the throat exceeds the throat radius. Flow calculations are made by a method that includes viscous effects in the generation of the flowfield (refs. 27, 29, and 30).

2.1.2.2 PLUG NOZZLE

A method for directly optimizing truncated aerospike or plug nozzles has not been developed. The bell-nozzle optimization procedure can be applied to plug nozzles, but to obtain a solution it is necessary to assume that the base pressure is zero. The results provide an efficient expansion of the gas on the contoured wall, but low base pressure. Currently, truncated ideal nozzles are used; these nozzles produce higher overall nozzle (base included) efficiency than the optimum nozzles with zero base pressure.

The plug nozzle is designed by starting with the Mach line of an ideal exit flowfield (fig. 9) and working upstream along a specific expansion surface. The Mach number of the exit flow is constant, and the flow angle is parallel to the axis. The ideal nozzle then is truncated to

20
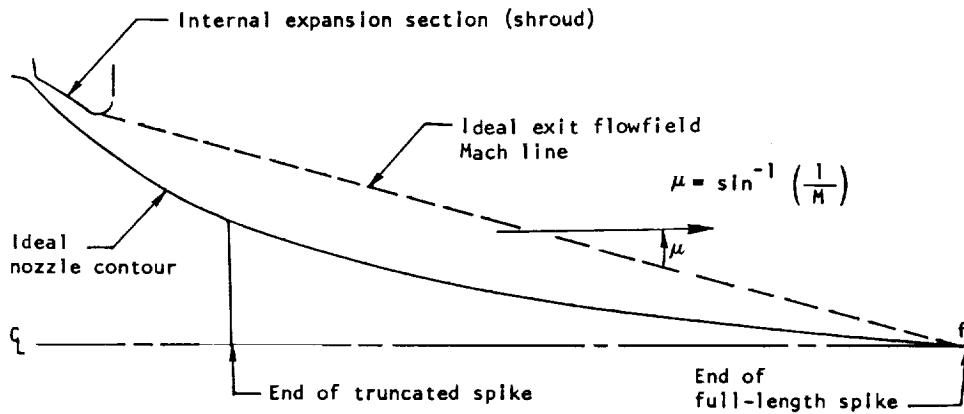
Figure 9. — Sketch illustrating nomenclature and configuration for ideal plug-nozzle design.

the desired length. The nozzle is designed without computing the transonic flow; the actual flowfield computed from the transonic wall geometry differs from the design flowfield. This difference may give rise to a predicted heat flux or pressure at some particular point different from the design value, but this deviation is not significant in terms of overall nozzle efficiency.

The flow angle at the throat relative to the axis in plug nozzles is equal to the Prandtl-Meyer angle corresponding to the design exit Mach number. For a single-expansion plug with an area ratio of 10, the angle is about 70° for typical rocket exhaust products. If internal expansion (i.e., a shroud) is used, the throat flow angle is the difference between the Prandtl-Meyer angles corresponding to the design exit Mach number of the plug nozzle and the exit Mach number for internal expansion. The combustion chamber, injector, and some ducting must be placed between the engine maximum diameter and the usable expansion exit area (fig. 9). For a fixed engine-envelope diameter, the usable expansion area ratio therefore is less for the unshrouded design. Also, the structure required for the combustion chamber is heavier than that needed when the throat flow is more nearly parallel to the axis.

Shrouded plug. — A shroud is a short outer wall (fig. 9). The shrouded nozzle design starts with the same ideal exit flowfield as that for an unshrouded nozzle, and therefore the performances of the two configurations are similar (the main difference is due to slightly different boundary-layer development and nonequilibrium effects), but the shrouded nozzle is longer. The shrouded nozzle provides a larger usable exit area for a given engine diameter. At very high thrust levels, the combustion-chamber length becomes small compared to the nozzle length, and the unshrouded plug nozzle provides a better overall package than does the shrouded configuration.

21

The procedure for design of annular-nozzle contours for high-energy propellants is fundamentally the same as the procedure for the bell: the shape of the short wall immediately downstream of the throat is selected to provide a relatively slow initial expansion; then the remainder of the nozzle is designed with the equilibrium method.

2.1.2.2.1 Base Design

The line of truncation for a plug nozzle forms a region referred to as the base. Recirculating gases from the main flow produce a pressure on the base. This base pressure over the area of the base is additive to the nozzle thrust. Additional thrust from the base can be generated by the addition of turbine exhaust or coolant gases.

Unless shielded by relatively cool bleed gases, the base region is subjected to recirculating gases with stagnation temperatures nearly equal to the combustion-chamber total temperature. In an engine with a gas-generator turbine drive (ref. 31), turbine exhaust gases are dumped into the nozzle base; for a preburner or expander cycle, no secondary flow is used, and the base must be cooled. The base pressure obtained for a given nozzle geometry and secondary flowrate, if used, depends on the base design and particularly on the method of introducing the secondary flow. The highest performance is obtained when the secondary flow is introduced with minimum axial momentum. Current designs inject the secondary flow through a porous plate covering the base (fig. 10(a)). The base plate is made concave to obtain the required rigidity from a structure considerably lighter than a flat base plate. Equal performance can be obtained with a deep-cavity base (fig. 10(b)) wherein secondary flow is introduced normal to the axis. The porous-plate configuration is favored, since it allows the volume that would otherwise be taken up by the deep cavity to be used for turbomachinery and other engine components.

(a) Porous-plate base   (b) Deep-cavity base
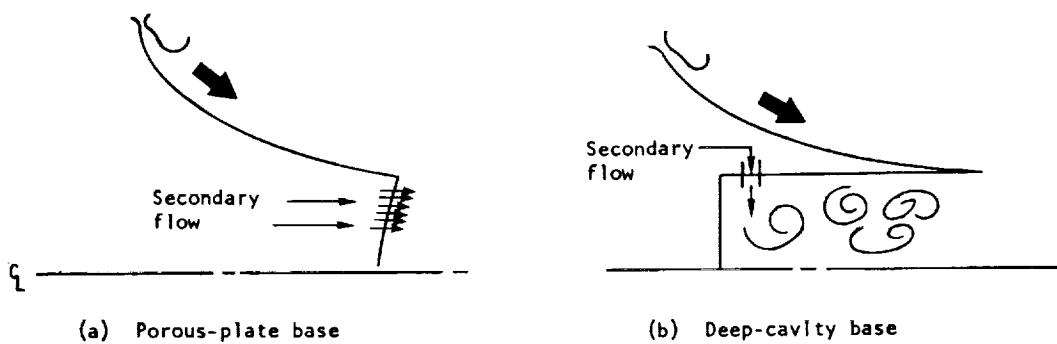
Figure 10. — Two types of base design for a plug nozzle.
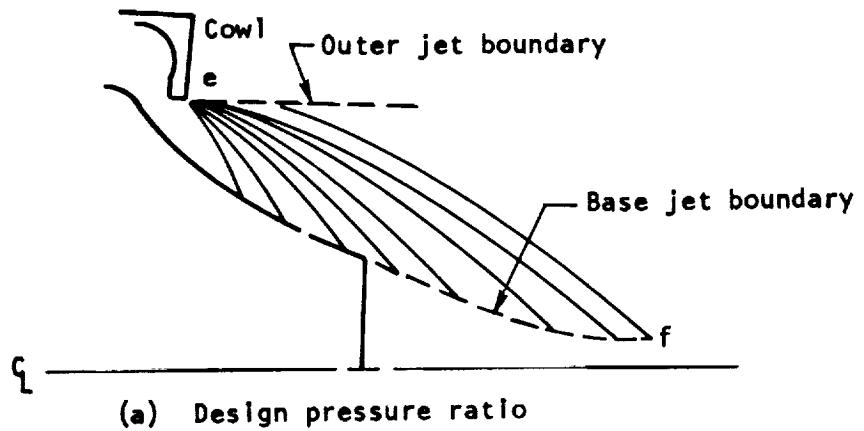
Most predictions of base pressure are made by a method that is based on scaling the results from a cold-flow model (ref. 32). The method is limited to truncated ideal plug nozzles because of the lack of test data for other configurations. Theoretical solutions for the base pressure require an analysis of the nozzle flowfield to obtain the boundary-layer solution and the potential flowfield at the nozzle exit. When little or no base bleed is introduced, the base region is analyzed by methods outlined in reference 33. The method described in reference 34 has been modified and used for designs with large base-bleed rates.

2.1.2.2.2 Overexpanded Nozzle
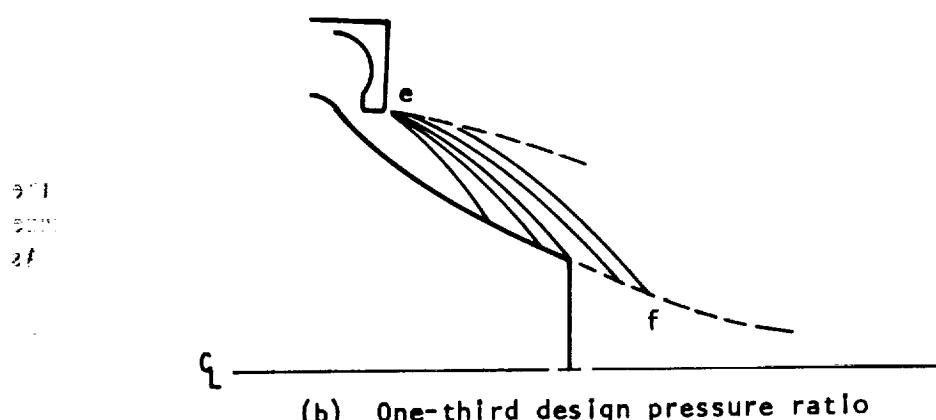
The flow phenomena that occurs during overexpansion of a plug nozzle are illustrated in figure 11. Figure 11(a) shows the flowfield of a plug nozzle expanding at the design pressure ratio (exit pressure for one-dimensional flow equals ambient pressure for the assumed gas properties). In this case, the exhaust gas separates from the outer wall when the velocity vector is parallel to the axis. For truncated ideal nozzles, the first wave that signals separation from the outer wall, e-f, passes far downstream of the plug base, and performance is unaffected. When the pressure ratio is decreased to about 1/3 of the design value (fig. 11(b)), the first wave from the outer jet boundary runs downstream of the contour and intersects the base jet boundary near the base, influencing thrust by raising the base pressure. At some lower pressure ratio, the first wave from the outer jet boundary intersects the nozzle, raising the wall pressure. When the nozzle operates in the slipstream of a moving vehicle, the outer jet boundary shape depends on the base pressure at the cowl, as shown in figure 11(c). The solution for the problem of interaction of slipstream and main flow is within present technology but has not been incorporated in available programs. For truncated ideal nozzles, recompression (reflection of exhaust gas from ambient jet boundary) is isentropic, i.e., no shocks occur; in nonideal nozzles, waves reflected from the jet boundary coalesce to form a shock that intersects the wall. The pressure peaks associated with recompression cause local areas of high heat flux, which move along the wall with changing pressure ratio and which must be considered in the design of the cooling system and structure of the nozzle.

2.1.3 Nozzle Contour Tolerances
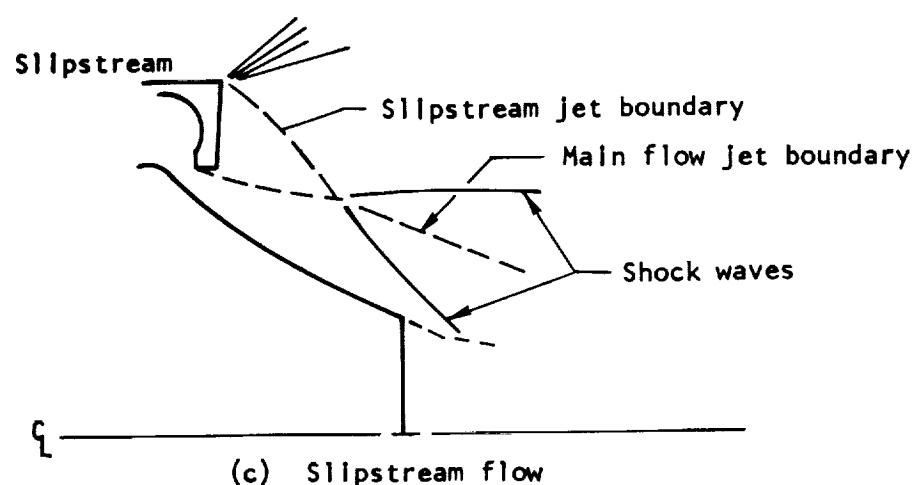
Theoretical analyses and model test programs (ref. 23) have shown that bell-nozzle performance is not sensitive to small deviations from the nominal wall shape. The nozzle contour tolerances ensure that the completed nozzle will approximate the selected nozzle shape sufficiently to obtain desired nozzle efficiency, thrust level, and thrust vector alignment. For the large-scale tube-wall nozzle of the J-2 engine, the tolerance on the 14.7-in. throat diameter is ±0.030 in. Allowable contour deviation on the circumference is 0.025 in./in. These tolerances are small in order to reduce geometric asymmetry that was suspected of contributing to side loads and to provide the required thrust alignment. The

23

(a) Design pressure ratio

(b) One-third design pressure ratio

(c) Slipstream flow

Figure 11. — Flowfield of a plug nozzle at three different expansion pressure ratios.

24

thrust-vector alignment tolerances for the J-2 engine are ±0.55 in. displacement at the gimbal center and ±0° 43' angle from the thrust chamber centerline. The F-1 engine has no tolerance values on the assembled nozzle per se; nozzle shape is controlled by tolerances on individual tubes, bands, jackets, and end ring. The F-1 actual thrust vector must fall within 0.60 in. of the gimbal center and be within 0° 30' of the engine centerline.

Closer tolerances on throat diameter must be used on an annular nozzle to achieve the same deviation of throat area allowable for a similar bell nozzle. For example, a plug nozzle with an area ratio of 80 and the same thrust and chamber pressure as the J-2 has a throat gap of a little over 0.45 in. The J-2 throat tolerance (±0.03 in.) would allow nearly 15-percent deviation from the nominal area in this case. The change in throat area from deflection of the walls due to pressure loads and thermal expansion is significant. Unless the inner and outer walls are both very nearly circular and the center lines coincide, the thrust vector may be displaced beyond the allowed deviation. Reliable rules for contour tolerances have not been established for annular nozzles.

2.2 NOZZLE STRUCTURE

The nozzle of a liquid rocket engine extends downstream from the convergent section of the combustion chamber to the exhaust-gas exit plane. The physical structure of a nozzle depends largely on the method used to cool the combustion chamber and the nozzle. As noted earlier and as shown in tables I and II, various combinations of cooling methods have been used. The treatment of nozzle structure herein emphasizes a regeneratively cooled chamber and basic nozzle combined with a regeratively cooled, film-cooled, ablation-cooled, or radiation-cooled nozzle extension. Discussion of the structure of ablation-cooled and radiation-cooled nozzles and nozzle extensions is limited because these subjects are treated in detail in references 1 and 2.

The nozzle structure transmits the pressure thrust to the combustion chamber and injector assembly, which in turn transmits the total engine thrust, usually through a gimbal block, to the vehicle frame. Nozzles are designed to minimize weight and, to some extent, cost, but not at the expense of performance. As a result of the emphasis on performance, the nozzle is the largest single component in most rocket engines and as such is a natural backbone for the engine structure. It is also a convenient place to mount other components such as coolant manifolds, hot-gas ducting, turbomachinery, and auxiliary equipment.

Figure 12 shows the thrust chamber and nozzle of the 200 000 lbf-thrust, pump-fed, regeneratively cooled J-2 engine. This thrust chamber assembly illustrates a typical placement of major components for a large engine. The basic combustion chamber and nozzle are made up of a bundle of tubes formed to the desired shape and externally supported by a continuous shell in the combustion chamber and throat region and by retaining bands over the balance of the nozzle. The fuel and turbine exhaust manifolds
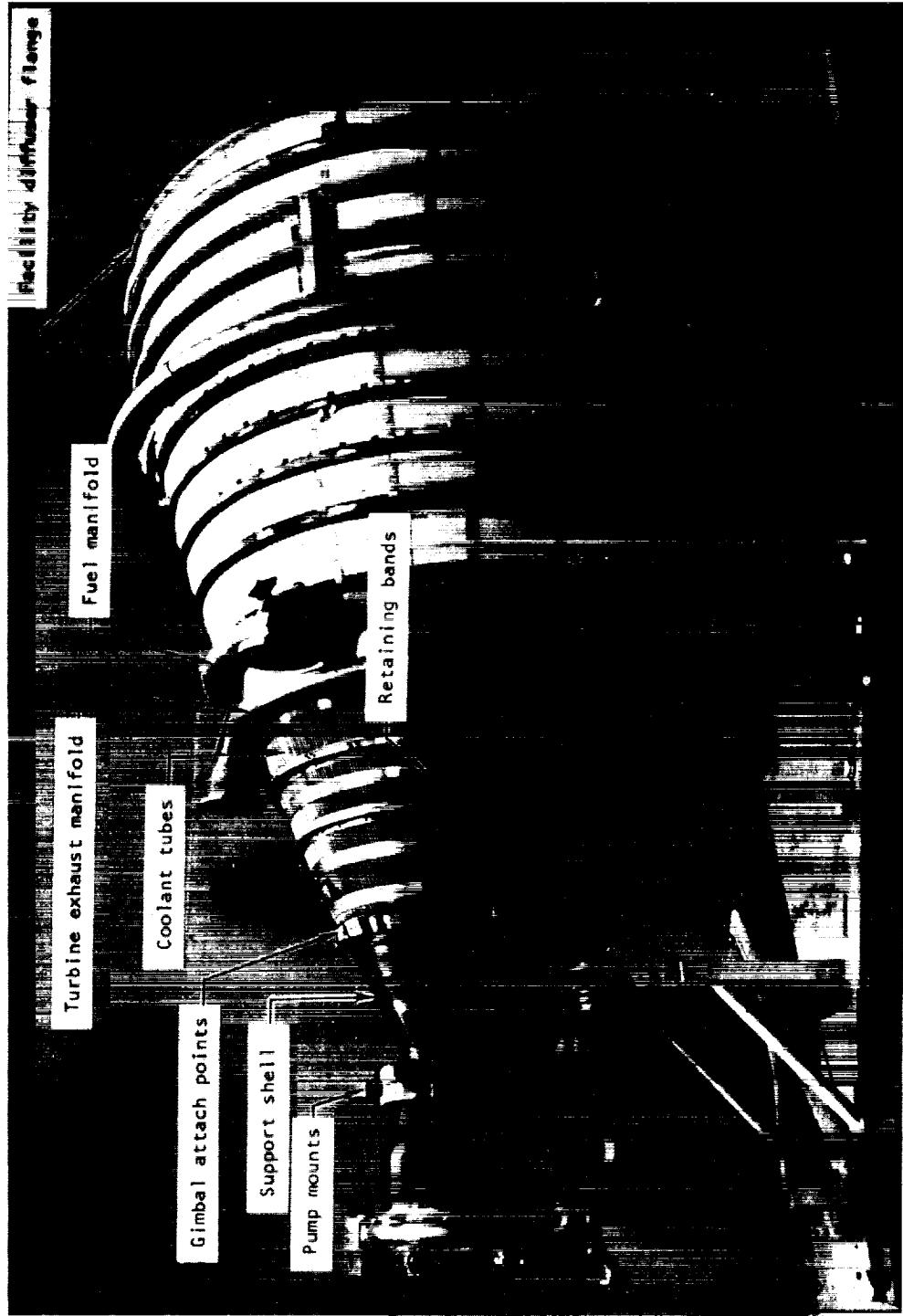
Figure 12. — Thrust chamber assembly for a large, pump-fed rocket engine (J-2).

attach to the nozzle and form an integral part of the structure. Mounts for the pumps, gimbal actuators, and other components are placed on major structural members to distribute the load over the relatively fragile tube bundle.

Mechanical design of the nozzle is complicated by the severe thermal environment and large dynamic loads that must be withstood by the nozzle. For example, during the initial boost phase, the nozzles of the core engine of the Titan III first stage are subjected to a severe thermal environment generated by the solid rocket motor strapons. To prevent damage, the external surfaces of the structure are protected by an insulation blanket while the nozzle inner surfaces are protected by a stageable exit-closure heat shield.

Nozzle structural failures often are due to inaccurate predictions of the gas expansion produced by the nozzle. A typical failure of this kind is the collapse of the nozzle from overexpansion during ground testing or from high side loads generated by severe accelerations of the exhaust gas resulting from unsteady, asymmetric separation of the expanding gases from the nozzle wall.

2.2.1 Regeneratively Cooled Nozzles and Extensions

In a regeneratively cooled thrust chamber, one of the propellants (usually the fuel) is used as a coolant for the chamber wall. As noted, the thrust chamber is made up of a bundle of thin-wall tubes or, more recently, a cylinder with coolant passages formed in the wall (ref. 35); the construction of the latter type of thrust chamber is illustrated in figure 13. The propellant is pumped at high velocities through the coolant tubes (or passages), separated from the combustion gases by a relativley thin wall. This cooling method can handle very high heat fluxes and provides a relatively lightweight thrust chamber. The energy transferred through the wall increases the energy of the propellants at the injector. All of the existing pump-fed engines are at least partially regeneratively cooled. Regenerative cooling is seldom used for pressure-fed engines because of the increased propellant tank pressure required for the coolant-jacket pressure drop. Reference 36 provides detailed treatment of the design of regeneratively cooled thrust chambers and also presents information on the assembly of tube-wall structures by brazing; much of the material therein is applicable to nozzle design and assembly.

2.2.1.1 INTERMITTENT RETAINING BANDS

Nozzle tube bundles have little resistance to external loads arising from side loads during startup, flow separation, or mechanical forces from attachments; therefore, either a continuous shell or intermittent rigid retaining bands are required for support of the tubes (fig. 14). Continuous support of the chamber shell (fig. 14(a)) commonly is stopped downstream of the chamber throat; intermittent retaining bands are then used down to the

27
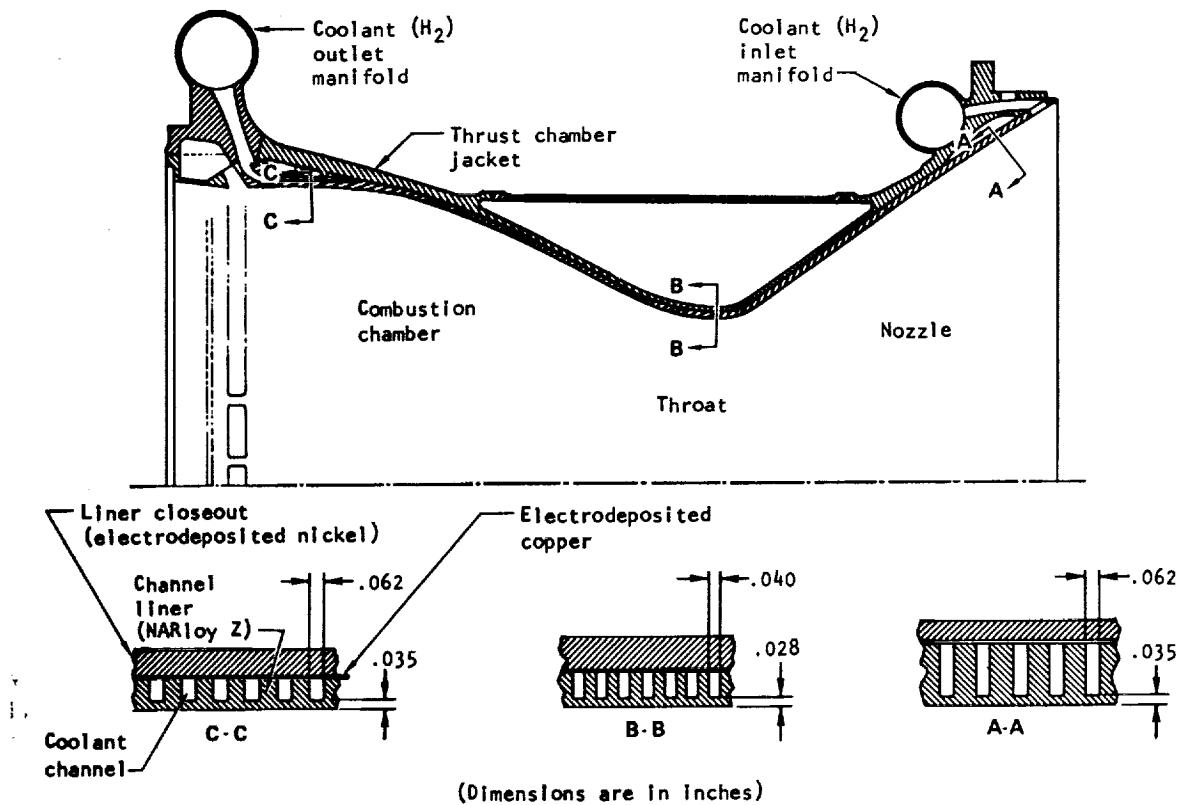
Figure 13. — Construction of channel wall for cooling thrust chamber of SSME.

(Dimensions are in inches)
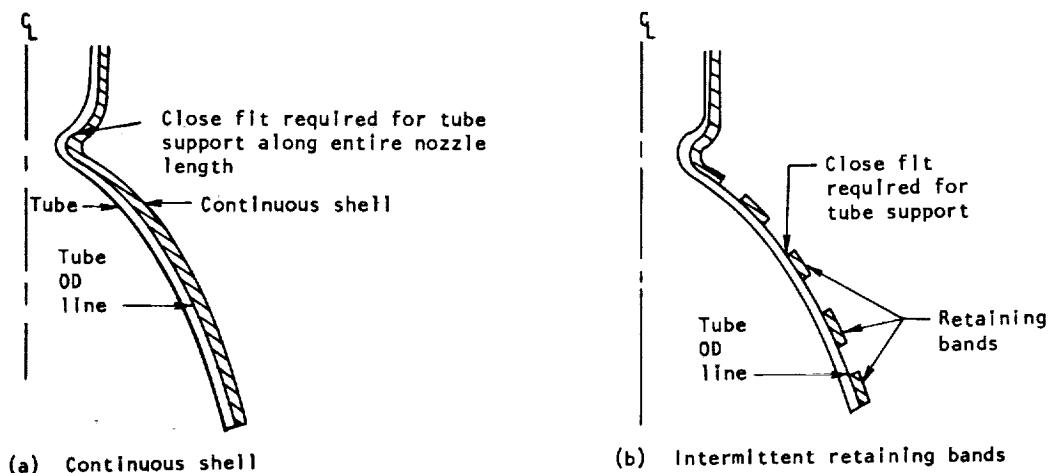
Figure 14. — Two basic methods for supporting coolant tubes.

nozzle exit on tube-wall rocket nozzles, as shown in figure 14(b). Such bands are feasible because of the rapid decrease of wall pressure aft of the throat; the bands are shaped and sized to withstand the various internal and external loads. This use of bands results in weight saving, cost reduction, and reduced nozzle fabrication problems. The weight reduction on the aft end of the nozzle is particularly advantageous in reducing moments on gimbaled engines. The major fabrication advantage of bands over the continuous shell is that the braze tolerance control is easier. In addition, less braze alloy is required.

Retaining bands can be made from fiberglass wrapping or wire windings, but normally are solid metal straps formed to fit around the nozzle over the tubes. The bands are designed to control tube-to-band fits so that each tube, after brazing, is supported by each band in the radial direction. Bands are sized structurally to withstand all internal-pressure hoop loads and external loads such as those caused by gas-flow separation, side loads, and accessory attachments. The tube-to-band braze joint ties the tube bundle to the retaining band so that the nozzle reacts to loads as a unit instead of as a group of individual components. The braze joint must also withstand the axial load caused by nozzle pressure being restrained in a diverging section.

Required retainer band spacing is determined by analyzing the unsupported tube length that can be allowed at operating (pressurized) conditions. Retainer band width depends primarily on band dimensions necessary to withstand the required operational loads. External mechanical and differential pressure loading have caused band buckling. In an early J-2 engine, side loads on the nozzle at startup caused localized buckling of an aft band early in intended chamber life. The fix described earlier (sec. 2.1.2.1.3) was adequate structurally but was expensive and heavy. For the nozzle on the J-2S (an improved version of the J-2 engine), the band was redesigned to be lightweight and easy to make and yet have good buckling resistance.

Problems and difficulties that accompany the use of retaining bands are illustrated in figure 15. Uniform tube-to-band tolerances are necessary for minimum gaps for braze joints. High-low tube conditions have produced excessive braze joint gaps (fig. 15(a)), which result in inadequate bonding of some tubes and in overstressing and failure of the bonded tubes where the bands rest on the high tubes. The same high-low tube conditions have resulted in high-tube crown depressions (fig. 15(b)) when the bands were forced to fit the low-tube dimensions in order to ensure proper braze gap. A variable contact angle or improper contact angle between the band and the tube (fig. 15(c)) has resulted in nonuniform tube-to-band gaps circumferentially around the nozzle with subsequent poor braze joints or dented tubes. Nondistributed external loads (fig. 15(d)) and band loading due to improper hardware fits or differential weld shrinkage (fig. 15(e)) have also caused tube damage. Local tube discontinuities such as joints and fairly abrupt changes in tube shape adjacent to or under bands can result in stress concentrations and early tube failure. Tube-to-band gaps resulting from poor fitup have been compensated for by inserting shim stock between the band and the tubes (fig. 15(f)).

29

(a) High-low tube alignment (excessive gap)

(b) High-low tube alignment (forced interference)

(c) Mismatch of tube to band angle

(d) Excessive external load

(e) External interference

(f) Gap repair with shim stock
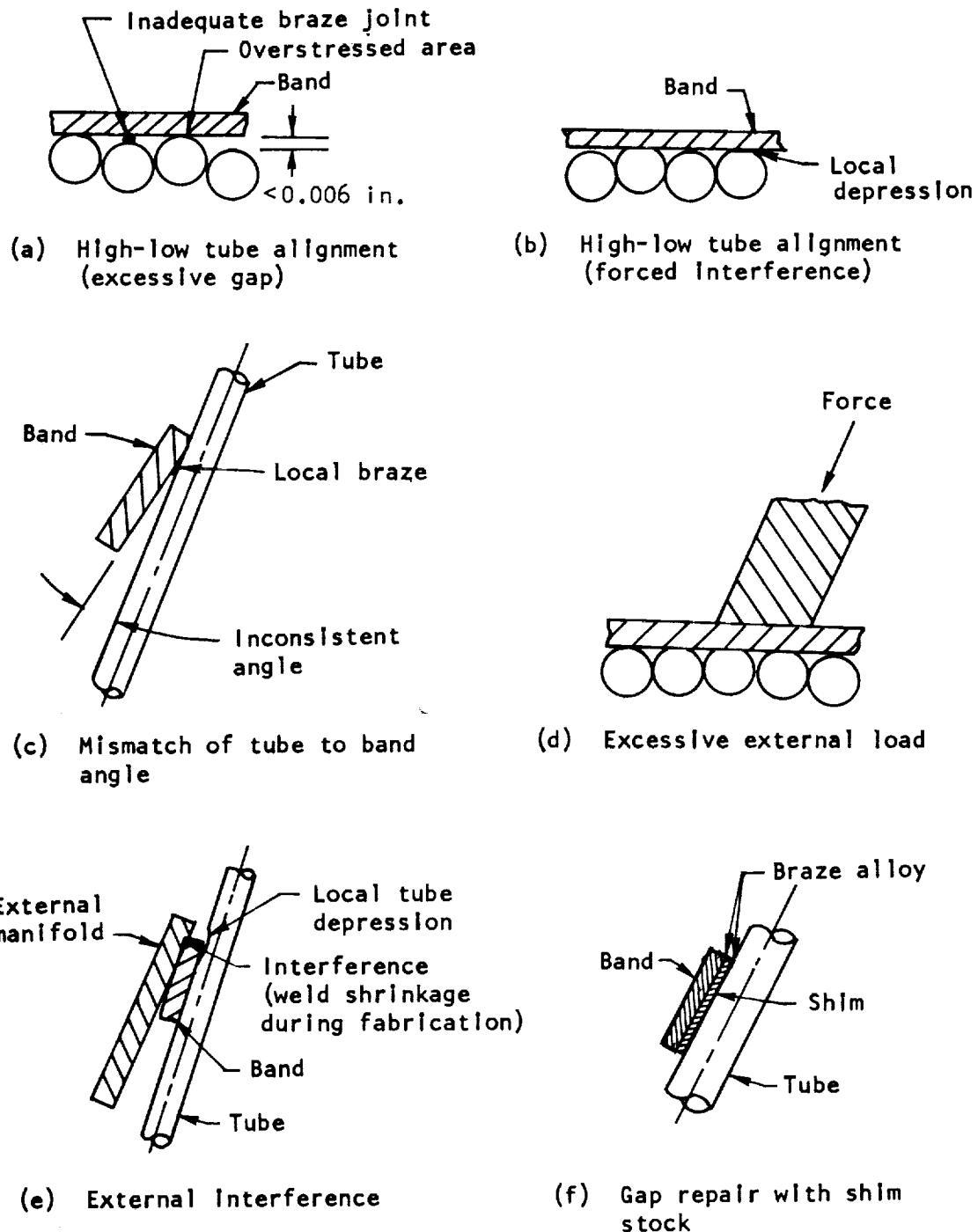
Figure 15. — Sketches illustrating problems with retaining bands.

30

The critical structural area in tube-to-band joints normally is that area where the braze attaches the tube to the band at the band edge. These intersections result in local strain discontinuities at the tube contact points. On the nozzle for the F-1 engine, which had rectangular retaining bands, tubes were instrumented and tested at the tube-to-band intersections. Concentration factors for axial stress up to 2.2 were measured; this value probably is low, because attaching instrumentation in sharp corners is very difficult. Analysis of these joints showed axial-stress concentrations as high as 2.8 and bending-stress concentrations as high as 2.45. No design changes were required on the F-1 nozzle, although tube failures occasionally have occurred at the tube-to-band joint after many tests. Reducing the band thickness at the edge of the band reduced the stress concentrations.

Vibration characteristics of the nozzle structure and attaching components play a critical role in hardware durability, but these characteristics are very difficult to predict. Structural vibration coupled with tube-to-band stress concentrations has caused many hardware failures. Vibrational stresses added to tube pressure and thermal loads have resulted in joint cracks at the retainer band-to-tube intersection. Analytical techniques described in references 34 and 37 have been used to predict chamber natural frequencies and dynamic loads resulting from anticipated vibration environments. Actual stress levels have been determined best at nominal hot-firing conditions with strain gages mounted at suspected high-stress tube-to-band joint intersections, and the results used to predict fatigue life.

Retaining-band material must be braze-compatible with the tube material either in the original or plated condition. A controlled cooldown cycle after furnace brazing has been used successfully to produce required mechanical properties with ageable band materials such as Inconel 718 and Inconel X-750. Coupons included in the furnace during the braze cycle are evaluated to verify mechanical properties of band material after the braze cycle.

2.2.1.2 TUBE SPLICE JOINTS

The circumference of a nozzle, a minimum at the throat, increases somewhat in the combustion chamber and greatly in the nozzle expansion section, especially for nozzles with high expansion-area ratios. For tube-wall nozzles, the amount of variation in circumference that can be obtained with a fixed number of tubes is limited by how much the tubes can be worked by tapering (varying the tube cross section) and forming. When the point at which the circumference cannot be further increased with the fixed number of tubes is reached, it is common practice to increase the number of tubes by using a tube "splice", in which for each tube coming into the splice two (or more) tubes leave the splice (fig. 16). The splice joint (also called a bifurcation joint or tube joint) occurs commonly in the nozzle and infrequently in the chamber. The joint location is determined from a tradeoff of heat transfer, weight, pressure drop, and fabricability.

31

(a) Rectangular splice joint

Metal braze foil
between tubes

Fusion
weld

"D"-shaped secondary
tubes

Preplaced wire braze

(b) "D"-shaped round-tube splice joint
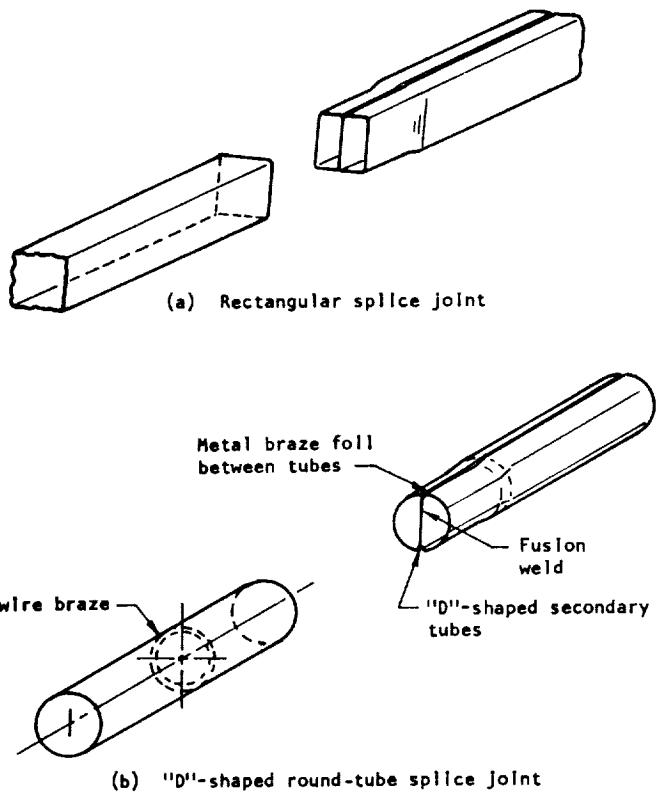
Figure 16. — Two types of coolant-tube splice joints.

At moderate expansion ratios ($\approx$8:1), nickel and stainless steel tubing can be tapered or otherwise formed successfully (Thor, Titan, and Atlas boosters). With the Inconel X-750 tubes of the F-1 engine, however, tapering became much more difficult and, in addition for the F-1, a bifurcated-tube design was lighter than a single tube to the 10:1 expansion ratio. The F-1 nozzle, therefore, has a splice joint at the 3:1 expansion ratio. (In an early F-1 design in which the nozzle was to be completely regeneratively cooled to the 16:1 point, two splice joints were planned.)

For very large expansion ratios, some method for increasing the number of tubes in the nozzle aft end is required. Even with stainless steel or nickel tubing, smaller tubes are used in order to reduce weight, increase cooling velocity, or make the tube fabricable. The Atlas sustainer (expansion ratio of 25) has a splice joint at about 7:1. In the J-2 and J-2S

(expansion ratios of 27-1/2 and 40, resp.) and the RL10, pass-and-a-half construction increases the number of tubes, and these nozzles do not require a splice joint. In all of the new Titan first- and second-stage engine systems, the tube bifurcation joint and its problems have been eliminated by employment of ablative extensions exclusively.

Rectangular splice joints (fig. 16(a)) have been used successfully for secondary tube widths of 0.5 in. or less (Atlas sustainer). In the F-1 engine, which has large tubes with relatively thin walls operating at high internal pressure, rounded tube crowns are necessary, and the "D" splice (fig. 16(b)) was developed. For this tube joint, the ends of the primary tube and the two secondary tubes are shaped as shown, and the secondary tubes are fusion welded together on the tube ends. Wire braze is preplaced in the primary tube and braze foil is inserted between the secondary tubes, and the assembly is induction brazed. The entire tube assembly is then used in stacking the chamber. The tube joint for the Atlas sustainer is made in a similar but simplified manner.

A sharp transition (joggle) in a secondary tube at the splice joint leads to stress concentrations. On the hot-gas side of the joint, thermal loads at these stress concentration points produce low-cycle plastic strains. With a material of good ductility and a limited number of cycles, as in the stainless steel tubes in the Atlas sustainer, leaks have not occurred. With the lower ductility Inconel X-750 of the F-1 nozzle, however, cracks in the secondary tubes developed. Although these cracks originally were thought to be, and had the appearance of, braze-joint cracks, investigation showed that the secondary tubes were cracking (fig. 17). Engines with a large number of restarts may suffer low-cycle fatigue of tube joints even with relatively ductile materials if the joint has a joggle in a hot-gas wall.
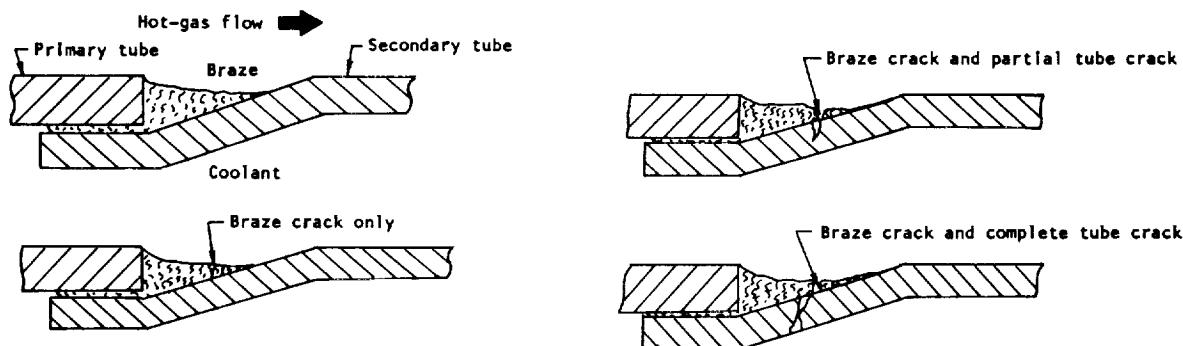
Figure 17. — Types of cracks in brazed joints of coolant tubes (F-1 engine).

33

2.2.2 Film-Cooled Extensions

The nozzle extension for the F-1 engine is the only example of a film (gas)-cooled extension in production. The F-1 engine is of more than ordinary importance because it is the highest-thrust single-chamber liquid rocket engine that has been operational to date. The design of the F-1 nozzle extension and the method of cooling it are unique and are therefore described in some detail in this section.

The regeneratively cooled section of the F-1 nozzle extends to a 10:1 expansion ratio, and the extension to 16:1. The extension is cooled by turbine exhaust gases. This method of exhaust-gas disposal is not only an effective method of cooling the extension but also reduces the overheating and afterburning problems that arise when turbine exhaust gases are discharged overboard through conventional ducts in nozzles. Turbine exhaust gases are injected along the extension wall at the joint attachment and also from shingles along the length of the extension (fig. 18). The extension consists of an outer skin connected by "Z" stringers to the inner shingles (fig. 19), all of Hastelloy C. The shingles overlap and form slots through which the turbine exhaust gas flows and protects the shingles from hot combustion gases. Retaining bands are attached to the outer skin, and the entire extension is bolted to the turbine exhaust manifold, which is an integral part of the regeneratively cooled nozzle section.

2.2.2.1 SLOTS

The slot design for the F-1 nozzle extension (fig. 18), which was based on references 38 and 39, was intended to maximize the effectiveness of the film-coolant flow. Since the F-1 slot design was developed, the effect of gas-stream separation has been quantitatively evaluated (ref. 40). The effect of slot height and slot turbulence intensity on the effectiveness of the film cooling is covered in reference 41. Reference 42 discusses the importance of lip thickness and injection angle. Reference 43 deals with large discontinuities and has also been used extensively for calculation of film-cooling effectiveness. References 44 and 45 indicate that, for injection of turbine exhaust gas into a supersonic nozzle area, the minimum amount of stream mixing and thus the most effective use of the film coolant occurs when the gaseous film coolant is injected parallel to the main gas stream, at the highest possible velocity, and with the smallest separation of the gas streams.

Permanent distortion of the shingles of nozzle extensions due to plastic flow caused by thermally induced stresses changes the slot geometry and produces unequal coolant distribution to the hot-gas wall. Total distortion is related to the number of thermal cycles rather than to the total firing time. Rigid shingle designs (fig. 20(a)) are subject to thermal distortion and have resulted in local liner failure. A design that limits deflection in both the up and down direction but allows axial and circumferential thermal growth has been used successfully in R&D hardware. The present F-1 nozzle uses a dimpled sheet design (fig.
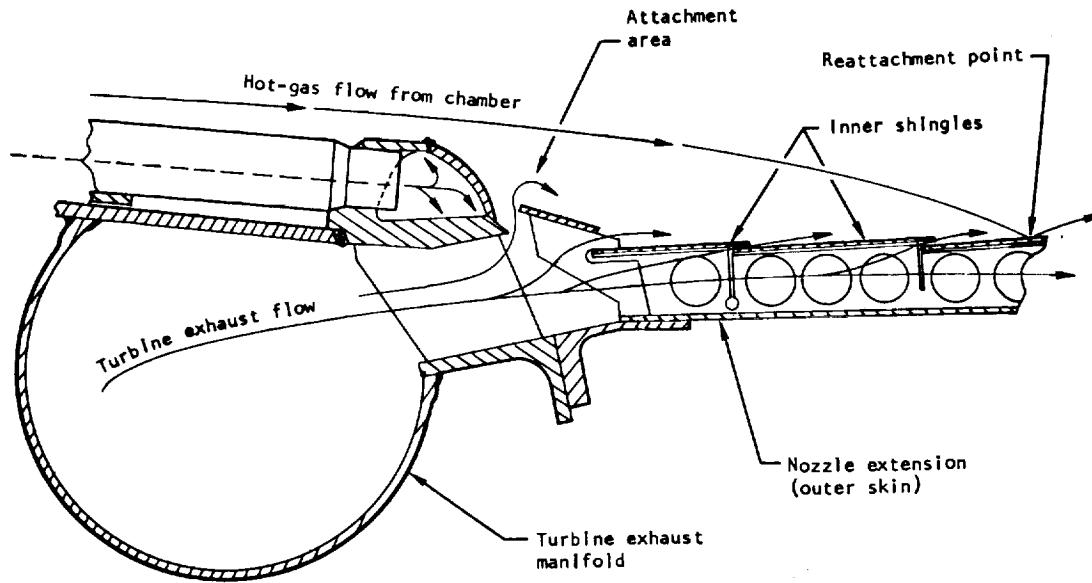
Figure 18. — Configuration for using turbine exhaust gas to cool nozzle extension (F-1 engine).
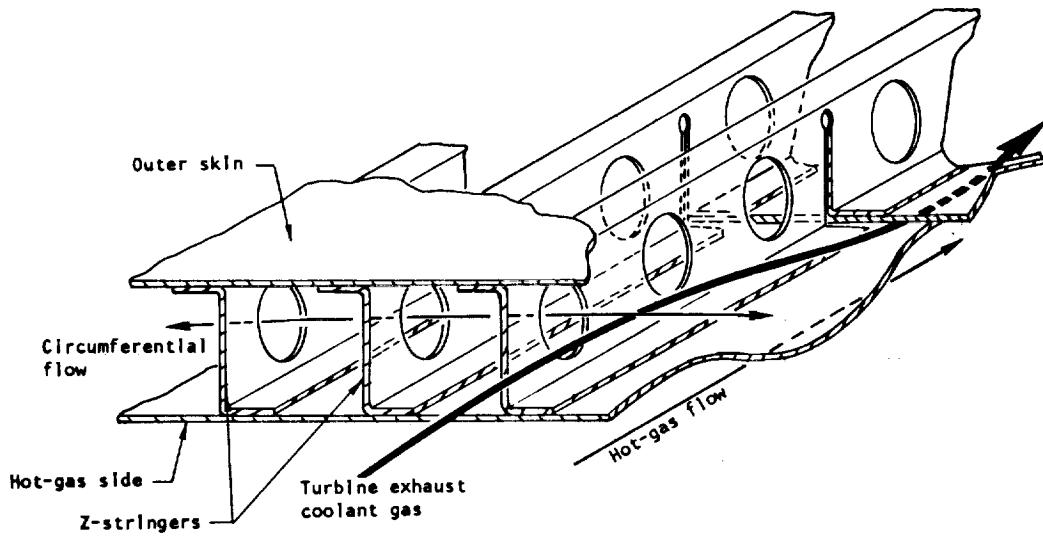
Figure 19. — Provisions for coolant crossflow in F-1 nozzle extension.

(a) Rigid shingle   (b) Dimpled sheet
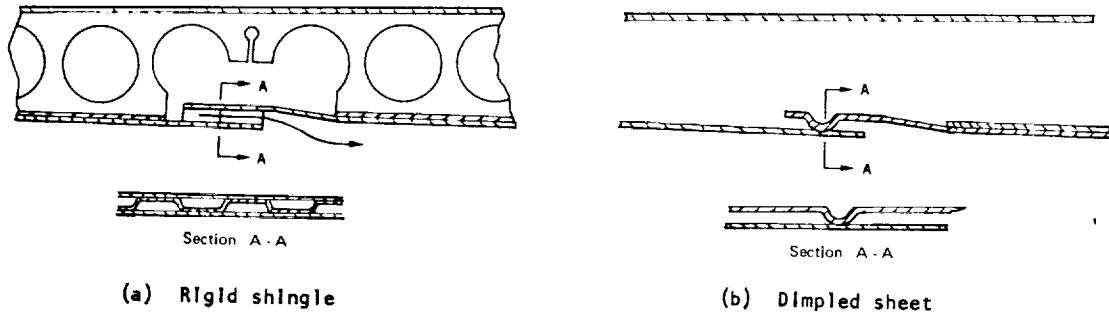
Figure 20. — Two designs for controlling distortion of coolant slot in film-cooled extension.

20(b)) that prevents the slot from closing but not from opening too wide and starving other slots. Ductile metals such as Inconel 625, Hastelloy C, or 347 CRES have been required as shingle and structural materials in order to avoid low-cycle thermal fatigue.

2.2.2.2 ATTACHMENT-AREA GEOMETRY

The geometry of the attachment area of the F-1 nozzle extension (fig. 18) is controlled by the regeneratively cooled exit end of the main chamber and the film-cooled upstream end of the nozzle extension. The large separation distance between the main-gas stream and the coolant-gas stream along with the nonparallel coolant-gas injection caused the main hot-gas flow to detach from the wall and then reattach at a point downstream. At this reattachment point, the protecting film-coolant layer was destroyed, and the shingles overheated, warped, and burned out. This problem of local reattachment and overheating was overcome by introducing a large proportion of the total film-cooling gas flow in the attachment region, but overheating occurred in the remainder of the nozzle extension because the coolant flow there was reduced. The actual proportion of the total coolant-gas flow (about 25 to 30%) that was required to prevent local overheating downstream of the attachment point while still leaving enough coolant to cool the remainder of the nozzle adequately had to be experimentally determined with full-scale hot-firing hardware. No analytical technique available at the time would adequately predict the results.

The cooling of the shingles just downstream of the attachment area is controlled by the same parameters that control the film cooling of the remainder of the extension (sec. 2.2.2.1). Injection of the film coolant parallel to the wall and with small gas-stream separation is more difficult in the attachment area.

2.2.2.3 EXTENSION STRUCTURE

An extension cooled by turbine exhaust gas is cooled with a fluid normally considered a hot gas; thus operating temperature, thermal stress, and thermal distortion are very important aspects of the design problem. Figure 19 shows the Z sections used to attach the outer skin to the inner skin for the F-1 nozzle extension. Circumferential maldistribution of the turbine gases caused local coolant starvation and produced warping of the shingles. Holes in the Z members as shown improved the distribution and eliminated the problem. Good structural and ductility characteristics at operating temperature are requirements for gas-cooled nozzle extensions. Inconel 625, Hastelloy C, and 347 CRES have satisfactory ductility, but the 347 CRES has considerably lower strength. Bands have been made from 347 CRES. In the highly loaded aft end, the band usually is made from Inconel 718.

Fusion welding of the Z members to the shingles resulted in protrusions on the hot-gas side of the shingle, boundary-layer interruption, and subsequent erosion and failure of the shingle. The use of spot welds and seam welds that were ground nearly flush with the parent metal eliminated this problem. The quality of resistance welds is quite difficult to control, however, and strict adherence to the requirements of reference 46 was necessary to ensure adequate quality.

During the start and stop transients on the F-1, large side loads result from asymmetric flow separation. Since the side loads move around the nozzle perimeter, the nozzle extension tends to "breathe", and the result is hardware failure. The calculation of these side loads is not very precise, and overdesign of the retaining bands has been necessary to ensure that the bands will not yield.

In order to minimize the weight of the bands, the heat transfer from the extension to the bands is reduced so that the band operational temperature is lower; this reduction is achieved by inserting insulation under the bands and under the aft band. In addition, the bands are scalloped along the weld joint between the band and the shell outer wall to reduce conduction to the bands. These insulating techniques, shown in figure 21, have increased the local thermal yielding of the outer shell, but the additional yielding has not been a serious problem. Contamination of the insulation with fuel is minimized by altering operational procedures. The band scallops also help drain the insulation.

Gross inner and outer wall buckling due to thermal and mechanical loads is reduced by close spacing of the nozzle bands. Figure 22 shows the effect of band spacing on the contour of the nozzle extension and on gas flow after several firings.

2.2.3 Ablation-Cooled Extensions

Ablation-cooled extensions offer advantages that make them attractive in some rocket applications. Because they are self-cooled, they are easily detached for ground testing of
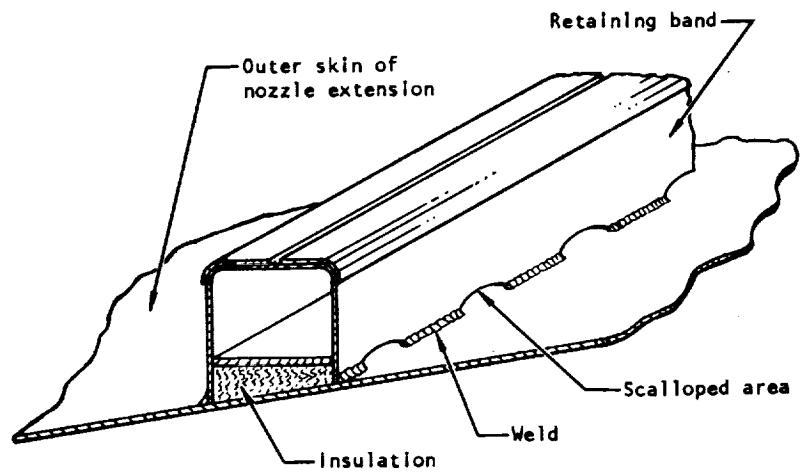
Figure 21. — Use of insulation and scalloped areas to reduce retaining-band temperature.

(a) Widely spaced retaining bands

(b) Closely spaced retaining bands
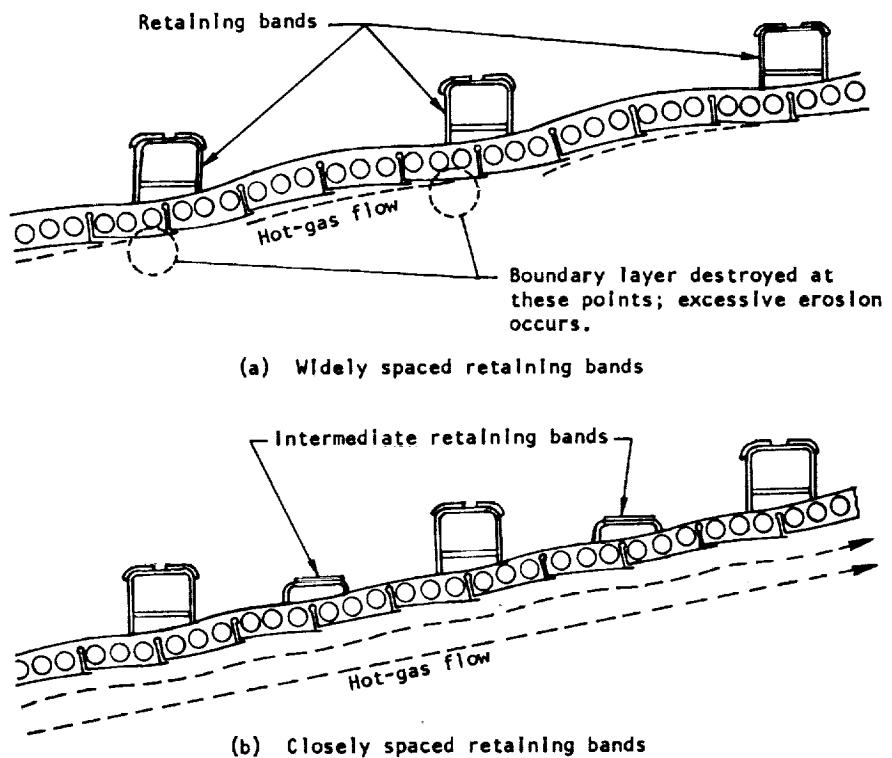
Figure 22. — Effect of retaining band spacing on contour of nozzle extension and gas flow after several firings.

altitude engines, so that nozzle-extension hardware is preserved and side loads from flow separation are precluded. Ablative nozzle extensions generally are lower in weight than film-cooled extensions and can operate continuously at a higher heat flux than can radiation-cooled nozzles. In addition, they are usually less expensive than film-cooled or regeneratively cooled extensions.

The composition, fabrication, and performance of ablative composites are discussed in references 1 and 2. As may be seen from the references, the support structure and performance characteristics of combustion chambers are different from those of the nozzle system. Erosion (sometimes chunking) or true ablation occurs in the chamber, where heat fluxes are high. In the nozzle, generally only charring occurs because the heat fluxes in this area are low enough to keep the wall surfaces intact. Attachment of the ablative extension to the nozzle requires special attention. Flange flexing or overall flexing due to handling, thermal distortion, or side loads from separated flow may cause bond failures and subsequent extension failure. In the successful attachment design for the Titan engines (fig. 23), the ablative extension is attached to the regenerative portion of the nozzle by a simple flange arrangement. No particular precautions or special sealing procedures are required. The
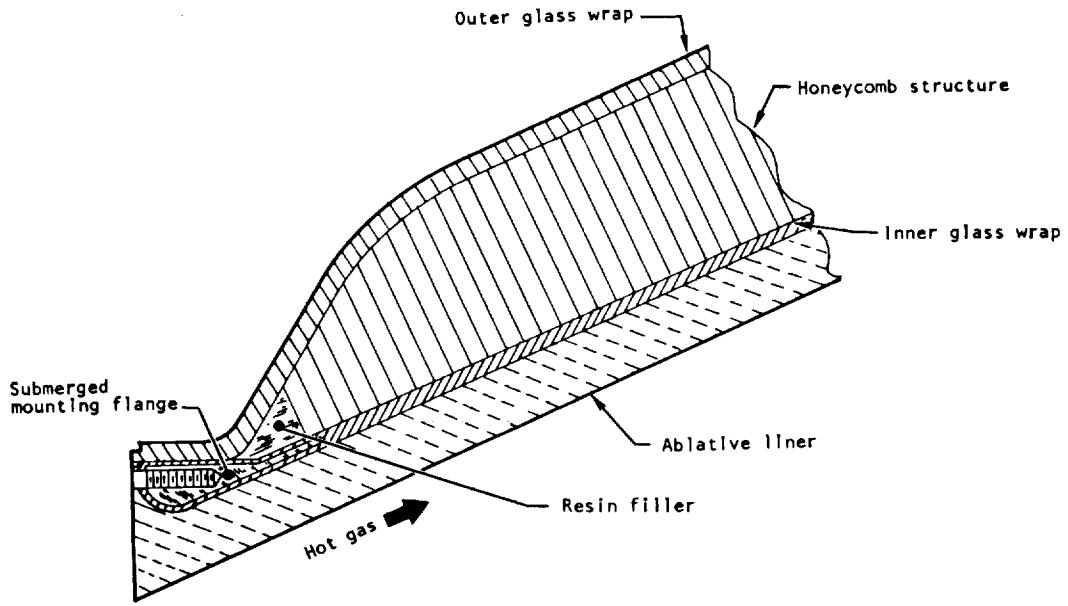
Figure 23. — Construction of ablative nozzle extension for Titan engines.

39

flange interface is horizontal and flat with a step machined into the liner at the hot gas side. A protruding lip from the chamber flange fits into the step to provide a simple method of positioning the extension squarely on the chamber. A leakproof seal is achieved by painting the flat surface of the flange with a silicone RTV sealant compound. The flange joint is fastened securely by bolts. In order to bolt into the ablative extension, 24 aluminum flange segments are bonded below the ablative flange surface; these segments are then drilled and tapped for thread inserts.

It should be noted in connection with the Titan nozzle extension that designs in which the aluminum segments were omitted (for simplicity) and the inserts installed directly into the ablative liner failed during the start transient. The failures occurred because the available inserts were intended for use with metal and lacked sufficient length to prevent shearing at the threaded interface. In addition, when inserts were installed directly into the ablative composite, the inherent creep characteristics of the material made it difficult to meet torque requirements.

Ablative material has limited mechanical strength and is sometimes backed by a honeycomb structure that is internally and externally wrapped with a glass/plastic composite. For example, in the Titan extensions, the tapewound ablative liners are strong enough to accommodate hoop loads from the internal nozzle wall pressures, which on the Titan systems range from 28 psi to 13 psi at the exit for the 15:1 nozzle. However, a glass-cloth/honeycomb-sandwich structure that constitutes 20 percent of the nozzle weight is employed to provide additional support for the liner during the start transient and gimbaling operation.

Gas evolution at the interface of the supporting structure can lead to pressure buildup sufficient to cause structural failure. To avoid this problem, all honeycomb channels are interconnected through drilled passages to allow free passage of gases to the atmosphere. In some designs of high-area-ratio ablative nozzles, the required strength is supplied by a thickened outer glass wrap.

2.2.4 Radiation-Cooled Extensions

Radiation-cooled nozzle extensions normally are used on pressure-fed space-engine systems, where high expansion ratios and minimum nozzle weight can be achieved at the lower operating pressure and thermal environment. The expansion ratio at the start of the extension is determined by the maximum heat flux that the extension can withstand at altitude. Variables affecting allowable thermal conditions, other than physical capabilities of the base material, include injector streaking characteristics, boundary-layer conditions, protective coatings on the extension, and external-shell emissivity. A generous fuel-rich boundary layer helps reduce heat flux but, of course, is detrimental to performance. Streaking injectors require that the extension be designed to the most extreme load

conditions, since circumferential heat transfer is quite low. A smooth transition between the nozzle and the extension minimizes heat loads from the gas boundary-layer attachment.

For low-temperature operation, titanium alloy AMS* 4917 has been satisfactory. For higher temperatures, hoop loads on titanium extensions have been taken up with molybdenum retaining bands fastened to the shell with a spot welder. For temperatures below 2000°F, both the cobalt-base L-605 (AMS 5537A) and the stainless steel N-155 (AMS 5532B) have been used successfully without protective coatings. At temperatures above 2000°F, refractory metals normally must be used for extensions. At these high operating temperatures, the most promising refractory alloys catastrophically oxidize or absorb gaseous products and become brittle. For columbium C-103, the aluminide coating NAA-85 has proved effective as an oxidation barrier. When a titanium extension was resistance welded to a columbium extension, the NAA-85 coating had to be left on the columbium to obtain a sound weld. Development problems in the use of refractory metals have been much greater than those that occur with "standard" metals that are limited to lower operating temperatures. The coating developed for a columbium chamber and nozzle extension in a technology development program is discussed in reference 47.

Flange yielding or nonuniform support on the extension increases the stresses in the joint and has led to cracking and leaking. Nonyielding flange designs and closely spaced high-temperature clamping bolts (e.g., those made of Rene 41) have minimized the difficulties, which are particularly severe for refractory extensions because of the higher temperatures. The use of a long heat-conduction path to the seal areas has allowed the use of elastomeric seals in some flange joints; elastomeric seals have considerably reduced the sealing problem, especially for large diameter seals. Asbestos seals have been used in initial development hardware with heavy flanges and relatively-short-duration testing in which the seal area has not become too hot. Pressure-assisted seals (e.g., Naflex and K seals) have been used successfully in flight hardware. Reference 48 provides detailed information on the design of joints and seals.

The high-temperature emissivity of metal surfaces can be increased by oxidizing and roughening the surface. The emissivity of aluminum can be increased from 0.1 for a clean surface to 0.9 for a dark anodized surface. Wall temperatures have been reduced by as much as 100°F by the use of an external emissivity coating.

Sea-level testing may induce severe structural loads from flow separation and also results in steady-state temperatures in the extension that are not the same as those achieved in space; thus, little if any sea-level testing is done with the nozzle extension in place.

---

*Aerospace Material Specification.

41

2.2.5 Circumferential Manifolds
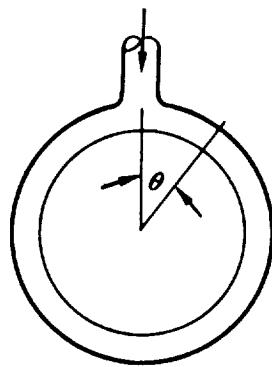
Circumferential manifolds for liquid rocket engine nozzles are used primarily for the following purposes:

- Direct fuel-rich turbine exhaust gas into the main gas jet

- Distribute turbine exhaust gases for gas-cooled nozzle extensions

- Distribute regenerative coolant around the nozzle for feeding the cooling tubes

- Direct the flow from the downcomer tubes to the upcomer tubes at the nozzle exit.
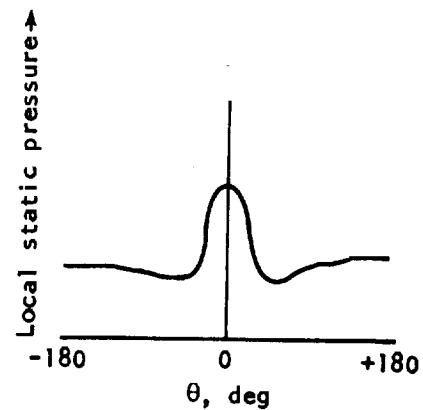
2.2.5.1 MANIFOLD HYDRAULICS

Weight limitations usually result in minimum manifold volumes and high fluid velocities. Holdup volumes affecting start and shutdown transients and wet weight are further considerations limiting the volume. Liquid velocities of 50 to 100 fps and gas velocities of Mach 0.25 to Mach 0.4 have resulted in maldistribution of the fluids, the consequence being tube starvation and inadequate local film coolant. With high fluid velocity in a radial inlet to a distribution manifold (fig. 24(a)), local static pressures will vary as shown in figure 24(b), and flow through the bleedoff ports will vary significantly along the manifold. Variations in static pressure near the inlet have been reduced by lowering the inlet velocity and also by providing multiple tangential inlets (fig. 24(c)), multiple low-velocity radial inlets (fig. 24(d)), or single or multiple radial inlets with turning vanes or deflector plates (figs. 24(e) and (f)). Variations in static pressure along the manifold in constant-area manifolds have been reduced by tapering the manifold (fig. 25).
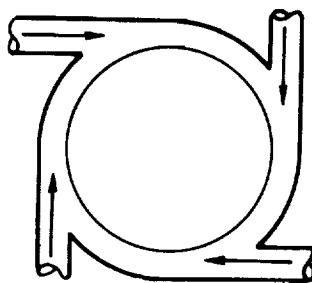
Basic hydrodynamic information is available in reference 49, and reference 50 contains information on hydrodynamic losses in branching manifolds. Local static-pressure profiles just downstream of the inlet duct normally cannot be calculated accurately, however, and experimental measurements must be made in critical areas. Since the flowrate through the bleedoff ports is affected by the cross velocity in the manifold as well as by the static pressure in the manifold, actual measurements of flow in bleedoff ports are often necessary. Even with a reasonably uniform pressure distribution near the inlet (produced by relatively low inlet velocity and a turning vane) with a tapered manifold, a pressure increase will occur at the final stagnation point in the manifold (fig. 26). Excess flow through the bleedoff ports near the final stagnation point can be reduced by increasing the flow resistance in or downstream of the bleedoff ports.
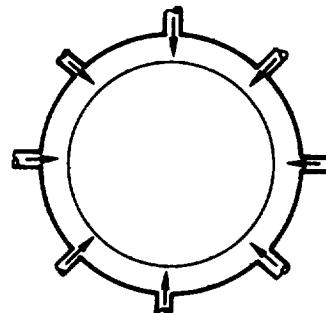
(a) Single, high-velocity inlet
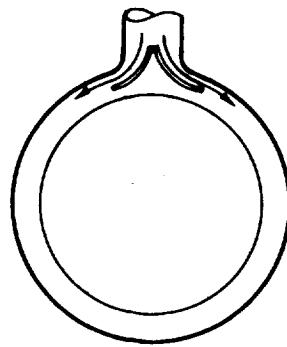
(b) Static-pressure profile for (a)
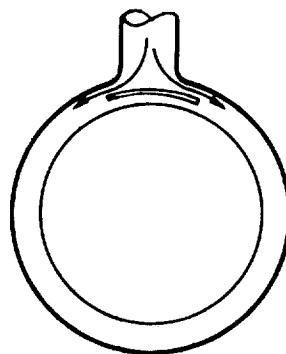
(c) Multiple tangential inlets

(d) Multiple low-velocity radial inlets
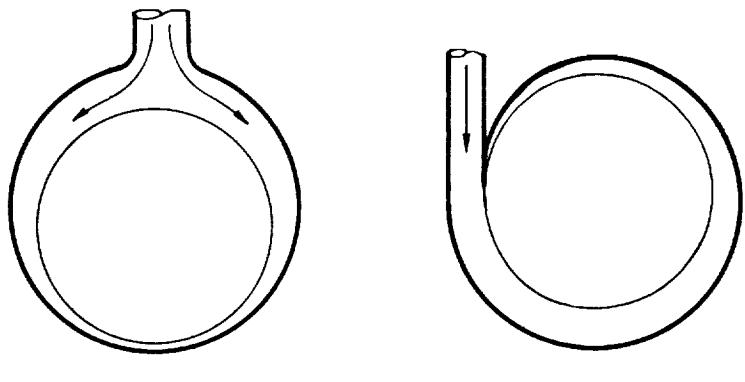
(e) Radial inlet with turning vane

(f) Radial inlet with deflector

Figure 24. — Types of manifold inlet configurations.

43

(a) Tapered manifold with radial inlet

(b) Tapered manifold with tangential inlet

Figure 25. — Two configurations for tapering a manifold to reduce variation of static pressure.
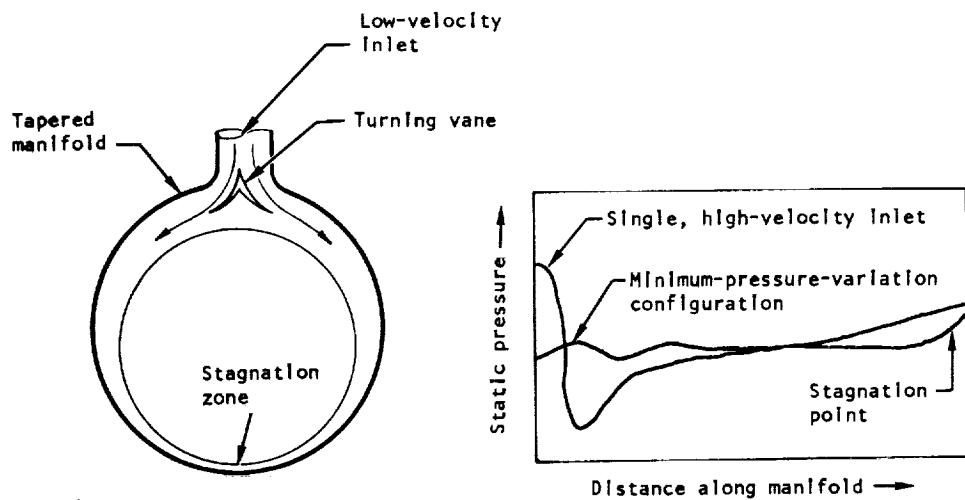
Figure 26. — Manifold configuration for minimum variation in static pressure.

2.2.5.2 VANES, SPLITTERS, DAMS, AND STRUCTURAL SUPPORTS

Maldistribution in flow often results from the high velocities associated with small-cross-section manifolds used to keep structural weight low and from the low pressure-drop requirements normally imposed on rocket engine flow system components. Vanes, splitters, and dams help correct these flow maldistributions. Large manifolds normally have relatively thin walls in order to minimize weight and are more flexible than the supporting structure. To prevent failure of these large manifolds, structural ties (supports) frequently are added. The hydrodynamic function of vanes and splitters sometimes is combined with the structural function of ties, and one member is used to do both jobs.

2.2.5.2.1 Turning Vanes

Although hydrodynamic correlations available in the literature (e.g., ref. 49) can be used to predict the pressure distribution in a manifold, the results frequently are not sufficiently accurate for design purposes. For very large, expensive manifolds with fabrication lead times of many months, it is impractical to recontour or move the turning vane on the basis of experimentally determined pressure profiles. For the inlet to the F-1 turbine exhaust gas manifold that was used to distribute gas film coolant around the chamber, the turning-vane contour design was based on available theory. Removable plugs were inserted in the auxiliary turning vanes (fig. 27), and pressure contours were determined with various combinations of plugs removed, without the necessity of physically moving the turning vanes.
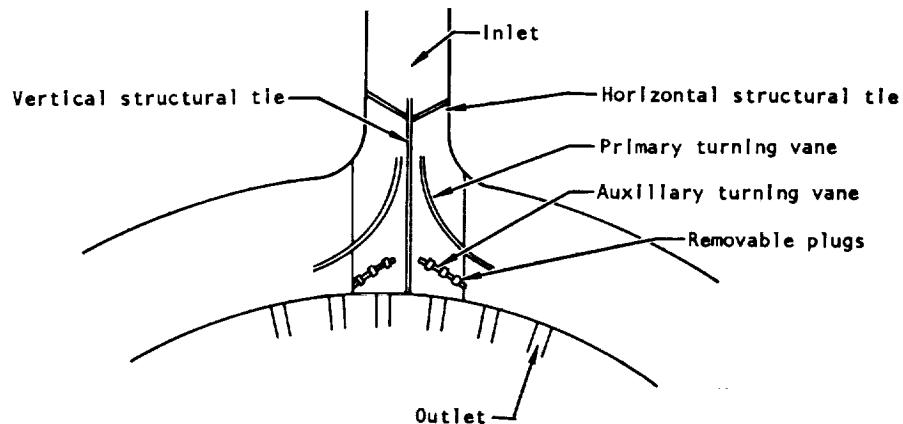
Figure 27. — Manifold design with removable plugs in auxiliary turning vanes.

2.2.5.2.2 Flow Splitters

Splitters have been used to provide an equal flow split for a nonsymmetrical entrance configuration (fig. 28); however, splitters located in the geometric center of the flow occasionally have caused increased maldistribution. The effectiveness of the splitter is sensitive to upstream flow conditions. If the upstream conditions change during operations (as from a variable-position valve), the flow split under some of these conditions may be considerably worse than it would have been without a flow splitter. Experimental determination of the pressure profile when upstream conditions are varied has been necessary to establish the effectiveness of flow splitters across the entire operating range. Splitters can be avoided with symmetrical entrance configurations such as those in figures 29(a) and (b). With nonsymmetrical configurations (fig. 29(c)), splitters may be avoided only if the entrance velocity and upstream velocities are kept low.
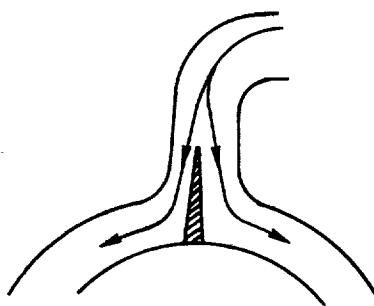
Figure 28. — Manifold flow splitter for nonsymmetrical entrance.

(a) Symmetrical elbow

(b) Symmetrical tee

(c) Nonsymmetrical entrance
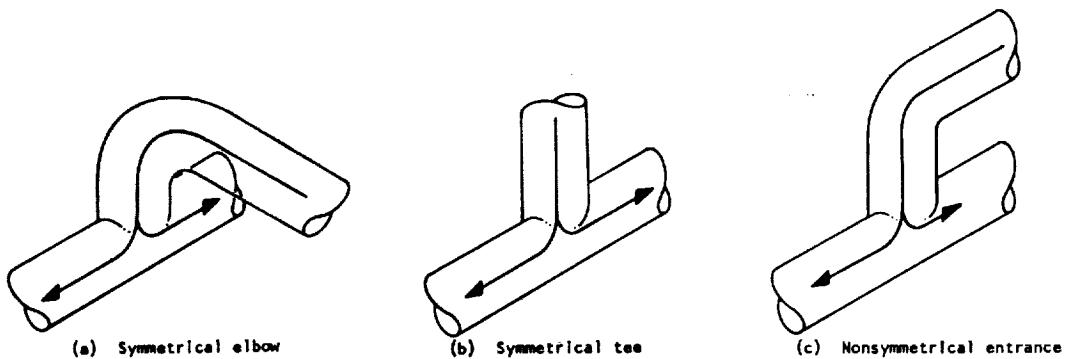
Figure 29. — Symmetrical and nonsymmetrical manifold entrances.

2.2.5.2.3 Dams

Dams are used to decouple fluid pressure perturbations and to help "fix" the pressure profile. In the fuel-return manifold at the end of the thrust chamber nozzle on the H-1 engine, a nonuniform inlet flow resulted in a variable cross velocity and variable distribution to the injector, and performance changed during test. A dam that covered 80 percent of the cross-sectional area of the fuel-return manifold and was located opposite the (upstream) fuel inlet for the main tube bundle considerably reduced the variations in cross velocity and stagnation-point location and eliminated the performance changes.

2.2.5.2.4 Structural Supports

Vanes, splitters, dams, and structural ties are subject to failure from differential thermal stress; fatigue from vibrational loads; fatigue from resonant flutter; and excessive static-pressure loading. Even when the failure does not result in a direct structural failure of the nozzle, it often produces a maldistribution of fluid flow and results in performance loss, combustion instability, or wall overheating. Toroidal manifold shells often are more flexible than the supporting structure and will "breathe" under pressure variation. Flow distributors and structural ties must be sufficiently flexible to grow with the shell and sufficiently rigid to support the shell locally, or they must be mounted on one side of the supporting structure with clearance left on the remainder of the circumference. Attachment of vanes, splitters, dams, and structural ties (figs. 30, 31, and 32) is extremely critical, since fatigue failure at the attachment location is a common failure mode.

Figure 30 shows some methods for attachment of turning vanes and splitters. The fillet weld is a generally unacceptable joint, while the full-penetration fillet weld is much better and usually acceptable. The butt weld is a good joint, and the integral casting has been excellent where it could be used.

Figure 31 shows two modifications of turning vanes that will prevent vane flutter in a large manifold. Flat surfaces are extremely subject to flutter, and large curved sections also have failed from fatigue. A splitter used in conjunction with vanes can produce a vibration-resistant structure.

Figure 32 shows several methods for welding dams in manifolds. Partial welds are the simplest but the most subject to fatigue failure. Continuous internal welds and internal-external welds are very good structurally but are limited to use adjacent to a manifold, because of the weld access requirements. Integral dams that are part of the parent metal constitute the best design from a structural standpoint and have in general been failure free.

47

(a) Fillet weld

(b) Full-penetration fillet weld

(c) Butt weld

(d) Integral casting
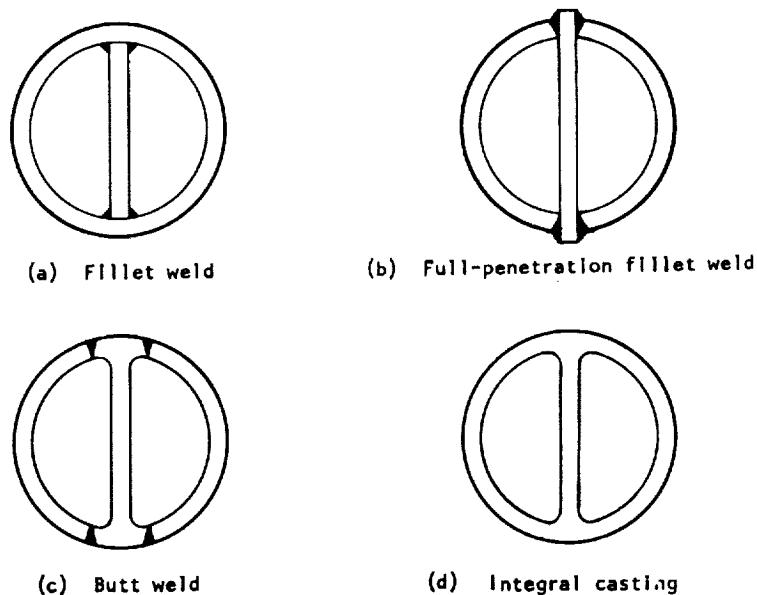
Figure 30. — Methods for attaching turning vanes and flow splitters to manifold.

Turning vane only

Splitter added

Dampeners added
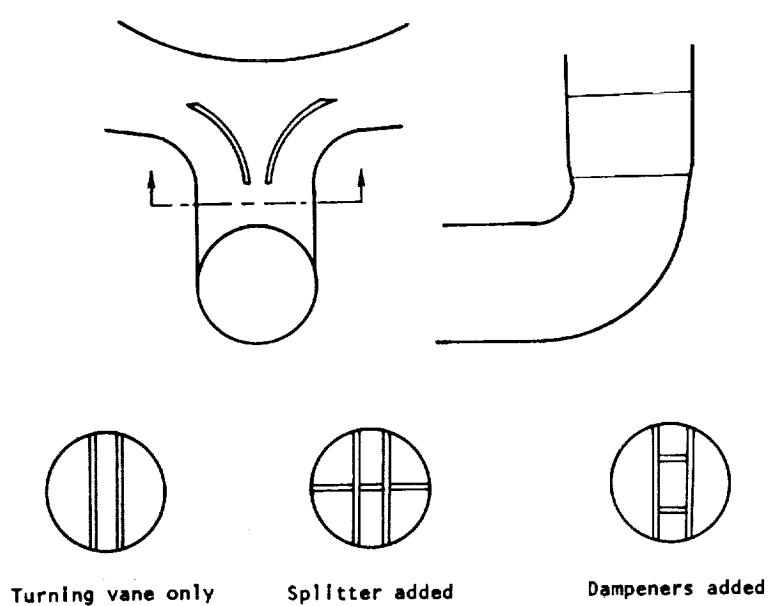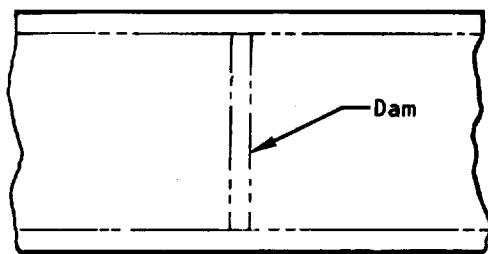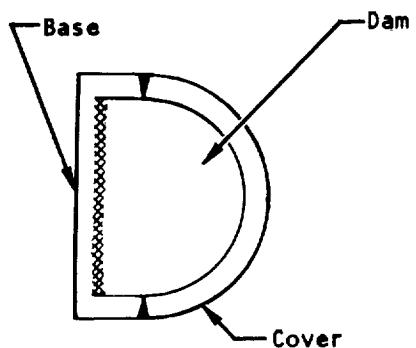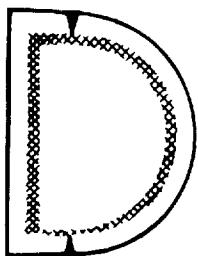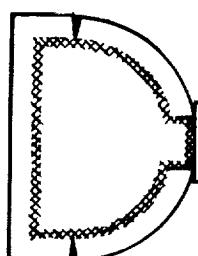
Figure 31. — Modifications of turning vanes to prevent flutter.

48
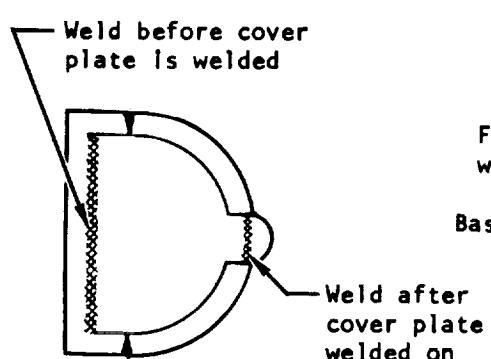
(a) Partial internal weld
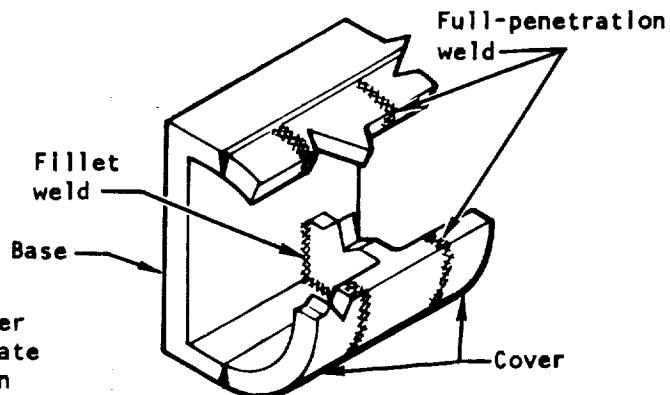
(b) Continuous internal weld (accessible)

(c) Internal-external weld (accessible)

(d) Weld is inaccessible after cover plate is welded on

(e) Weld is inaccessible after cover plate is welded on

Figure 32. — Methods for welding dams in manifolds.

49

2.2.5.3 HOT-GAS MANIFOLD

In early Atlas vehicles in which the booster-engine exhaust gases were ducted axially, the fuel-rich turbine exhaust gases caused boattail fires. Canting the exhaust ducts outwardly directed the gases into the slipstream and prevented recirculation. In the Atlas sustainer engine, the exhaust gases were conducted around the end of the nozzle where they were entrained in the main jet and ejected axially. In the Jupiter and Thor vehicles, the engines were more exposed to the slipstream, and no serious problems resulted. Each of the four gimbaled outboard H-1D engines of the Saturn S-1B had an exhaust-stream disposal system like that of the Atlas sustainer engine.

In the F-1 engine, the turbine exhaust gas is used as film coolant for the nozzle extension. In the J-2 engine, the turbine exhaust gases are dumped into the main gas stream through "cat-eyes"*. The tubes downstream of the J-2 turbine exhaust dump are partially film cooled but primarily regeneratively cooled. The Titan stage I turbine exhaust gases leave the turbine at 1200°F at 30 psi and are ducted through the oxidizer superheater, where additional heat is extracted in raising the temperature of the oxidizer pressurant. From the superheater, the exhaust gases are conducted through a short duct to the outside where they impinge on the ablative extension. The resultant side loads resolved into axial and lateral components are 90 ± 20 lbf and 360 ± 50 lbf, respectively. The axisymmetric nature of the applied loads from both turbine exhausts is calculated to induce a vehicle roll moment of approximately 250 ft-lbf. Thermal damage is prevented by an insulation blanket placed over the nozzle.

In the single-nozzle engine system for Titan stage II, roll is corrected by the use of an additional small conical nozzle that employs turbine exhaust gases. Impingement of these gases on the ablative surfaces of the main engine nozzle extension, during swiveling, caused local heating and structural damage. This problem was corrected by bonding low-density silica matt over the exposed extension areas directly below the roll-control nozzle.

The contribution by the turbine exhaust gas to the overall engine performance can be significant, the thrust potentially produced by the turbine exhaust gas being usually in the vicinity of 1/2 percent of the total thrust. This exhaust gas can also introduce a nonaxial thrust or an axial thrust with a moment. For large potential-thrust values (16 000 lbf for the F-1), careful attention must be given to the structures that must withstand these added loads.

A looped-tube configuration to allow the turbine exhaust gas to pass into the nozzle gases was used on an experimental Atlas sustainer engine. The fuel-rich cutoff left RP-1 trapped in pockets in the exhaust-gas manifold, and detonations resulting from LOX/RP-1 gel formation occurred at the start of the following test. The J-2 had a similar potential trap,

*Long, narrow openings between coolant tubes.

but the use of cryogenic propellants that evaporated between runs eliminated the problem. The J-2 system with cat-eyes and a hot-gas manifold is expensive but has not had significant hardware failure.

The primary problem with large hot-gas manifolds is the yielding that occurs when the thermal growth is restricted. The F-1 turbine exhaust manifold has a potential thermal growth of approximately 1/2 in. radially. Restraining thermal growth has caused innumerable hardware failures in various hot-gas manifolds. Many designs have been successful despite the restriction on thermal growth. In these cases, the cyclic life has been increased to the required value by fixes that reduced the local plastic yielding but did not eliminate it.

The present F-1 turbine-exhaust manifold (fig. 33) is a tapered hot-gas torus rigidly attached to the cooled exit ring. "Omega" expansion joints placed around the torus shell allow the torus to expand. Expansion of the flame shield results in shield bending, but the plastic
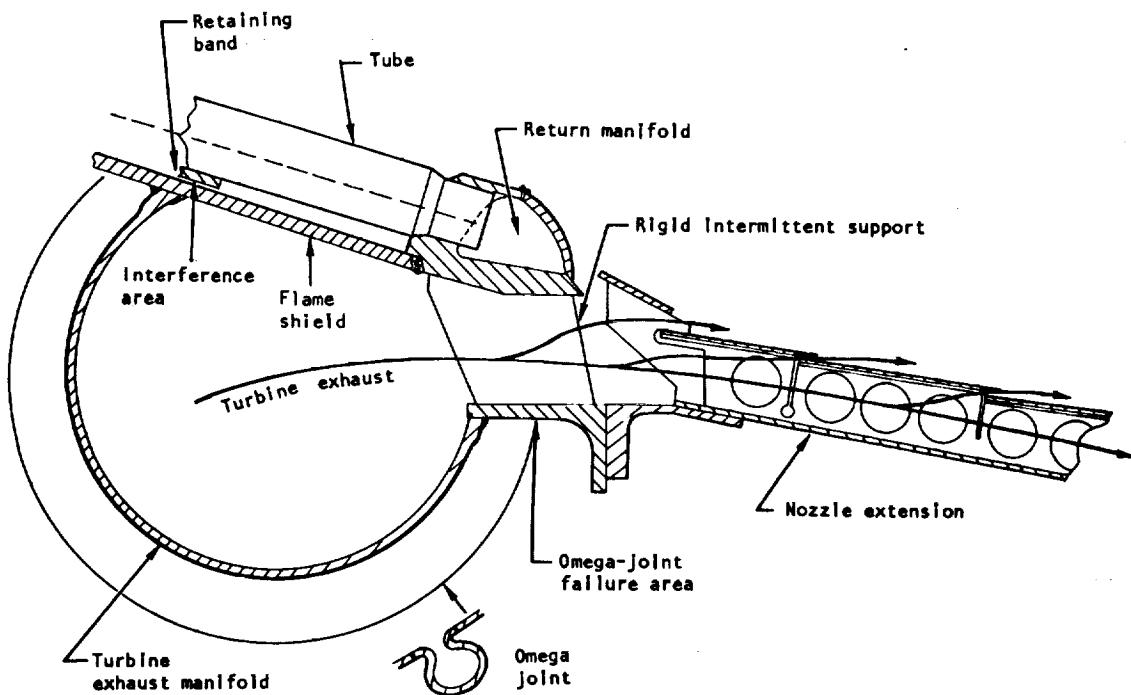
Figure 33. — Construction of junction of turbine exhaust manifold and film-cooled nozzle extension (F-1 engine).

strain is low enough that 50 or more cycles can be achieved without cracking. The major problem area has been at the intersection of the omega joints with the outer ring. This ring is restrained by being rigidly attached to the stronger cooled exit ring, so that the ring bends between attachments. The base of the omega joint attaches to this ring; on cooldown, tension cracks develop. Doublers added to the omega joints to distribute the load over a longer base have resulted in increased cycle life. Distortion of the hot-gas manifold during fabrication and operation has resulted in interference between the flame shield and the tube retaining band, the result being denting of tubes. This problem was caused basically by an inability to control adequately the dimensions of large, flexible manifolds that were subject to much welding, a braze cycle, and subsequent deformation during operation. This F-1 tube denting was eliminated by increasing the clearance between the flame shield and the retaining band from a few thousandths to about four-tenths of an inch.

Classic sliding-pin and A-frame designs that allow unrestrained thermal expansion have been used successfully for a long time in turbojets and ramjets and are applicable to hot-gas manifolds in rocket engines. One such design was proposed for the F-1 but was not used because the local thermal stresses in the production design were reduced enough to allow successful repeated operation. In the F-1 turbopump, radial pins were used to solve a problem in differential thermal expansion. In one of the original F-1 turbine exhaust manifold designs, sliding pins and slotted clevises were employed to eliminate thermal stresses. Because of a combination of insufficient installation clearances, mechanical loads that were too high, pins that were too small and too short, and thermal clearances that were inadequate, the pins were overloaded and were bent. This design was dropped because of difficulties of reworking it within the required schedule, and the hardware was modified to the present type shown in figure 33. The J-2 turbine exhaust manifold has no removable gas seal and thus can be somewhat simpler. The difference in expansion between the hot duct and the cold tube bands is taken primarily by bending in the base plates.

For designs in which the thermal loads are kept low enough to maintain the material in the elastic state, relatively brittle materials have been used (e.g., Waspaloy and Rene 41 in turbojet designs). When thermal loads on a structure are high (e.g., the F-1 turbine-exhaust manifold), materials that retain ductilities of about 20 percent or higher at elevated temperatures are required (e.g., 347 CRES, Hastelloy C, Inconel 625, and L-650).

Flanges often are heated rapidly during operation and sustain major thermal gradients that cause warping and dishing and resultant seal leakage. Splitters or other external attachments increase this problem by inducing additional thermal and mechnical loads. Very thorough analysis of the distortions caused during startup and operation can help reduce but probably not eliminate the problems. Some seal-surface deflection for low-pressure seals can be allowed by using self-energizing pressure-actuated seals, which can allow flange deflection of up to 0.010 in. per leg and still give seal tip contact to the flange. Bolt preloads on flanges must be sufficient to keep the flanges in contact under the high thermal and mechanical loads that develop during operation.

2.2.5.4 COOLANT-RETURN MANIFOLD

A coolant manifold is positioned at the end of a regeneratively cooled chamber for either single-pass (an inlet manifold) or double- or multiple-pass system (a return manifold). The term "single-pass" or "multiple-pass" refers to the number of times the coolant flows through the axial coolant passages in the nozzle wall before it is used in the injector. The same coolant flows alternately upstream and downstream a selected number of times in order to provide adequate nozzle cooling surface area with a given size of individual passages. Both inlet and return manifolds are subject to similar problems, primarily overheating and inadequate braze joints. The double-pass coolant-return manifolds used on all Titan engine systems are included as an integral part of the extension attachment flange. The arrangement simplifies construction and eliminates extensive welding, thus decreasing the incidence of weld leakage and reducing fabrication expense.

Good cooling is provided by using individual 180° tube elbows for propellant flow reversal at the nozzle exit. A support ring, which is often required for nozzle attachments, is not provided by this method. The chamber is extremely difficult to drain, and removal of solid contaminants (chips, broken seals, etc.) often is impossible. Continuous manifolds into which the tubes are inserted provide support for attachments and are much easier to drain and clean.

Tubes with swaged square ends have been inserted into slots in the coolant manifold (fig. 34(a)). Problems have resulted from the (1) required insertion of fillers or powder into the
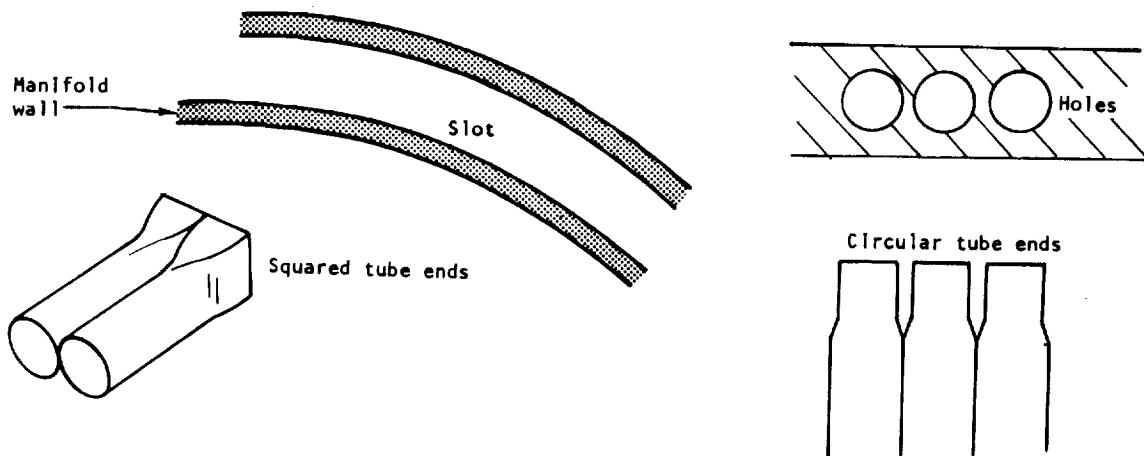
Figure 34. — Configurations for attaching tubes to manifolds.

53

corners because the tubes could not be made with sharp-enough corners; (2) peeling of the braze joint; (3) "oil canning" of the flat tube walls; and (4) difficult tolerance control. Tubes with circular ends inserted into round holes in the manifold (fig. 34(b)) have produced much more successful bonds. Expansion of the tube end while it is in place within the manifold (F-1 technique) has remained within the closely controlled braze gap tolerance, and bonds produced have been highly successful. Braze foil preplaced throughout the entire braze joint has been investigated and looks promising. Most production chambers now use powder or paste successfully. Depending on the particular design, maximum braze gaps of 0.004 to 0.006 in. have been satisfactory. A braze-joint length of at least one tube diameter usually has produced acceptable joint strength. Incompatible plating materials and materials with dissimilar brazing characteristics and thermal expansion coefficients have resulted in unsatisfactory joints. The inclusion in the furnace of braze samples of a new joint design during the brazing of a chamber with an existing joint design has helped to point out potential problems in the new joint design. Verification of final material properties as affected by material aging characteristics has been obtained by including braze samples during production-chamber furnace brazing. Although hand-brazed chambers have been successfully built, furnace brazing has produced a much more reliable product.

Complete braze bonding throughout the joint length, even when it is not needed for basic strength, increases heat-transfer contact area and improves ring and joint cooling. Braze gaps can interrupt the heat-conduction path between tubes (fig. 35). Voids and heat-transfer barriers have resulted in overheating during operation. Minimum sections in manifolds have produced cooler manifolds.
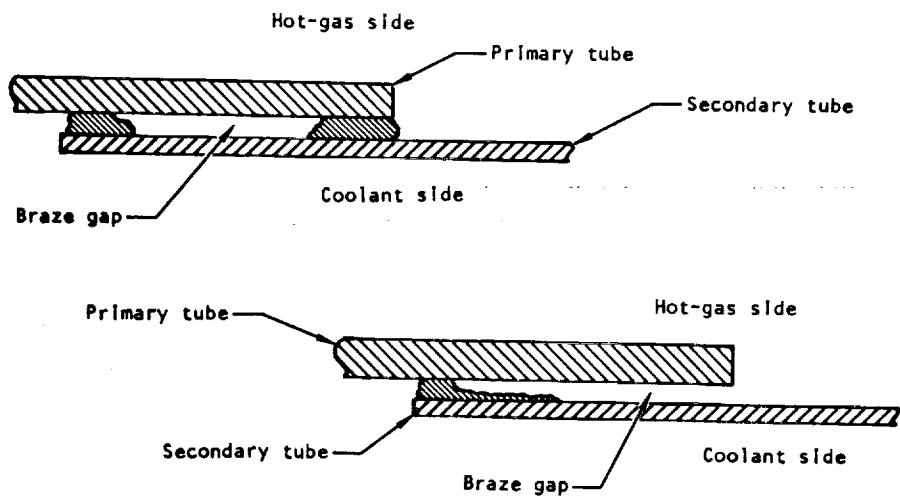
Figure 35. — Two types of braze gaps that interrupt the heat-conduction path between tubes.

54

Coolant manifolds that project into the main hot-gas stream have been subject to overheating, erosion, and leakage. Manifolds that are not in direct contact with the gas stream have not had such problems. Overheating typically is more severe for the down-tube/manifold joint than for the up-tube/manifold joint, because the thin, just-developing boundary layer results in a higher liquid-side film coefficient along the up-tube joint.

2.2.6 Nozzle Attachments

Major structural loads such as those from turbopumps or gimbal arms normally are taken through the chamber section, where heavy construction is already required for chamber-pressure loads. The majority of nozzle and nozzle-extension loads result from the mass of and attachment techniques for

- Propellant manifolds and turbine exhaust-gas manifolds

- Thermal insulation

- Small plumbing and instrumentation and associated brackets

- Side load supports

- Restrained attached or adjacent major ducting

- Handling lugs and brackets

2.2.6.1 ATTACHMENT TECHNIQUES

Tube-wall chambers have failed as a result of severe local stress concentrations produced by direct attachments to the tubes or to thin structural sections. Welding in general has not been acceptable because of local tube stresses and the problems of welding thin-wall sections; brazing has been more successful. Better practice has been to connect attachments to a nozzle structural member such as a retaining band rather than directly to the tubes. Excessive local external loads have resulted in tube depressions and early tube failures.

The welding of attachments to nozzle structural members that are age hardened during furnace brazing has resulted in failure of the structural member due to loss of the age-hardened induced strength; welding the attachments prior to furnace brazing has solved this problem. Local weld distortions and internal stresses have also resulted in failure of relatively thin nozzle structural parts where the attachments were welded; careful design and fabrication in these areas has been sufficient to resolve these problems in most cases.

55

Major nozzle load inputs must be analyzed not only for local attachment adequacy but also for their effect on the overall load-carrying capability of the nozzle. These loads are amplified as gimbal accelerations increase. Early F-1 engine testing revealed insufficient nozzle bending resistance at the end of the continuous jacket, and axial stiffeners had to be added. Increased nozzle loads result from support of components adjacent to but not integral with the nozzle, such as the turbine exhaust manifold inlet, turbine exhaust ducting, propellant ducting, and thermal shields or barriers. Loads from these items often are significant and must be included in the original design, not added as an afterthought. Gimbaled nozzles support only the aft portion of hardware that is gimbaled, but in many cases this portion includes fairly heavy turbine-exhaust and propellant plumbing.

Addition of accessory structures that have operating temperatures considerably higher than those of the nozzle structure causes thermal loads that are unacceptable if relative movement between the assemblies is precluded (sec. 2.2.1.1.3).

2.2.6.2 EXTENSION JOINT FOR LARGE CHAMBERS

For large thrust chambers, the nozzle/nozzle-extension joint normally consists of two large-diameter (up to 120 in.) flanges, with one flange sometimes considerably cooler than the other during operation. Designing this joint with enough flange thickness and heel length to provide sufficient rigidity to prevent flange distortion, rotation, and general yielding during handling and operation would require heavier flanges than are normally allowable. Designs and manufacturing techniques developed to reduce the weight of these large assemblies usually result in hardware conditions that are more representative of sheet-metal tolerances than the normal machine tolerances. This condition in turn results in connect-flange conditions that produce out-of-roundness and waviness because of weld distortions, flange distortion due to low-rigidity flanges, general yielding, and surface finishes that do not meet regular seal requirements.

Overall flange out-of-roundness between mating flanges of as much as 1.5 percent of the flange diameter has been compensated for by using oversized bolt holes, radial bolt slots on one or both flanges, and portable assembly alignment tools to allow bolt insertion in out-of-line bolt holes. The radial bolt holes also allow differential thermal expansion between the two flanges. A bolt spacing equal to the bolt head diameter plus twice the flange thickness has been found adequate to minimize unsupported areas and force the two flange contours to conform closely to each other.

Flange waviness resulting from fabrication techniques and from rotation, flange distortion, and flange surface irregularities – all require seals that have large crush or compression ratios, are flexible, and still produce an adequate sealing force after being crushed or compressed up to 50 percent. Elastomeric seals have been effectively utilized for joint temperatures up to 500°F. Specially constructed "tadpole" asbestos seals (fig. 36) with
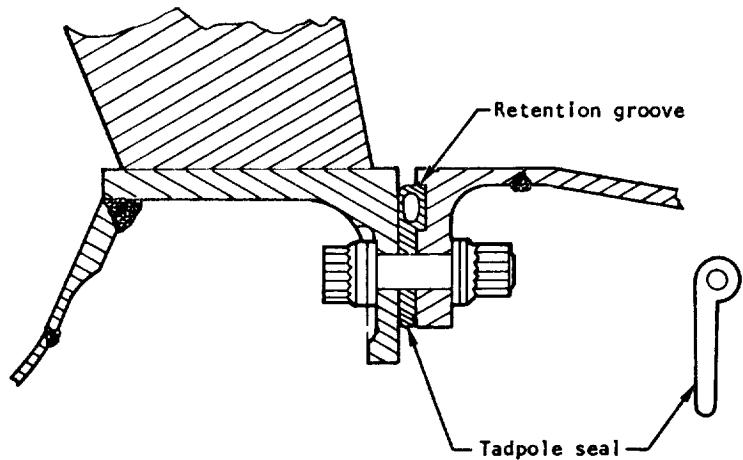
Figure 36. — Flange and seal design for use in high operating temperatures.

Inconel-mesh rope cores have been used for higher operating temperatures; these seals have been retained better when one of the flange surfaces was grooved. For seals designed to have the crush portion match the groove area, the groove edges have added seal points to prevent local leak paths. Continuous seals or seals with flat joints have been found necessary to prevent seal leakage or flange distortion due to local areas of increased seal thickness.

The tadpole type of seal yields during installation and has been nonreusable because of mismatch of flange imperfections and lack of resilience upon reassembly. In nonflight-type, noncritical seal areas (e.g., the J-2 nozzle-mounted diffuser-to-chamber joint), simple asbestos rope has been satisfactory.

2.2.7 Instrumentation Provisions

Most nozzles in the course of design and development are ground tested to verify the design and evaluate performance. In these full-scale hot-firing tests, hot-gas-side wall temperature, static pressure on the nozzle wall, and stress (strain) at key stations in the nozzle structure must be measured. Current methods for making these measurements require that the nozzle designer make provision during design to accommodate the necessary instruments, materials, and associated equipment.

2.2.7.1 TEMPERATURE MEASUREMENT

Attempts to measure the temperature of the nozzle hot-gas wall have been difficult in the past. Radiation methods have not been satisfactory. Attachment of thermocouples to the liquid side of the tube hot crown has resulted in leakage where the thermocouple wires pierced the back side of the tube, and has produced liquid-side boundary-layer disturbances that resulted in erroneous temperature measurements. Standard-size thermocouples attached to the hot side of the tube crown have burned out or have produced erroneous temperature measurements because the thermocouple disturbed the gas-side boundary layer. Development of microminiature thermocouples has resulted in satisfactory measurement of tube-wall temperatures on the hot-gas side. Measurements with 0.010-in. microminiature thermocouples bonded to the hot-gas side of the tube crown in the chamber of the Atlas sustainer engine revealed that temperature spikes of 100 millisecond duration were occurring after one-half to one minute of mainstage operation and were causing tube failure (ref. 51).

2.2.7.1.1 Thermocouples

Early thermocouple assemblies that stuck out from the thrust chamber frequently were damaged by handling during engine assembly or by vibration during testing. Thermocouple tip breakage during installation was eliminated by annealing tips that had been work hardened during the flattening process.

Thermocouple assemblies that were inoperable or that provided erroneous measurements of temperature have been produced by improper installation techniques. Reference 52 contains the recommendations developed for installation of microminiature thermocouples on the thin-wall tubes of the J-2 thrust chamber. For tubular chambers that have already been furnace brazed, a heated tungsten probe has been used to melt the tube-to-tube braze and produce a local tube-wall indentation or dimple (refs. 53 and 54). Chamber tubes have often been pierced by this technique, however, and repairing the leaking tubes has been a difficult and time-consuming process. Thermocouples have also been run along the tube crevice from the nozzle exit in order to avoid damaging the tubes with the heated probe while making the tube indentation; this technique has been satisfactory near the nozzle exit. A much superior technique in comparision with the heated-probe method is to predimple the tubes before stacking (ref. 44) and place a Refrasil cord in the dimples to prevent their filling up with braze alloy during furnace brazing. The dimples have been placed in adjacent tubes rather than in the tube to which the thermocouple is to be attached, in order to avoid restricting the flow in the tube for which the wall measurement is to be made (ref. 55). The thermocouple is inserted through the dimple between the tubes (whether the tubes are predimpled or dimples are produced by the heated tungsten probe), the tip of the thermocouple is tack welded to the tube, the thermocouple is brazed to the tube, and the dimple and exposed thermocouple sheath are brazed over. Thermocouples have been brazed

58

onto the tube surface by combustion torches, argon plasma-arc torches, quartz lamps, and Dalic-process gold plating (ref. 56).

Although thermocouple installations would be much better if the thermocouple were brazed to the tube before tube stacking and brazing, the junction between the microminiature thermocouples and the standard thermocouple wires has not yet been developed to the point at which it can with certainty withstand a furnace braze cycle.

Directing the thermocouple tip in the upstream direction, relative to the hot gas, has produced a minimum interference with the boundary layer and resulted in a truer temperature measurement. Reference 57 contains a discussion of measurement errors introduced by thermocouple installation and measurement techniques. The actual junction location for these high-resistance microminiature thermocouples can be determined within a few thousandths of an inch by means of a Wheatstone bridge having a precision of ± 0.1% (ref. 58). The junction location has been changed by tack welding upstream of the original junction.

A technique for measuring gas-side wall temperatures that consists of spot welding a single Platinel* thermocouple wire less than 0.001 in. in diameter to the stainless-steel thrust-chamber tube is presented in reference 59. The thermocouple wire is sheathed in a quartz insulator with a diameter of less than 0.003 in. Nickel or copper is then electroplated over the thermocouple and insulator. Installation techniques are included in the reference.

2.2.7.1.2 Braze Patches

Attempts to use temperature-sensitive paints, crayons, and patches on the inside of thrust chambers to determine maximum tube-wall temperatures have been unsuccessful. Braze patches, however, have been used successfully to determine limiting tube-wall temperature. A large range of melting temperatures is available (e.g., from about 361°F for Sn-37Pb to 1832-1868°F with Cu-35Au) (ref.60). A thin patch is melted onto the hot-side tube wall and an "X" scribed on the patch. When the patch reaches its melting point, the "X" is obliterated. Braze patches are easier to apply than thermocouples, especially in small tubular annular thrust chambers and in already completed chambers. Large numbers of braze patches can be readily applied and are especially valuable in indicating temperature profiles around or along the tube walls. However, the braze patch technique is subject to several problems, as follows:

- A braze patch that is too thick or too low in conductivity will result in the braze-patch surface reaching a significantly higher temperature than the tube surface would have reached without the braze patch (ref. 61).

*Registered trademark of Englehard Industries, Inc. U.S. patent 3,066,177, Nov. 27, 1962.

- Patch material must be compatible with the tube material to avoid stress-corrosion cracking (ref. 60).

- Patch erosion may obliterate the "X" without the patch having reached the remelt point (ref. 62).

2.2.7.2 PRESSURE MEASUREMENT

The measurement of static pressure on the nozzle wall requires pressure taps in the wall. Provisions for these taps are made during nozzle design and assembly. At designated locations in the nozzle, the designer provides for dimpling of the tubes during the tube forming process as discussed above for installation of thermocouples. During assembly, a ceramic rod or Refrasil cord is placed in the dimple to prevent the braze from filling the dimple. Following the furnace brazing of the tube assembly, the rod or cord is removed, and a pressure-pickup tube is inserted in the dimple and brazed in place. Care is taken to ensure that the pressure tap does not project into the hot-gas stream, but remains level with the inner wall. The length of the pickup tube from tap to recording device is kept as short as possible to achieve a high degree of accuracy in the measurement.

2.2.7.3 STRESS (STRAIN) MEASUREMENT

As noted earlier, stress concentrations due to retaining bands and local attachments on nozzles often result in tube failures. Stress of course is not measured directly, but is determined from strain measurement. Very small strain gages have been used to monitor strains in the fillet of the tube-to-band joint close to the maximum stress-concentration point. Strain gages have also been used to determine deflection of bands subject to external loads from accessories.

The nozzle designer is not involved in making any particular provisions for stress (strain) measurements. On the completed nozzle, strain gages are installed at designated stations by specialized trained personnel. The area of attachment is cleaned mechanically and chemically and wiped dry; the gage then is cemented on with epoxy or cyanoacrylic resin. Preferably, the strain gage is mounted on a flat surface that will not be exposed to elevated temperature. Small gages (< 0.030 in. in length) act like heaters, and require cooling by conduction. The gage is checked out electrically, and preset strain or resistance is read on a meter. Bonding to the metal is checked by observing the amount of drifting on the readout instrument. Measured strain values are converted to stress values by the stress analysts.

2.3 TESTING

Full-scale hot-firing tests of rocket components are used to isolate potential engine-system failures. The structural strength, cooling capacity, and performance of the nozzle are

checked by full-scale thrust-chamber firings. Full-scale static firing of the complete engine at altitudes near those of flight is the final demonstration of structural integrity and performance prior to actual flight of the vehicle. Model testing is used to verify the accuracy and applicability of analytical techniques and to study nozzle problems that cannot be solved accurately by analysis. Standard procedures for calculating rocket engine performance and recommendations for testing and data acquisition are presented in references 63 and 64.

2.3.1 Full-Scale Testing

2.3.1.1 GROUND TESTING

Ground testing of altitude engines has been the source of problems in several development programs. As shown in the following examples, early engine development programs underestimated the problems associated with flow separation.

The Nomad engine had an area ratio of 25 and a chamber pressure of 160 psi; it was predicted that during ground static test firing the nozzle would run "separated," but it was assumed that the flow separation would affect only performance and could easily be corrected. Actually the separated flow was unstable and asymmetric and caused large oscillatory loads on the thrust chamber. The test stand had to be strengthened to restrain the engine.

The J-2 engine has a large expansion area ratio (27 to 1), a slow pressure buildup during start, and an adverse pressure gradient in the nozzle. Very large unsteady side loads due to flow separation during both startup and steady-state operation caused nozzle structural failures (ref. 23). The nozzle structure was strengthened, but it was not practical to build a flightweight structure that could absorb the startup loads. As noted earlier, support arms were added from the test stand to the nozzle during start and detached remotely during the test run to allow gimbaling of the engine; in addition, a short bolt-on diffuser was attached to the nozzle to eliminate flow separation during mainstage operation.

Early tests of the Titan I stage II engine were conducted at sea-level conditions with ablative extensions from area ratio 6 to exit area ratio of 25. Separation occurred approximately 8 in. forward of the exit, resulting in a recirculation of atmospheric oxygen and severe erosion at the separation plane. A clam-shell "corset" was placed about the throat and combustion chamber during these tests to provide the additional support required because of the separation loads.

2.3.1.2 PERFORMANCE EVALUATION

To evaluate nozzle performance, the stagnation pressure downstream of the plane where combustion is essentially complete must be accurately known. Static-pressure measurements

at the injector face, corrected for heat addition (Rayleigh flow), can be used to calculate the stagnation pressure at the nozzle throat only under certain conditions such as liquid injection, efficient combustion, and uniform pressure distribution on the injector face. The method of measuring static pressures along the wall in the combustion chamber and correcting for the local gas velocity provides accurate nozzle stagnation pressures. Figure 37 shows the static-pressure distribution measured along a combustion-chamber wall (ref. 65). The rise in wall pressure upstream of the throat is produced by turning of the flow near the wall at the start of contraction.
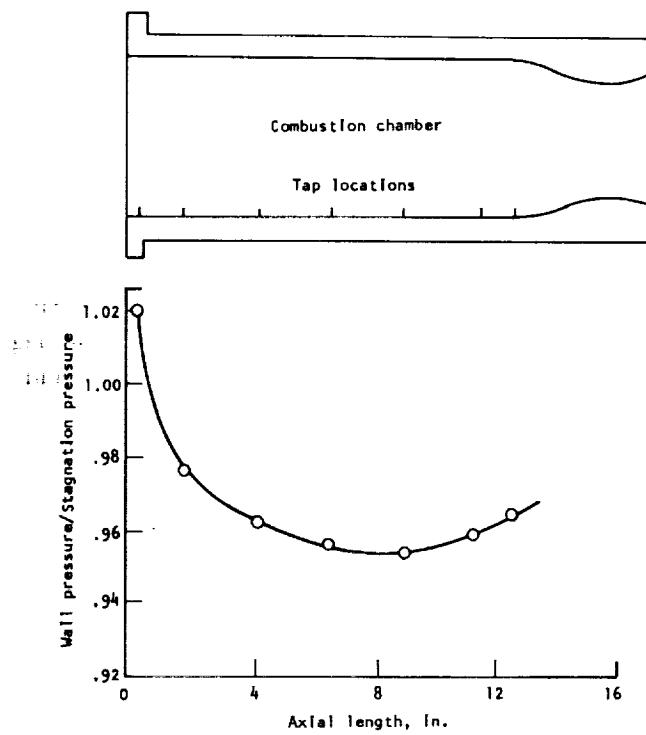
Figure 37. — Distribution of static pressure measured along combustion-chamber wall (ref. 65).

2.3.2 Model Testing

The accuracy of nozzle efficiencies obtained from model tests is directly proportional to the accuracy of the measurements of thrust, total pressure, and flowrate. Since nozzle-efficiency differences of 0.2% generally are considered significant, great care must be taken to obtain

62

the required accuracy in measuring these parameters. Model size must be large so that errors in wall shape are minimized. When only a portion of the nozzle is being studied, near-full-size cold-flow studies often are possible.

An important limitation of cold-flow testing is the large difference between the expansion characteristics of typical hot-firing exhaust products and typical cold-flow gases. Most exhaust gases have a specific heat ratio γ of 1.1 to 1.3; most cold-flow tests are conducted with air, which has a γ of 1.4. Gases with lower γ values that are inexpensive, incombustible, nontoxic, and noncondensing during expansion are not known. Tetrafluoromethane (CF_4) has been used for cold-flow testing because of its low γ ($\gamma = 1.2$); however, losses of up to 3 percent due to nonequilibrium expansion have been observed in model testing with CF_4. A complicated analysis is required to account for the nonequilibrium expansion loss.

An accurate method for scaling from cold-flow results at $\gamma = 1.4$ to hot-firing conditions does not exist. The most satisfactory method is to use cold-flow results to develop and verify a calculation technique, then use the calculation procedure to predict hot-firing results.

A frequent problem in cold-flow testing is condensation of the gas during the expansion process (ref. 66). Room-temperature air condenses at an expansion ratio of about 14 with a total pressure of 100 psi. The expansion ratio at which condensation begins can be increased by decreasing the total pressure; however, total pressures of less than 50 psi generally are not practical because, as total pressure is decreased, the magnitudes of forces, flowrates, and pressures that must be measured decrease proportionally. Condensation can best be detected by comparing the measured wall-pressure/total-pressure profile at several total pressures with calculated values. When condensation occurs, the actual wall pressure will deviate from the predicted curve, becoming higher than predicted (fig. 38).

Optical methods are particularly suited to cold-flow testing; however, most of the data taken are only qualitative. Quantitative data can be obtained with interferometry, but the sensitivity and expense of the system eliminates it for most facilities. Shadowgraphs provide limited information. Most optical measurements of nozzle flowfields are made with schlieren systems. Very short exposure times are required to obtain sharp definition. A high-intensity short-duration light source such as an electrical-discharge spark gives good results.

63
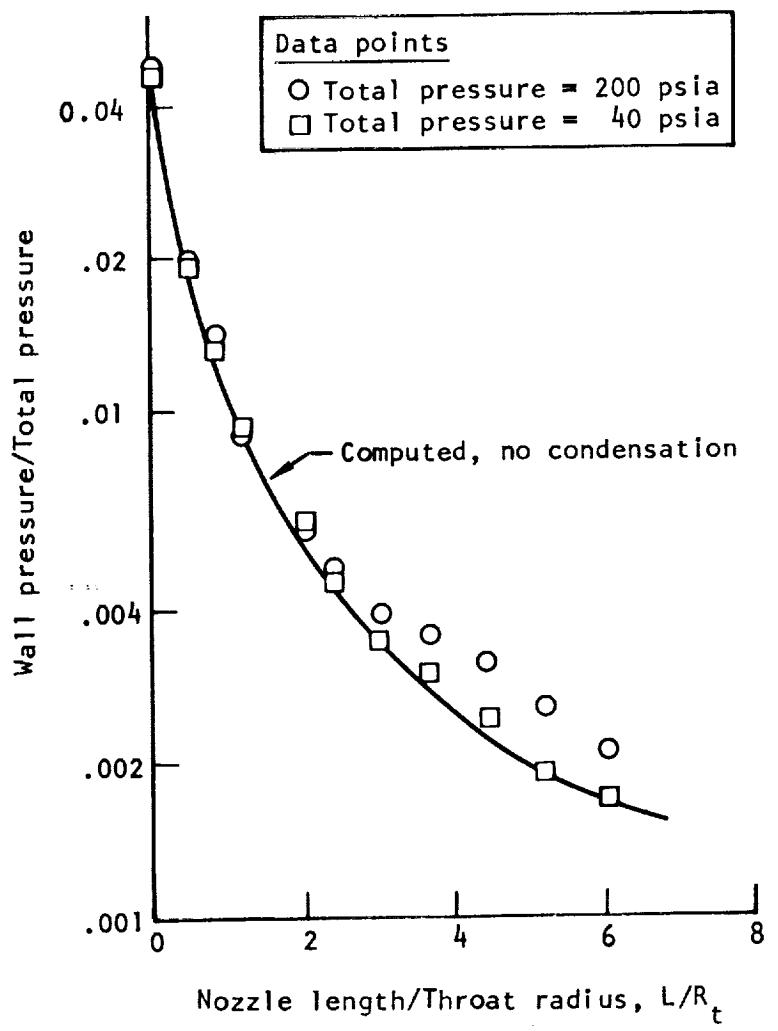
Figure 38. — Calculated and observed values for wall pressure/total pressure
as a function of L/R_t.

3. DESIGN CRITERIA and

Recommended Practices

3.1 NOZZLE CONFIGURATION

3.1.1 Throat Geometry

3.1.1.1 UPSTREAM WALL

The throat upstream-wall geometry shall be based on a trade of length against performance and shall minimize the wall surface area in the region of maximum heat load.

Bell nozzles should have a constant-radius arc for the upstream walls, the ratio of wall radius to throat radius being kept greater than 0.6. To obtain the best compromise of nozzle efficiency and throat surface area exposed to gas conditions near Mach 1, maintain the upstream-wall radius ratio at about 1.0.

Annular nozzles should have a constant-radius upstream wall, with the inner wall radius equal to the outer wall radius, which is equal to the throat gap. When the two wall radii are not equal, make the smaller radius either equal to the product of throat gap and the ratio of the larger radius to the smaller radius, or three times the throat gap, whichever value is less. Avoid geometries with one wall concave to the flow upstream of the throat.

Use a reference-streamline series-form transonic solution (e.g., ref. 4) or the method of reference 5 to obtain a line along which supersonic flow properties are known for the selected transonic geometry; this line then serves as a starting line for the nozzle design or flow analysis. Employ a 29-term series for the commonly used radius ratio of 1.5. Increase the number of terms for small approach radii to obtain a close fit to the desired wall geometry. Use a constant specific heat for the calculation of the transonic solution for typical rocket nozzle designs.

3.1.1.2 DOWNSTREAM WALL

The throat downstream-wall geometry shall minimize the overall nozzle length, but shall provide an expansion rate low enough to minimize losses due to chemical nonequilibrium.

Use a constant-radius-arc transition between the throat and contoured wall. When nonequillibrium losses are not a consideration, the radius should be the smallest that can be economically fabricated. For tube-wall nozzles, the minimum tube-bend radius should be twice the tube outside diameter for round tubes of stainless steel, nickel, or copper.

65

When nonequilibrium losses must be considered, select the downstream transonic wall geometry in conjunction with the supersonic wall contour design, using the procedure described in section 3.1.2.1.1.2.

3.1.2 Expansion Geometry

3.1.2.1 BELL NOZZLE

3.1.2.1.1 Optimum Contour

3.1.2.1.1.1 Equilibrium Flow

For equilibrium flow, the expansion geometry shall provide maximum nozzle performance for the given flowrate, combustion products, and envelope.

For bell nozzles (equilibrium flow), select the transonic wall geometry and solve the transonic flowfield. On the basis of a starting line from the transonic solution, the selected downstream transonic wall, and equilibrium gas properties, compute the flowfield from the starting line to the end of the downstream transonic wall; design the remaining wall to a selected length and exit area, employing a bell-nozzle design program based on reference 14 or 16. Consult reference 67 (Appendix A) or reference 68 for a list of available programs.

3.1.2.1.1.2 Nonequilibrium Flow

When performance losses due to nonequilibrium effects in the throat region are significant, the geometry from the throat to an area ratio of approximately 3 shall control the initial expansion to maintain composition near equilibrium.

Select several wall geometries just downstream of the throat, and compute the flowfield to the end of the controlled-expansion section. On the basis of the flow properties at the end of the controlled-expansion region as a starting line, design the remainder of the wall with a bell-nozzle design program for equilibrium flow.

Use simple wall geometries for the controlled-expansion wall: circular arcs with large radii when the expansion is controlled to area ratios of less than 3, and combinations of circular arcs and straight segments to control expansion to area ratios greater than 3. For all but extreme cases, very small gains in performance can be obtained with more complex shapes, and the added freedom introduced in the contour selection complicates the design problem unnecessarily.

66

3.1.2.1.2 Nonoptimum Contour

When performance losses of the order of 0.25 percent are tolerable or when rigorous optimization methods do not exist. The expansion geometry shall be a simple curve that provides the best performance.

For the first condition, a canted-parabola contour as shown in figure 5(a) is recommended for the expansion wall. For conditions where rigorous optimization methods do not exist (e.g., short nozzles with high area ratio), the truncated ideal nozzle of reference 14 or a parabolic wall contour is recommended. From the extrapolated region of figure 5(b), get a trial estimate of the initial and final wall angles for the parabolic contour. To maximize performance, vary the trial angles and compute the efficiency of each configuration.

Design three-dimensional nozzles by computing the performance of a set of shapes and selecting the nozzle with highest performance. A good first attempt is an equilibrium optimum plane-flow or axisymmetric contour that approximates the three-dimensional shape.

3.1.2.1.3 Overexpanded Nozzle

Whenever possible, the contour of the nozzle for an altitude engine that must be ground tested at overexpansion pressure ratios shall not lead to separated flow.

Design an optimum nozzle contour (ref. 14) and check for flow separation (fig. 39). If the
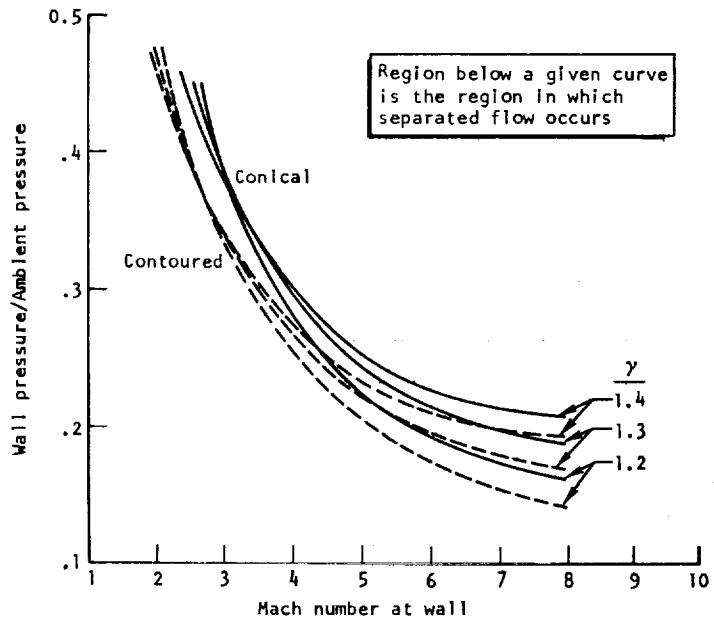
Figure 39. — Mach number vs pressure ratio for separated flow for three specific-heat ratios (ref. 25).

67

exit wall pressure is within 20 percent of the separation pressure, reduce the expansion ratio or select a nonseparating, nonoptimum contour. Predictions of separated flow should be regarded as development guides only. Verify marginal nozzles by full-scale operation.

To select a nonoptimum contour for overexpanded operation, generate a series of parabolic contours and compute the flowfield of each. Examine the pressure profile from throat to exit. Look for regions of increasing pressure towards the exit. A desirable contour will always provide a continuously decreasing wall pressure. Therefore, if the wall pressure does not continuously decrease, change the nozzle contour to a parabola with a smaller initial wall angle or a larger exit wall angle. Select a contour that raises the exit-wall pressure above the separation value, provides a continuously decreasing wall pressure, and produces acceptable performance.

Consult section 3.3.1.1 for recommendations on testing nozzles with separated flow.

3.1.2.1.4 Nozzle Extension

A nozzle extension shall be a simple geometric shape that provides near-maximum performance for the nozzle plus extension.

When adding a short extension to an existing nozzle with area ratio in the range 10 to 20, use a straight wall from the end of the nozzle to the selected end point. Select several extension angles and compute the performance of each extended nozzle within the available space envelope. Select the final configuration on the basis of a performance/weight tradeoff.

When the existing nozzle area ratio is less than 10 or when long extensions are added, use contoured extensions such as the canted parabola or optimized extension-wall contours.

3.1.2.1.5 Small Nozzle

3.1.2.1.5.1 Geometry

The throat wall geometry of a small nozzle shall limit boundary-layer buildup, and the nozzle shall have a simple shape that facilitates fabrication.

For nozzles with throat Reynolds numbers less than 1×10^4, keep values for R_u/R_t less than 2 when a high discharge coefficient is desired. See figure 8 for discharge coefficient versus radius ratio for small nozzles.

68

Convergent and divergent sections should be straight-walled, with wall angles of 25° to 45°. Keep the expansion area ratio low.

3.1.2.1.5.2 Flow Analysis

Methods for flow analysis of small nozzles shall include viscous effects in the generation of the core.

Analyze the flow by a method similar to that of reference 30, which includes viscous effects in the supersonic-core solution. Do not employ an inviscid-core solution corrected by a boundary-layer perturbation.

3.1.2.2 PLUG NOZZLE

The plug-nozzle configuration shall maximize nozzle performance including the thrust from the base.

For gas-generator engine cycles, use truncated ideal nozzles with base bleed. For topping cycles, regeneratively cool the base plate without base bleed, or bleed the minimum fuel required to cool the base.

Shrouded nozzles are recommended for area ratios higher than 40 and thrust levels less than 1×10^6 lbf; for other conditions, select the nozzle configuration on the basis of a rough layout that compares the shrouded and unshrouded nozzles. For very large engines, use an unshrouded nozzle with an injector that is made up of a number of segments.

With a shrouded nozzle, use an up-pass cooling circuit to obtain the high rate of curvature at the throat that will result in a high rate of heat transfer to the coolant.

3.1.2.2.1 Base Design

3.1.2.2.1.1 Performance

The base design shall provide maximum base thrust from the gas bleed available.

With a deep-cavity base, introduce the bleed gas radially inward or outward at low velocity; with a porous base plate, inject the secondary gas through the plate.

69

Scale the results of cold-flow model tests (ref. 32) to predict base pressures for truncated ideal nozzles. Use theoretical base-pressure methods (refs. 33 and 34) for other annular-nozzle configurations or for examining the effects of exit flowfield on base pressure.

3.1.2.2.1.2 Packaging

The base design shall provide room for engine components.

In most cases the best engine package can be obtained with a porous-plate base cover near the nozzle end, the base cavity then being left available for major engine components (e.g., turbomachinery).

3.1.2.2.1.3 Cooling

The base bleed shall cool the base region.

Distribute the bleed gases evenly or bias the distribution to introduce most of the gas in the outer perimeter of the base. Either of these distributions will tend to shield the base from the high stagnation temperature of the primary exhaust gases and produce high base performance. Base heating rates can be predicted only approximately and must be verified experimentally.

3.1.2.2.2 Overexpanded Nozzle

The contour of a plug nozzle for booster application shall minimize the effect of shocks impinging on the wall of the nozzle during recompression.

Use contours of the truncated ideal nozzle to minimize the strength of shocks incident on the wall during low-altitude operation. If incident shocks are expected (e.g., when nonideal contours are used), analyze the nozzle flowfield to determine if boundary-layer separation occurs. Design the cooling circuit in the separated-flow area to handle heat flux from separated flow.

3.1.3 Nozzle Contour Tolerances

The tolerances on nozzle contours shall ensure that a nozzle falling within tolerance limits will produce the required thrust and thrust-vector alignment.

For bell nozzles, set a tolerance on the average throat diameter such that a nozzle within tolerance provides throat areas consistent with the thrust requirements and allowable

70

chamber pressure. Set the tolerance on the circumferential variation in throat diameter to limit the throat configuration so that the thrust vector is within the gimbal adjustment range. For annular nozzles, regulate the throat-area variation by tolerances on the mean throat gap and mean distance from the nozzle axis to throat gap. Control throat-gap variation by specifying a tolerance on the mean throat gap and a tolerance on the gap deviation from nominal.

Establish tolerances that limit wall angles downstream of the throat to $\pm 1°$ of the design contour for the first $10°$ of overturning and $\pm 2°$ for the rest of the nozzle.

3.2 NOZZLE STRUCTURE

3.2.1 Regeneratively Cooled Nozzles and Extensions

3.2.1.1 INTERMITTENT RETAINING BANDS

3.2.1.1.1 Structural Adequacy

Retaining bands shall accept all nozzle hoop loads.

Shape and size the retaining bands for start-transient, overexpansion, and gimbal loads. Do not require the tube bundle to withstand any loads from exhaust gas or mechanical forces.

Make the bands rigid rather than flexible.
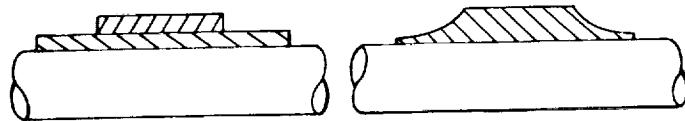
Calculate structural-dynamics characteristics by the structural-analysis methods of references 37 and 69.

Instrument the tubes and retainer bands at the areas that will be subject to high stress during operation.
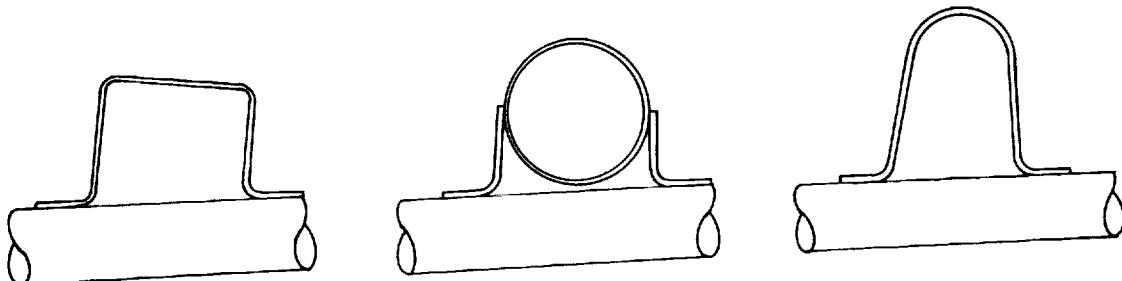
3.2.1.1.2 Tube-Bundle Rigidity

Retaining bands shall provide rigidity to the tube bundle.

Use simple flat-band designs such as those in figure 40(a) for configurations with low buckle-resistance requirements, and more rigid designs such as those of figure 40(b) for configurations with high buckle-resistance requirements. Within a given nozzle, in most cases, bands of the (a) type are adequate for regions near the throat, whereas bands of the (b) type often are required near the exit.

71

(a) Low buckling resistance

(b) High buckling resistance

Figure 40. — Recommended designs for retaining bands to provide desired degree of tube-bundle rigidity.

3.2.1.1.3 Tube Support

Each retaining band shall provide support in the radial direction for each tube.

Maintain minimum braze gaps between tube and band consistent with the braze alloy.

Do not force bands against tubes by local external loads (fig. 15(d)), interference with an external manifold (fig. 15(e)), or an inconsistent band angle (fig. 15(c)).

Fill in excess gaps in the tube-to-band fit with shims as shown in figure 15(f).

Do not place a band over or next to a sudden change in tube shape or a tube discontinuity.

Use a thin band section at the edge of the band as in figure 40(a) rather than a thick section.

3.2.1.2 TUBE SPLICE JOINTS

Tubes shall not be subject to increased wall temperature and leakage at splice joints.

72

Whenever possible, coolant tubes should be single continuous units without splice joints. To allow a high taper ratio, specify a high-ductility tube material such as 347 CRES or nickel.

If a splice must be made, use a one-and-a-half pass or similar construction to increase the number of tubes in the aft end of the nozzle. Contour the splice smoothly.

Avoid stress concentrations on the tube crown by using a secondary tube with a straight hot side as shown in figure 41(b) rather than one with a joggle in the hot side as in figure 41(a). Do not form small-radius bends or breaks in the tube.

(a) Tube with joggle on hot-gas side

(b) Tube with joggle removed from hot-gas side
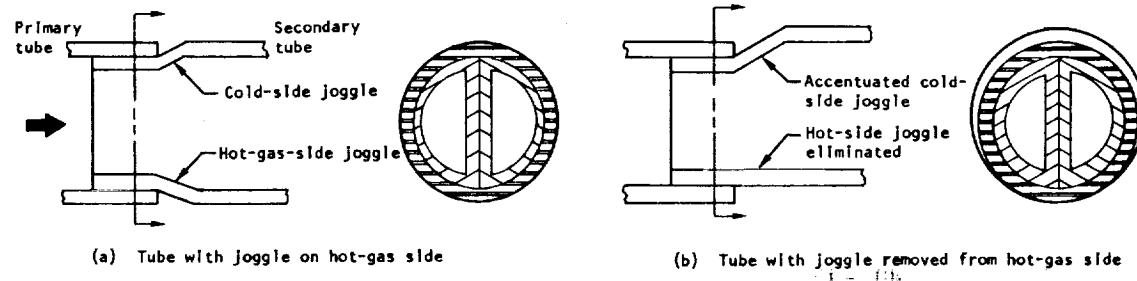
Figure 41. — Recommended design for avoiding coolant-tube joggle on hot-gas side of tube.

For tubes with diameters greater than 0.5 in., the "D" joint of figure 16(b) is recommended over the rectangular joint of figure 16(a).

3.2.2 Film-Cooled Extensions

3.2.2.1 SLOTS

The extension shall provide for thermal growth without distortion of the slot.

A design such as that of figure 42 will accommodate thermally induced growth. Avoid designs that restrict thermal growth and produce permanent deformation.

For the shingles and body, employ ductile materials such as Inconel 625, Hastelloy C, or 347 CRES.

Avoid large steps in the wall contour at the skirt attachment point. If there is a large separation between gas streams, then mainstream detachment and reattachment,

73
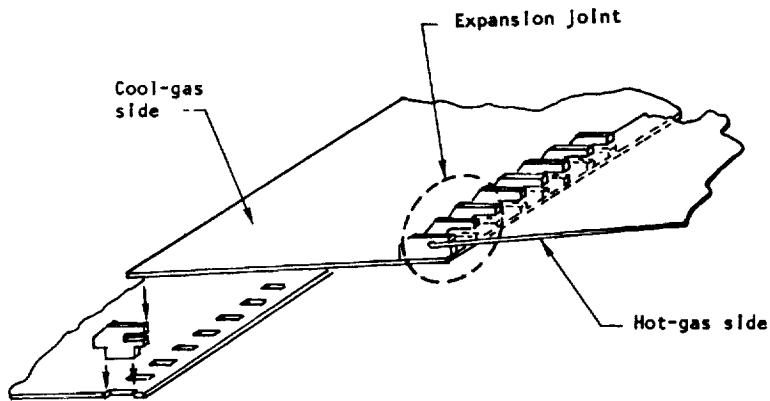
Figure 42. — Recommended joint configuration to allow for shingle expansion in film-cooled nozzle extension without distortion of the slot.

accompanied by increased local heating, occur. Provide additional film cooling at the attachment point. Determine the amount of film required experimentally, using full-scale hardware. Calculate film-cooling effectiveness by the methods of references 38 through 40; modify the results as necessary by the methods of references 41, 42, 43, and 70.

3.2.2.2 ATTACHMENT-AREA GEOMETRY

The geometry of the attachment area shall produce minimum mixing of the main supersonic gas stream and the gas film coolant.

Maximize the coolant injection velocity, minimize the gas-stream separation distance, and inject parallel to the main gas stream, with a geometry such as that shown in figure 43.

3.2.2.3 EXTENSION STRUCTURE

3.2.2.3.1 Inner Supports/Coolant Distribution

Internal structure-reinforcing members shall not lead to uneven coolant distribution.

Punch holes in the center of the vertical leg of each member, as shown in figure 19. Make the hole diameter equal to about 2/3 of the Z height, and space the holes about one
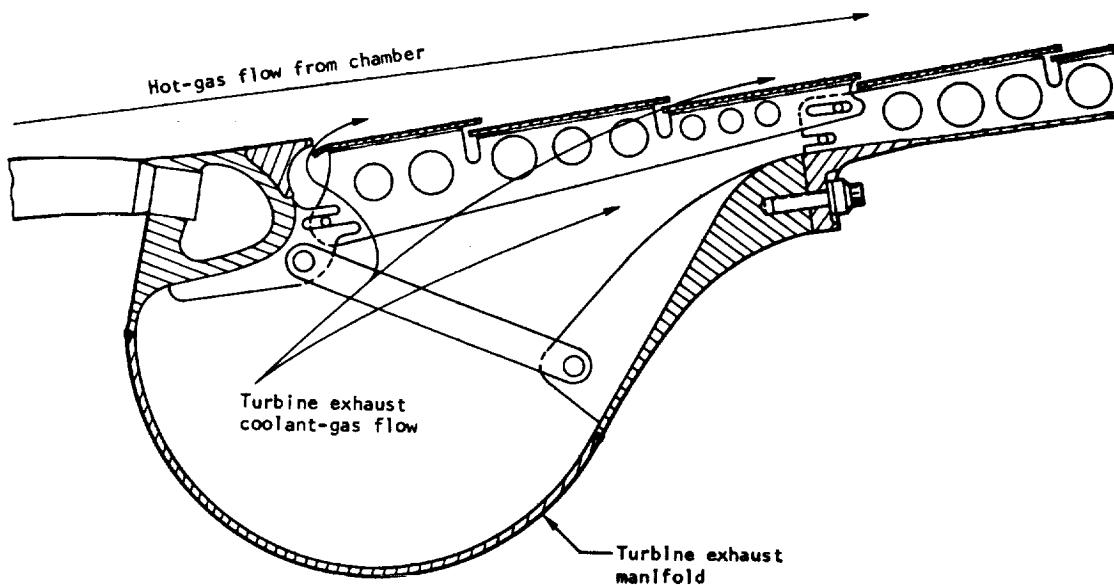
Figure 43. — Recommended attachment-area geometry for minimum mixing of chamber gas and coolant gases in a film-cooled extension.

diameter apart to minimize the resistance to circumferential flow without greatly reducing the rigidity of the structure.

3.2.2.3.2 Attachment of Inner Supports

The attachment of inner support members to the inner wall shall minimize the disturbance to the hot-gas boundary layer.

Attach the support members with spot or seal welds; grind the welds nearly flush with the parent metal.

3.2.2.3.3 Structural Stiffness

The extension shall not be subject to excessive flexing.

The recommended designs for retaining bands are shown in figure 40; construct the aft retaining band as shown in figure 44. Overdesign aft retaining bands by 50 percent during

the initial design to allow for the uncertainties of the start-transient loads.

Put insulation under the bands and scallop the band edges (fig. 21) to reduce band temperature if necessary.

Space the nozzle bands to limit rippling of the hot gas wall and avoid disruption of the hot-gas boundary layer (fig. 22). See section 3.2.1.1 for recommended procedures for design of retaining bands.
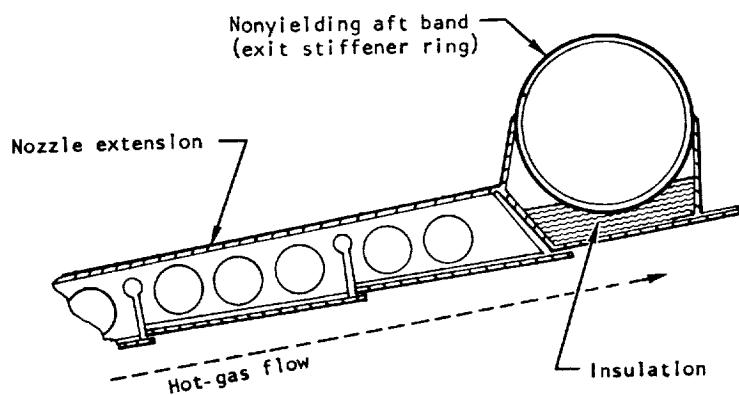
Figure 44. — Recommended construction of a nonyielding aft retaining band.

3.2.3 Ablation-Cooled Extensions

3.2.3.1 EXTENSION/NOZZLE JOINT

The extension attachment shall withstand all operating loads and shall not be subjected to high-temperature environments.

Design the extension joint so that all handling, ground, flight, and thermal loads are carried through the external structure (honeycomb or simple glass wrap) and not through the ablative liner.

Use a positive interlocking attachment technique as shown in figure 23 with a long heat-conduction path to the submerged mounting flange.

3.2.3.2 HONEYCOMB SUPPORT STRUCTURE

Honeycomb structures shall not be subject to overpressures from gas evolution.

Interconnect all honeycomb channels through drilled passages leading to the atmosphere.

3.2.4 Radiation-Cooled Extensions

3.2.4.1 TEMPERATURE CONTROL

Radiation-cooled extensions shall not be subject to failure induced by local overheating.

Employ an injector that provides a fuel-rich boundary layer and minimum streaking.

Provide a smooth transition between the nozzle and the extension. To obtain high emissivity, oxidize and roughen the outer wall surface, or use an emissivity coating.

3.2.4.2 MATERIAL COMPATIBILITY

The material in radiation-cooled extensions shall be compatible with the combustion gases.

For operation below 2000°F, specify metals that do not react rapidly with the combustion gases (e.g., L-605, N-155, or titanium alloy AMS 4917).

For operation above 2000°F, employ protectively coated refractory liners (e.g., NAA-85 on columbium C-103).

3.2.4.3 NOZZLE/EXTENSION JOINT

The nozzle/extension joint shall be nonyielding and provide for thermal growth.

Use closely spaced high-temperature clamping bolts such as those fabricated from Rene 41.

Make the heat-conduction path long enough to maintain the joint temperature below the limit for elastomeric seals.

Pressure-assisted seals such as Naflex or K seals should be utilized in flight hardware if elastomeric seals will not work. Consult reference 48 for specific design practices. Use

simple asbestos or elastomeric seals for heavy-duty development hardware that does not reach high temperatures during the test.

In low-thrust rocket chambers, with a nozzle extension joint up to 4 in. in diameter, prevent axial movement by using buttress threads in a threaded collar that has segmented fingers to absorb thermal deflections without yielding.

Do not subject flight-type joints to side loads induced by sea-level testing of a nozzle extension.

3.2.5 Circumferential Manifolds

3.2.5.1 MANIFOLD HYDRAULICS

Manifolds shall maintain a uniform static pressure that provides uniform flow through the manifold bleedoff ports.

Keep the fluid velocities in the manifold as low as possible, preferably less than 60 fps for liquids and less than Mach 0.25 for gases.

Incorporate several tangential inlets or multiple low-velocity radial inlets (fig. 24) in the manifold design.

For a single-inlet configuration, a tapered manifold and a tangential inlet (fig. 25) is recommended. Tapering the manifold increases the cost since the fabrication becomes more difficult. When only a few units are made, a circular torus in which the cross section is made to vary by boring the inner walls off center will accomplish approximately the same result.

If a single radial inlet is used, a tapered manifold with splitter vanes or deflector plates is recommended. Do not use a single radial inlet for high-velocity fluid without making provisions for reducing the static-pressure variation in the vicinity of the inlet.

For a given design, calculate as closely as possible the local pressure and velocity fields within the manifold and the resulting bleed-port flowrates, using available information and techniques such as those in references 53 and 54. Then measure the actual bleed-port flowrates with either cold-flow mockups or actual hardware.

Avoid the requirement for a flow splitter by reducing the incoming velocity head. In the final stagnation region, increase the flow resistance in or downstream of the bleedoff ports.

78

3.2.5.2 VANES, SPLITTERS, DAMS, AND STRUCTURAL SUPPORTS

3.2.5.2.1 Turning Vanes

Turning vanes shall minimize maldistribution of manifold pressure.

Design turning vanes by the method of reference 49. Experimentally verify the manifold pressure profile over the range of operating conditions. Provide for easy replacement, repositioning, and recontouring of turning vanes.

Large manifolds should have provisions for minimizing pressure variations around the manifold without moving the turning vanes. Install easily removable plugs in auxiliary turning vanes (fig. 27). Measure the manifold pressure distribution with various combinations of the plugs removed to obtain the configuration with minimum pressure gradient. Provide for the ports in the structural design of the manifold.

3.2.5.2.2 Flow Splitters

Flow splitters shall provide an equal division of flow in manifolds with nonsymmetrical inlet conditions.

The flow splitter is basically a fix for an existing design that for various reasons cannot be redesigned. In any new design, avoid the need for a flow splitter by using a symmetrical entrance for the manifold or by reducing the incoming velocity head.

If a flow splitter must be used, experimentally determine the size, shape, and location of the splitter that provides equal distribution of flow. Measure the pressure in each branch of the manifold downstream of the splitter, and obtain the pressure profile across the entire operating range. Adjust the flow splitter until the desired flow split is achieved.

3.2.5.2.3 Dams

Full or partial dams shall minimize variations in manifold cross velocity.

Insert a partial or a full dam near the stagnation point opposite the manifold inlet, or insert dams between multiple inlet locations.

3.2.5.2.4 Structural Supports

Structural supports for manifolds shall prevent structural failure of the manifold, but shall not result in flow maldistribution that leads to performance loss, combustion instability, or wall overheating.

External supports or heavier walls are recommended over internal supports whenever possible. Use integral vanes, splitters, dams, and structural ties whenever possible.

For welded-in turning vanes and splitters, the butt weld is first choice when it can be used, and next the full-penetration fillet weld. Avoid the fillet weld except under light loading and low vibration. Examples of these welds are given in figure 30.

For welded-in-dams, use the joints of figures 32(a), (b), and (c) for designs that are internally accessible and the joints of figures 32(d) and (e) for designs that are internally inaccessible. The fillet weld should be avoided, except possibly for very light loading and low-vibration conditions.

Avoid large unsupported sections, particularly flat ones. If such sections must be used, incorporate flutter dampeners as shown in figure 31.

3.2.5.3 HOT-GAS MANIFOLD

3.2.5.3.1 Manifold Outlet

The system for introducing the turbine exhaust gas into the nozzle shall minimize the disturbance to the main jet.

Introduce the turbine gas into the nozzle through gaps in the nozzle wall (e.g., fig. 45(a)) or parallel to the mainjet through an annulus at the nozzle exit (fig. 45(b)), or use a film-cooled extension.
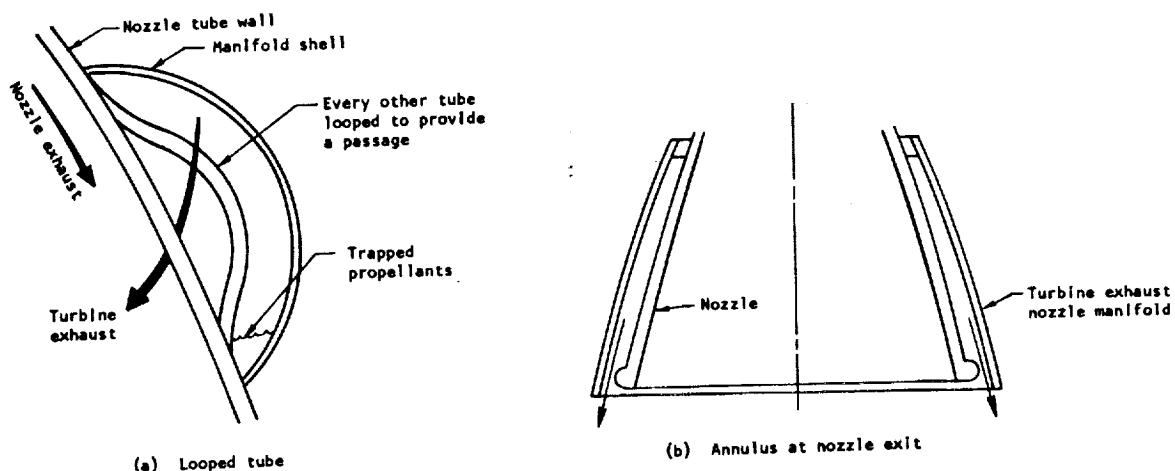
Figure 45. — Two methods recommended for introducing turbine exhaust gas into nozzle.

80

3.2.5.3.2 Manifold Drainage

Turbine exhaust manifolds for noncryogenic propellants shall not trap propellants.

Do not use a turbine exhaust manifold and tube-wall configuration such as that in figure 45(a) for noncryogenic propellants. Use the exit dump method (fig. 45(b)), or a film-cooled extension.

3.2.5.3.3 Thermal Growth

Hot-gas manifolds and associated joints shall allow for thermal expansion.

Use sliding-pin, A-frame, or other designs that allow unrestrained thermal expansion of the heated portion of the manifold.

Absorb thermal deflections in bending in relatively flexible members such as the flame shield in figure 33 or the baseplate in figure 46.
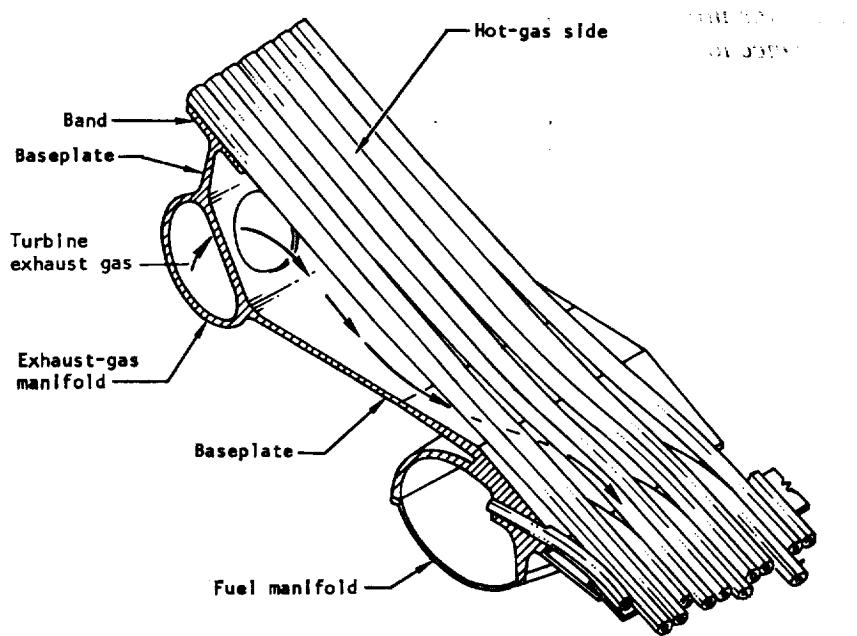
Figure 46. — Manifold design for absorbing thermal deflections in flexible baseplate.

Distribute the thermal loading at highly stressed points with doublers or similar devices.

Specify ductile materials (e.g., 347 CRES, Hastelloy C, Inconel 625, or L-605) with an elongation of 20 percent or more across the operating temperature range.

Allow larger-than-normal clearances between tubes or bands and the manifold structure to account for shrinkage from multiple welding, thermal distortion during brazing or operation, and difficulty in fitting together large flexible ducts.

3.2.5.3.4 Manifold Seals

Seals for hot-gas manifolds shall provide for flange warpage from thermal and mechanical loads.

Self-energizing pressure-actuated seals are recommended for hot-gas manifolds.

3.2.5.4 COOLANT-RETURN MANIFOLD

3.2.5.4.1 Drainage

The coolant-return manifold shall be easily drained and cleaned.

Use a continuous coolant-return manifold rather than individual tube elbows. Install drain plugs so that the manifold can be drained with the engine upright or horizontal.

3.2.5.4.2 Tube-to-Manifold Joint

3.2.5.4.2.1 Tube Ends and Manifold Openings

Tube ends shall conform closely to the manifold opening to which they are to be mated.

Insert circular tubes into round holes in the manifold (fig. 34(b)) rather than square tubes into a slot (fig. 34(a)). Expand the tube end while it is in place within the manifold.

Ensure that the brazing characteristics of the plating material are compatible with the tube and manifold materials. Tube and manifold materials should have similar brazing characteristics and expansion coefficients; preferably both tubes and manifolds should be constructed of the same material.

Include a braze sample during production furnace brazing to verify the resulting material properties.

82

Use furnace brazing in preference to hand brazing of tube bundles.

3.2.5.4.2.2 Braze Joint

The braze joint between the manifolds and tubes on the hot-gas side shall provide a continuous conduction path between the hot wall and the coolant.

Maintain the recommended braze joint for the full length of the joint on the hot gas side. This practice will preclude breaks in the connection between the hot wall and the coolant tube as shown in figure 35.

Remove manifolds from direct contact with the exhaust gas (fig. 47) to reduce the heat-transfer rate at the braze joint, thereby eliminating the criticality of obtaining a continuous braze.

(a) Manifold exposed to direct flow of hot gas

(b) Manifold removed from contact with direct flow of hot gas
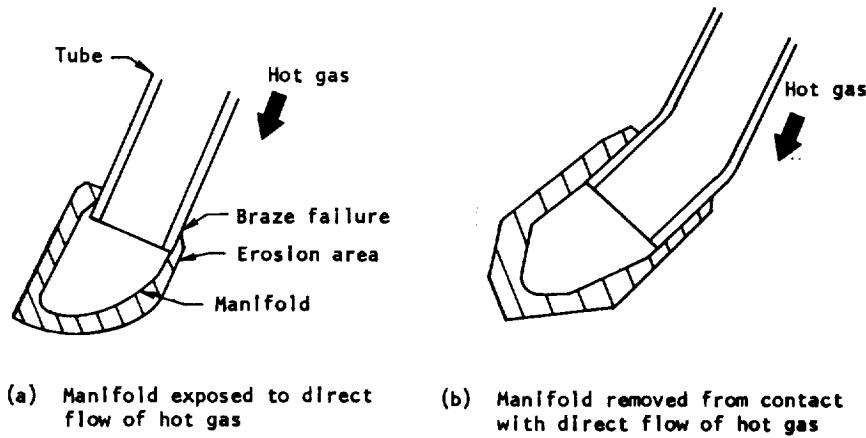
Figure 47. — Method for avoiding failure of manifold from exposure to hot-gas flow.

3.2.6 Nozzle Attachments

3.2.6.1 ATTACHMENT TECHNIQUES

The method for making attachments to the nozzle shall distribute the loads to the tubes and preclude local stress concentrations.

Connect attachments to nozzle structural members (e.g., manifolds or retaining bands) rather than directly to the tubes.

83

If attachments must be made directly to the tubes, braze them; do not weld attachments to thin-wall tubes. The configurations shown in figure 48(a), not those of figure 48(b), are recommended for brazing attachments to tubes. Note that the recommended method is to braze only one side.

(a) Good - attachment configuration and brazing on one side produce acceptable stresses on tubes

(b) Bad - attachment configuration and brazing on both sides produce high local stresses on tubes
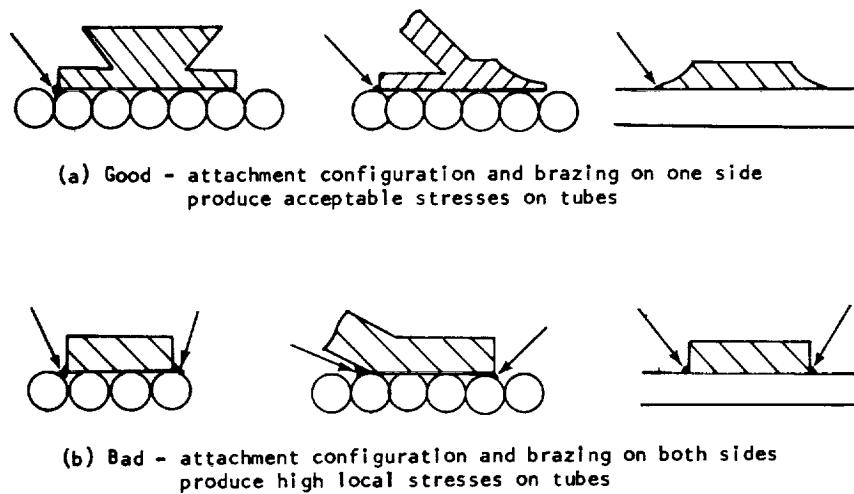
Figure 48. — Good and bad methods for brazing attachments to tubes.

3.2.6.1.1 Welding

Weldments to thin nozzle structural parts shall not induce distortion and internal stresses.

For structural members that are hardened during the furnace braze cycle, weld the attachments to the structural members before furnace brazing.

3.2.6.2 EXTENSION JOINT FOR LARGE CHAMBERS

The nozzle/nozzle-extension joint for large thrust chambers shall be sealable, assemblable, and lightweight.

Design to keep differential expansion within limits. Design the flanges with oversized bolt holes and radial bolt slots on one or both flanges. Use alignment tools in assembling the configuration.

Make the flange bolt spacing equal to the bolt-head diameter plus twice the flange thickness.

84

Use elastomeric seals up to 500°F. Use tadpole-type asbestos-and-wire mesh seals above 500°F and groove one flange face (fig. 36).

3.2.7 Instrumentation Provisions

3.2.7.1 TEMPERATURE MEASUREMENT

3.2.7.1.1 Thermocouples

3.2.7.1.1.1 Installation

Nozzle tube bundles shall provide for the installation of thermocouples at required stations.

Before stacking the chamber tubes, predimple the tube next to the tube on which the thermocouple is to be installed. Place Refrasil cords in the dimples during furnace brazing. See reference 71 for detailed recommendations.

For thermocouples positioned near the nozzle exit, run the thermocouple along the tube crevice from the nozzle exit (fig. 49).
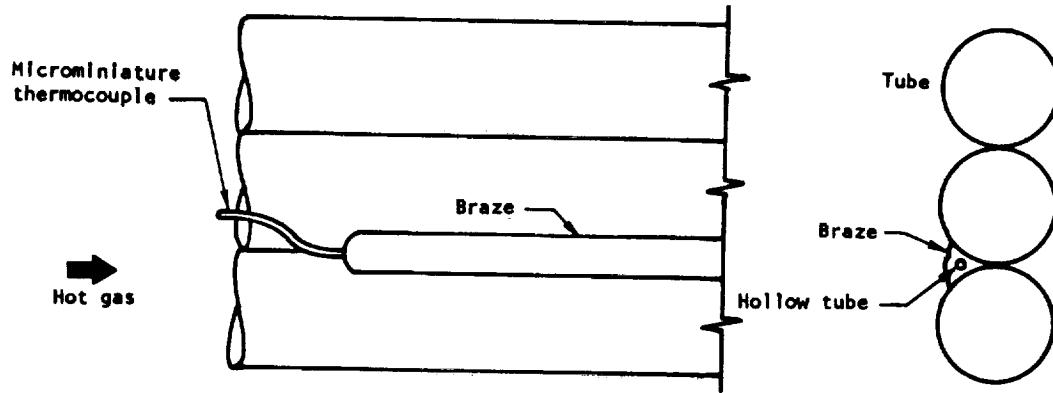
Figure 49. — Method for mounting thermocouple near nozzle exit.

85

Avoid inserting thermocouples between tubes in already brazed thrust chambers. If a thermocouple must pierce an already brazed tubular thrust chamber, use a heated tungsten probe to melt the tube-to-tube braze and produce a local tube-wall indentation on the tube next to the tube on which the thermocouple is to be installed. See reference 52 for detailed installation recommendations.

Braze the thermocouple to the tube crown with a miniature argon-plasma arc torch. During installation of the thermocouple, monitor temperature with the thermocouple itself.

3.2.7.1.1.2 Thermocouple Type

Thermocouples installed on tube hot walls shall withstand installation, handling, and operation without damage.

A damage-resistant thermocouple assembly such as the armored microminiature design (ref. 72) is recommended. With the flattened-tip thermocouple, use annealed thermocouples. Tack weld the tip of the thermocouple to the tube crown. Braze the thermocouple to the tube at an angle and fill the dimple and cover the exposed thermocouple sheath with braze material by means of a miniature argon-plasma arc torch. Consult reference 52 for detailed recommendations or reference 59 for the NASA electroplating technique.

Avoid thermocouple installations that project from the thrust-chamber outer surface significantly, or installations that have sufficient mass to be prone to vibration damage.

3.2.7.1.2 Braze Patches

Braze patches used as temperature indicators shall show whether a specific temperature limit is exceeded.

Braze patches must be compatible with the base tube material. Select the material for the required limiting temperature on the basis of remelt data in reference 60.

3.2.7.2 PRESSURE MEASUREMENT

3.2.7.2.1 Installation

Nozzle tube bundles shall provide for pressure taps at required stations.

Dimple the tubes at the designated points during tube forming process. Place ceramic rod or Refrasil cord in each dimple during brazing, so that the opening for the pressure tap is not filled by the braze.

3.2.7.2.2 Measurement

The pressure pickup shall provide accurate measurement of static pressure of the nozzle wall.

After furnace brazing of the tube assembly, insert a pressure-pickup tube into each dimple and braze in place. Make sure that the pressure tube does not project into the hot-gas stream. Use a short run from tap to recording device.

3.2.7.3 STRESS (STRAIN) MEASUREMENT

The stress-measurement materials and procedures shall provide accurate values for stress in the nozzle structure.

Select a strain gage that is appropriate for the application and is accurately calibrated. Use trained specialists and approved techniques for installation. Avoid placing a gage at a location exposed to elevated temperatures or steep temperature gradients. Protect the gage from exposure to moisture and from air currents that could change its temperature. Avoid small gages (< 0.030 in. in length).

For determination of stress concentrations, carefully select the areas that will be subject to maximum stress concentration. These places often are in the fillet of tube-to-band joints and at locations where attachments to the tubes have been made.

3.3 TESTING

3.3.1 Full-Scale Testing

3.3.1.1 GROUND TESTING

Upper-stage engines required to run at ground-level back pressures either shall not develop separated flow or shall be capable of absorbing the loads associated with unstable asymmetric flow separation.

For altitude engines, use bolt-on nozzle extensions that can be removed during ground testing to reduce the area ratio sufficiently to preclude separated flow. Provide restraining arms from the nozzle to the test stand to absorb startup side loads in high-area-ratio engines with slow thrust buildup. Make the arms remotely detachable after start to allow gimbaling. On the basis of the worst case of asymmetric separation, size the nozzle structure to resist collapse or being forced out of round.

87

Use a fast-start system for high-area-ratio nozzles.

Eliminate flow separation on marginal nozzles during mainstage by employing a short bolt-on diffuser.

Avoid nozzles with adverse wall-pressure gradients.

3.3.1.2 PERFORMANCE EVALUATION

Altitude performance extrapolated from ground-test data shall be based on results for which the extent of overexpansion is accurately known, and the pressure used for evaluating nozzle performance shall approximate the nozzle total pressure.

Compute altitude performance from ground-test results on nozzles with unseparated flow.

Use a static-pressure distribution along the combustion-chamber wall as shown in figure 37 to obtain the nozzle total pressure for hot-firing tests.

3.3.2 Model Testing

3.3.2.1 MODEL SIZE

The size of the cold-flow test model shall facilitate accurate fabrication and reliable measurements.

Make the models as large as possible to obtain close reproduction of the desired wall geometry. The chamber pressure should be high enough to allow accurate static-pressure measurements. The large model and high pressure will provide more accurate thrust and flowrate measurements.

3.3.2.2 PROPERTIES OF TEST GAS

The gas used for cold-flow tests shall not condense in the nozzle and shall simulate the average γ of the hot gas during expansion.

Use dry filtered air except for tests involving nozzles with very high area ratios. Exercise caution in interpreting performance data obtained with high-molecular-weight gases such as CF_4. Avoid CF_4 in nozzles with low total pressure or in small annular nozzles where nonequilibrium effects may be large.

88

When testing nozzles with air at area ratios greater than 15, total pressures should be low enough to reduce condensation of air in the nozzle. Detect condensation by measuring wall static pressure at several different total pressures; do not rely on optical methods to detect condensation of air in cold-flow models.

3.3.2.3 FLOWFIELD OBSERVATION

Optical methods for cold-flow-model testing shall provide qualitative flowfield visualization.

A spark-illuminated schlieren system is recommended for observing the flowfields of the nozzle model.

APPENDIX A

GLOSSARY

Symbol	Definition
A_c	area of combustion chamber at maximum cross section
A_e	geometric flow area of nozzle at exit plane
A_t	geometric flow area of nozzle at throat
A_t^*	aerodynamic flow area of nozzle throat (geometric flow area corrected for the effects of nonuniform transonic flow)
alt	altitude
C_d	discharge coefficient
$C_{d\,pot}$	discharge coefficient (potential flow)
D_e	diameter of nozzle at exit
D_t	diameter of nozzle at throat
G_t	throat gap (width of annular throat)
L	nozzle length
M	Mach number (ratio of fluid velocity to velocity of sound in the fluid)
R_d	radius of nozzle wall downstream of throat
R_t	radius of nozzle throat
R_u	radius of nozzle wall upstream of throat
Re	Reynolds number (ratio of momentum forces to viscous forces in fluid flow)
sl	sea level
vac	vacuum
x	axial distance from a given reference plane

Symbol	Definition
α	nozzle divergence half-angle
γ	ratio of specific heat at constant pressure to specific heat at constant volume
ϵ	nozzle expansion area ratio, $\epsilon = A_e/A_t$
θ	momentum thickness of the boundary layer; this thickness represents a loss in momentum of the exhaust gas
$d\theta/dx$	rate of change of momentum thickness with respect to axial distance along the wall
μ	Mach angle (the angle between the direction of supersonic flow and the characteristic line)

Term	Definition
ablative cooling	use of a material on the nozzle wall that evaporates or chars during engine firing and thereby cools the nozzle
aerodynamic performance	portion of the nozzle performance due to nozzle divergence efficiency (the degree of perfection of the nozzle contour)
aerodynamic throat area	effective flow area of the throat, which is less than the geometric flow area because the flow is not uniform
aerospike nozzle	annular nozzle that allows the gas to expand from one surface — a centerbody spike — to ambient pressure
altitude engine	rocket engine that is designed to operate at high-altitude conditions
annular nozzle	nozzle with an annular throat formed by an outer wall and a centerbody wall
area ratio	ratio of the geometric flow area of the nozzle exit to the geometric flow area of the nozzle throat; also called expansion area ratio
asymmetric separation	separation of the exhaust jet from the nozzle wall nonuniformly or at localized regions not in the same plane
base area	truncated area of a plug nozzle
base cavity	the opening in the base of a plug nozzle

Term	Definition
base pressure	static pressure in the base cavity
bell nozzle	nozzle with a circular opening for a throat and an axisymmetric contoured wall downstream of the throat that gives the nozzle a characteristic bell shape
bifurcation joint	junction of two tubes or passages with a single larger tube or passage
boattail	aft end of a rocket that contains the propulsion system and its interface with vehicle tankage
boundary layer	film of gas or liquid next to the nozzle wall; its thickness is usually taken as the radial distance from the wall to a point at which gas velocity reaches 99% of freestream gas velocity
"cat-eyes"	long, narrow openings between coolant tubes for the purpose of discharging turbine exhaust gases
channel construction	use of machined grooves in the nozzle wall to carry coolant
characteristic line	mathematical line inclined to the direction of flow used to compute the flowfield
coupon	a piece of material, representative of the material used in a part, that accompanies the part during processing and subsequently is used as a test specimen to evaluate properties
dam	baffle or flat plate inserted perpendicularly into a fluid manifold in order to partially or fully separate two streams approaching from opposite directions
discharge coefficient	ratio of the actual flowrate to the ideal flowrate calculated on the basis of one-dimensional inviscid flow
displacement thickness	distance by which the outer streamlines are shifted (displaced) as a result of the formation of the boundary layer
divergence efficiency	ratio of thrust calculated for the actual nozzle contour (potential flow) to the thrust of an ideal-flow nozzle
downcomer	nozzle tube in which coolant flows in the same direction as the exhaust gas
E-D nozzle	expansion-deflection nozzle, which has an annular throat that discharges exhaust gas with a radial outward component

93

Term	Definition
equilibrium composition	chemical composition that the exhaust gas would attain if given a sufficient time for reactants to achieve chemical balance
expansion ratio, or expansion area ratio	see area ratio
external expansion	gas expansion from the throat directly without a controlled expansion wall
flow angle	direction of gas flow at any point in the nozzle referred to nozzle axis
flowfield	aerodynamic and thermodynamic states of the gas flow in the nozzle
flow separation	detachment of the exhaust-gas flow from the nozzle wall
frozen composition	chemical composition of the exhaust gas that does not change during expansion
holdup volume	large-capacity propellant supply reservoir
ideal nozzle	nozzle that provides theoretically perfect performance for the given area ratio when analyzed on the basis of one-dimensional point-source flow
internal expansion	gas expansion within a controlled expansion wall or shroud
K seal	flexible metal seal shaped like a K
kinetic performance	that portion of the nozzle performance that depends on the equilibrium state of the chemical reaction during gas expansion
momentum thickness	thickness of the potential flow with a momentum equal to that lost in the boundary layer as a result of wall shear forces
MR	mixture ratio: $\dfrac{\text{mass flowrate of oxidizer}}{\text{mass flowrate of fuel}}$
Naflex seal	flexible metal seal developed by North American Aviation, Inc.*
nonequilibrium composition	chemical composition of the exhaust gas resulting from incomplete chemical reaction of the products of combustion in the exhaust gas

*Now Rockwell International Corporation.

94

Term	Definition
nozzle extension	nozzle structure that is added to the main nozzle in order to increase expansion area ratio or to provide a change in nozzle construction
oil canning	flexing of unsupported sheet metal
omega joint	expansion joint shaped like the upper-case Greek letter omega in the wall of a manifold; used to relieve stresses due to thermal growth
overexpansion	expansion of the gas to an ambient pressure that is higher than that for which the nozzle was designed
plug nozzle	annular nozzle that discharges exhaust gas with a radial inward component: a truncated aerospike
potential flow	flow with effects of viscosity not considered
Prandtl-Meyer angle	angle through which the supersonic flow turns during expansion
pressure ratio	ratio of chamber pressure to ambient pressure
radius ratio	ratio of radius of curvature of the wall in the throat section to the throat radius (1/2 throat diameter)
Rayleigh flow	steady frictionless flow in a constant-area duct with heat being added or removed
recompression	reflection of exhaust gas from ambient jet boundary
reference streamline	path of the flow along which the velocity is assumed for transonic flow calculations
regenerative cooling	cooling of the nozzle wall with one of the propellants before it is burned in the combustion chamber
right characteristic	characteristic line that travels downstream and to the right of the supersonic flow direction
shroud	short extension of the outer wall of the plug nozzle downstream of the throat
slip effects	discontinuities in momentum and temperature in the boundary layer due to rarefaction of the exhaust gas
slipstream	flow of ambient air around the nozzle

Term	Definition
stacking	assembling the coolant tubes vertically on a mandrel that simulates the chamber/nozzle contour; this procedure facilitates fitting and adjusting the tubes to the required contour prior to brazing.
storable propellant	a propellant with a vapor pressure such that the propellant can be stored in a specified environment (earth or space) at moderate ullage pressures without significant loss over a specified period of time
streamline	line tangent to the velocity vector at each point in a flowfield; in steady flow, a streamline is the pathline of the fluid element
tadpole seal	a flange seal whose cross section resembles the shape of a tadpole
taper	gradual reduction in or englargement of coolant-tube diameter
taper ratio	ratio of maximum coolant-tube diameter to minimum tube diameter; usually kept below 4
temperature jump	difference in temperature between the nozzle wall and the layer of gas molecules next to the wall, a result of rarefaction of the exhaust gas
thermally perfect gas	gas that obeys the equation of state $PV = RT$ and has specific heats with values independent of temperature
throat gap	width of the annular passage at the throat of an annular nozzle
tube crown	portion of the coolant tube that forms the outer wall of the cooling jacket
tube-wall construction	nozzle wall that consists of a series of parallel metal tubes that carry coolant
upcomer	nozzle tube in which coolant flows in a direction opposite to that of the exhaust gas flow
velocity slip	velocity of the gas molecules next to the nozzle wall, a result of rarefaction of the exhaust gas

Material[1]	Identification
columbium C-103	alloy of 89 percent columbium, 10 percent hafnium, and 1 percent titanium

---

[1] Additional information on metallic materials herein can be found in the Aerospace Material Specifications, SAE, Two Pennsylvania Plaza, New York, NY.; in MIL-HDBK-5B, Metallic Materials and Elements for Aerospace Vehicle Structures, Dept. of Defense, Washington, D.C., Sept. 1971; and in Metals Handbook (8th ed.), Vol. 1: Properties and Selection of Metals, Am. Society for Metals (Metals Park, Ohio), 1961.

Material	Identification
CRES·	corrosion-resistant steel
Dalic plating	selective metal-plating process for small areas; the method employs a swab wetted with electrolyte and wrapped around a movable electrode
Hastelloy C	trade name of Stellite Division of Cabot Corporation for austenitic nickel-molybdenum-chromium-iron alloy (AMS 5530C)
Inconel 625 718 X-750	trade names of International Nickel Co. for nickel-base alloys (AMS 5599, 5597A, and 5598, resp.)
IRFNA	inhibited red fuming nitric acid, propellant grade per MIL-P-7254
L-605	cobalt-base alloy per AMS 5537A
LH_2	liquid hydrogen, propellant grade per MIL-P-27201
LOX	liquid oxygen, propellant grade per MIL-P-25508
MMH	monomethylhydrazine, propellant grade per MIL-P-27404
MON	mixed oxides of nitrogen
N-155	iron-base alloy per AMS 5532B
NAA-85	designation of North American Aviation, Inc.* for a sprayable metal coating made from a slurry of powder containing 98 percent aluminum
N_2H_4	hydrazine, propellant grade per MIL-P-26536
N_2O_4	nitrogen tetroxide, propellant grade per MIL-P-26539
NARloy Z	silver-zirconium-copper alloy developed by North American Rockwell Corp.*
Refrasil	trade name of HITCO for a group of high-purity silica-base materials having outstanding high-temperature resistance; acronym for refractory silica
Rene 41	trade name of General Electric Co. for an austenitic nickel-chromium-cobalt-molybdenum alloy

*Now Rockwell International Corporation.

Material	Identification
RP-1	kerosene-base hydrocarbon fuel, propellant grade per MIL-P-25576
silicone RTV	room-temperature-vulcanizing organosiloxane polymer
UDMH	unsymmetrical dimethylhydrazine, propellant grade per MIL-P-25604
Waspaloy	trade name of Pratt & Whitney Aircraft for austenitic nickel-base alloy (AMS 5544B)
50:50	mixture of 50% hydrazine and 50% unsymmetrical dimethylhydrazine, propellant grade per MIL-P-27402
347	designation for columbium-stabilized austenitic stainless steel

ABBREVIATIONS

Organization	Identification
AIAA	American Institute of Aeronautics and Astronautics
ARS	American Rocket Society
ASME	American Society of Mechanical Engineers
CPIA	Chemical Propulsion Information Agency
ICRPG	Interagency Chemical Rocket Propulsion Group
JANNAF	Joint Army-Navy-NASA-Air Force
M.I.T.	Massachusetts Institute of Technology
NACA	National Advisory Committee for Aeronautics
NAR	North American Rockwell Corporation*
SAE	Society of Automotive Engineers
WPAFB	Wright-Patterson Air Force Base

*Now Rockwell International Corporation.

APPENDIX B

Conversion of U.S. Customary Units to SI Units

Physical quantity	U. S. customary unit	SI unit	Conversion factor[a]
Angle	degree	radian	1.745×10^{-2}
Area	in.^{2}	cm^2	6.452
Force	lbf	N	4.448
Length	ft	m	3.048×10^{-1}
	in.	cm	2.54
Load	lbf	N	4.448
Mass	lbm	kg	4.536×10^{-1}
Pressure	psi (lbf/in.^{2})	N/cm^2	6.895×10^{-1}
Roll moment	ft-lbf	N-m	1.356
Specific impulse	lbf-sec/lbm	N-sec/kg	9.807
Temperature	°F	K	$K = \frac{5}{9} (°F + 459.67)$
Temperature difference	°F	K	$K = \frac{5}{9} (°F)$
Thrust	lbf	N	4.448

[a]Multiply value given in U.S. customary unit by conversion factor to obtain equivalent value in SI unit. For a complete listing of conversion factors for basic physical quantities, see Mechtly, E. A.: The International System of Units. Physical Constants and Conversion Factors. Second Revision, NASA SP-7012, 1973.

REFERENCES

1. Anon.: Liquid Rocket Engine Self-Cooled Combustion Chambers. NASA Space Vehicle Design Criteria Monograph, NASA SP-8124 (to be published).

2. Anon.: Solid Rocket Motor Nozzles. NASA Space Vehicle Design Criteria Monograph, NASA SP-8115, June 1975.

3. Back, L. H.; Cuffel, R. F.; and Massier, P. F.: Influence of Contraction Section Shape and Inlet Flow Direction on Supersonic Nozzle Flow and Performance. J. Spacecraft Rockets, vol. 9, no. 6, June 1972, pp. 420-427.

4. Anon.: User's Manual for Subsonic-Transonic Flow Analysis. PWA 2888, Suppl. 4, Pratt & Whitney Aircraft Div., United Aircraft Corp. (East Hartford, CT), 1966.

5. Kliegel, J. R.; and Levin, J. N.: Transonic Flow in Small Throat Radius of Curvature Nozzles. AIAA J., vol. 7, no. 7, July 1969, pp. 1375-1378.

6. Cuffel, R. F.; Back, L. H.; and Massier, P. F.: The Transonic Flowfield in a Supersonic Nozzle with Small Throat Radius of Curvature. AIAA J., vol. 7, no. 7, July 1969, pp. 1364-1366.

7. Back, L. H.; and Cuffel, R. F.: Flow Coefficients for Supersonic Nozzles With Comparatively Small Radius of Curvature Throats. J. Spacecraft Rockets, vol. 8, no. 2, February 1971, pp. 196-198.

8. Oswatitsch, K.; and Rothstein, W.: Flow Pattern in Converging-Diverging Nozzle. NACA TM X-1215, 1949.

9. Kliegel, J. R.; and Quan, V.: Convergent-Divergent Nozzle Flows. AIAA J., vol. 6, no. 9, September 1968, pp. 1728-1734.

10. Back, L. H.; Massier, P. F.; and Cuffel, R. F.: Flow Phenomena and Convective Heat Transfer in a Conical Supersonic Nozzle. J. Spacecraft Rockets, vol. 4, no. 8, August 1967, pp. 1040-1047.

11. Back, L. H.; Massier, P. F.; and Gier, H. L.: Comparisons of Measured and Predicted Flows Through Conical Supersonic Nozzles, With Emphasis on the Transonic Region. AIAA J., vol. 3, no. 9, September 1965, pp. 1606-1614.

12. Back, L. H.; and Cuffel, R. F.: Detection of Oblique Shocks in a Conical Nozzle With a Circular-arc Throat. AIAA J., vol. 4, no. 12, December 1966, pp. 2219-2221.

13. Back, L. H.; Cuffel, R. F.; and Massier, P. F.: Laminarization of a Turbulent Boundary Layer in Nozzle Flow — Boundary Layer and Heat Transfer Measurements With Wall Cooling. J. Heat Transfer, Trans. ASME, Series C, vol. 92, August 1970, pp. 333-344.

14. Aulberg, J. H.; Hamilton, S. A.; Migdal, D.; and Nilson, E. N.: Truncated Perfect Nozzles in Optimum Nozzle Design. ARS J., vol. 3, no. 5, May 1961, pp. 614-620.

15. Miele, A.: Theory of Optimum Aerodynamic Shapes. Academic Press (New York), 1965, pp. 151-183.

16. Rao, G. V. R.: Exhaust Nozzle Contour for Optimum Thrust. Jet Propulsion, vol. 28, no. 6, June 1958, pp. 377-382.

17. Taylor, Allan A.; and Hoffman, Joe D.: Design of Maximum Thrust Nozzles for Nonequilibrium Chemically Reacting Flow. AIAA J., vol. 12, no. 10, October 1974, pp. 1299-1300.

18. Ranson, V. H.; Hoffman, J. D.; and Thompson, H. D.: Three-Dimensional Supersonic Nozzle Flow Field Calculations. J. Spacecraft Rockets, vol. 7, no. 4, April 1970, pp. 458-462.

19. Alber, I. E.: Comparison and Evaluation of Computer Program Results for Rocket Engine Performance Prediction. SN-82, Dynamic Sciences Div., Marshall Industries (Monrovia, CA), April 1968.

20. Elliott, O. G.; Bartz, D. R.; and Silver, S.: Calculation of Turbulent Boundary Layer Growth and Heat Transfer in Axisymmetric Nozzles. Tech. Rep. 32-387, Jet Propulsion Lab., Calif. Inst. Technology (Pasadena, CA), February 1963.

21. Waldman, B. J.; and Shuster, E. B.: Fluorine-Hydrogen Performance Evaluation, Phase I, Part II: Nozzle Performance Analysis and Demonstration. Final Report, NASA CR-72038, Rocketdyne Div., North American Aviation, Inc. (Canoga Park, CA), April 1967.

22. Migdal, D.; and Landis, F.: Characteristics of Conical Supersonic Nozzles. ARS J., vol. 32, no. 12, December 1962, pp. 1898-1901.

23. Anon.: J-2 Bimonthly Progress Report, November-December 1965. R-6300-3, Rocketdyne Div., North American Aviation, Inc., January 1966.

24. Schilling, M. T.: Flow Separation in a Rocket Nozzle. M. S. Thesis, University of Buffalo, June 1962.

25. Crocco, L.; and Probstein, R.: The Peak Pressure Rise Across an Oblique Shock Emerging from a Turbulent Boundary Layer Over a Plane Surface. Princeton University (Princeton, NJ), March 1964.

26. Schmucker, R. H.: Status of Flow Separation Prediction in Liquid Propellant Rocket Nozzles. NASA TM X-64890, November 1974.

27. Touryan, K. J.; and Drake, R. M., Jr.: Flow Investigations in Delaval Supersonic Nozzles at Very Low Pressures. Rarefied Gas Dynamics, Vol. II, Proc. Third Int'l Symposium on Rarefied Gas Dynamics (Paris, France) 1962, J. A. Laurmann, ed., Academic Press, Inc., 1963, pp. 402-434.

28. Massier, P. F.; Back, L. H.; Noel, M. B.; and Saheli, F.: Viscous Effects on the Flow Coefficient for a Supersonic Nozzle. AIAA J., vol. 8, no. 3, March 1970, pp. 605-607.

29. Spisz, E. W.; Brinich, P. F.; and Jack, J. R.: Thrust Coefficients of Low-Thrust Nozzles. NASA TN D-3056, October 1965.

30. Rae, W. J.: Some Numerical Results on Viscous Low-Density Nozzle Flows in the Slender-Channel Approximation. AIAA J., vol. 9, no. 5, May 1971, pp. 811-820.

31. Anon.: Turbopump Systems for Liquid Rocket Engines. NASA Space Vehicle Design Criteria Monograph, NASA SP-8107, August 1974.

32. Martinez, A.: Aerodynamic Nozzle Study, Vol. I. R-6582, Rocketdyne Div., North American Aviation, Inc., July 1966.

33. Alber, I. E.; and Lees, L.: Integral Theory for Supersonic Turbulent Base Flows. AIAA J., vol. 6, no. 7, July 1968, pp. 1343-1351.

34. Chow, W.; and Addy, A.: Interaction Between Primary and Secondary Streams of Supersonic Ejector Systems and Their Performance Characteristics. AIAA J., vol. 2, no. 4, April 1964, pp. 686-695.

35. Wagner, W. R.; and Shoji, J. M.: Advanced Regenerative Cooling Techniques for Future Space Transportation Systems. AIAA Paper No. 75-1247, SAE 11th Propulsion Conf. (Anaheim, CA), Sept. 29 - Oct. 1, 1975.

36. Anon.: Liquid Rocket Engine Fluid-Cooled Combustion Chambers. NASA Space Vehicle Design Criteria Monograph, NASA SP-8087, April 1972.

37. Zienkiewicz, O. C.; and Cheung, U. K.: The Finite Element Method in Structural and Continuum Mechanics. McGraw-Hill Publishing Company, Ltd. (London), 1967.

38. Sellers, J. P., Jr.: Gaseous Film Cooling with Multiple Injection Stations. AIAA J., vol. 1, no. 9, September 1963, pp. 2154-2156.

39. Tribus, M.; and Klein, J.: Forced Convection from Non-isothermal Surfaces. Ch. 8, Heat Transfer Symposium, University of Michigan Press (Ann Arbor, MI), 1953.

40. Burns, W. K.; and Stollery, J. L.: The Influence of Foreign Gas Injection and Slot Geometry on Film Cooling Effectiveness. Intl. J. Heat and Mass Transfer, vol. 12, August 1969, pp. 935-951.

41. Kacker, S. C.; and Whitelaw, J. H.: The Effect of Slot Height and Slot Turbulence Intensity on the Effectiveness of the Uniform Density, Two-Dimensional Wall Jet. J. Heat Transfer, Trans. ASME, Series C, vol. 90, 1968, pp. 469-475.

42. Sivasegaram, S.; and Whitelaw, J. H.: Film Cooling Slots: The Importance of Lip Thickness and Injection Angle. J. Mech. Engrg. Science, vol. 11, no. 1, February 1969, pp. 22-27.

43. Mukerjee, T.; and Martin, B. W.: Film Cooling of Air Injection Through a Backward-Facing Annular Tangential Slot into a Supersonic Axisymmetric Parallel Diffuser. Proceedings of the 1968 Heat Transfer and Fluid Mechanics Institute, Univ. of Washington (Seattle, WA), June 17-18, 1968.

44. Abramovitch, G. N.: The Theory of Turbulent Jets. MIT Press, 1963.

45. Vulis, L. A.; and Kashkarov, V. P.: Theory of Viscous-Fluid Jets. Moscow, 1965. Available translated as FTD-HT-23-669-67 (AD-673687), Foreign Technology Div., Air Force Systems Command (WPAFB, OH), Dec. 19, 1967.

46. Anon.: Welding, Resistance: Aluminum, Magnesium, etc.; Spot and Seam. Military Specification MIL-W-6858C, Dept. of Defense, Oct. 20, 1964.

47. Senneff, John M.: Final Report for Space Shuttle Orbit Maneuvering Engine Reusable Thrust Chamber Program. Rep. 8693-950-001, Bell Aerospace Co., Division of Textron, May 1975.

48. Anon.: Liquid Rocket Disconnects, Couplings, Fittings, Joints, and Seals. NASA Space Vehicle Design Criteria Monograph, NASA SP-8119 (to be published).

49. Anon.: Aerospace Applied Thermodynamics Manual. Committee A-9, Aero-Space Environmental Systems, SAE, January 1962.

50. Ornstein, H. L.; and Kunz, H. R.: Experimental Investigation of Heat Rejection Problems in Nuclear Space Powerplants. Rep. PWA-2227, Pratt & Whitney Aircraft Div., United Aircraft Corp. (East Hartford, CT), June 1963.

*51. Bockstahler, A. J.: S-4 Thrust Chamber Hot-Gas Wall Microminiature Thermocouple Test Results and Analysis. CDR 6124-2000, Rocketdyne Div., North American Aviation, Inc., unpublished, December 1966.

*52. Blendermann, W. H.; and Garrett, A. J.: Procedure for Installation of Microminiature Thermocouples on J-2, J-2SE, and J-2X Thrust Chambers to Obtain Coolant Tube Hot Gas Side Wall Temperatures. IL 6124-2026, Rocketdyne Div., North American Aviation, Inc., unpublished, May 1966.

*53. Gill, G. S.; Koenig, W. R.; and Garrett, A. J.: Installation of Microminiature Thermocouples in Liquid Rocket Thrust Chambers. NAR 50633, Rocketdyne Div., North American Aviation, Inc., unpublished, April 1966.

*54. Garrett, A. J.: Limitation of Probing Between Thrust Chamber Tubes With a Tungsten Spatula for the Purpose of Inserting Microminiature Thermocouples. CDM 6124-2006, Rocketdyne Div., North American Aviation, Inc., unpublished, July 1966.

*55. Lum, J. H.: Tube Dimple Effect on Coolant Flow and Maximum Gas Side Wall Temperature. IL 6124-4075, Rocketdyne Div., North American Aviation, Inc., unpublished, June 1966.

*56. Garrett, A. J.: Installation of Gas-Side-Wall Thermocouples in the Toroidal Type Thrust Chamber. CDM 6124-2003, Rocketdyne Div., North American Aviation, Inc., unpublished, March 1966.

---

*Dossier for design criteria monograph "Liquid Rocket Engine Nozzles." Unpublished. Collected source material available for inspection at NASA Lewis Research Center, Cleveland, Ohio.

*57. Cook, R. T.: Objectives and Significance of Local Heat Transfer Measurements in Tubular Thrust Chambers; Previous Experience, Required Accuracy, and the Influence of Installation Induced Errors. APM 6-168-138, Rocketdyne Div., North American Aviation, Inc., unpublished, May 1966.

*58. Bockstahler, A. J.: Resistance Method for Determining Hot Junction Location in Microminiature Thermocouple Assemblies. CDR 6124-2006, Rocketdyne Div., North American Aviation, Inc., unpublished, August 1966.

59. Huff, R. G.: A Thermocouple Technique for Measuring Hot-Gas-Side Wall Temperatures in Rocket Engines. NASA TN D-5291, June 1969.

*60. Roeder, E. R.: Brazing Alloys and Solders for Temperature Indicators of Tubular Wall Thrust Chamber Hot Gas Side Wall Temperature Profiles During Hot Firing Tests. MPR 6-175-178, Rocketdyne Div., North American Aviation, Inc., unpublished, March 1966.

*61. Cook, R. T.: Brazing Alloys as Temperature Indicators; Influence of Braze Alloy Thickness on Indicated Temperatures. APM 6-168-29, Rocketdyne Div., North American Aviation, Inc., unpublished, March 1966.

*62. Cook, R. T.: Post Test Observation of Braze Alloy Deposits (Temperature Indicators) on High P_c (SA-6201) 45° Nickel Thrust Chamber. APM 6-178-74, Rocketdyne Div., North American Aviation, Inc., unpublished, April 1966.

63. JANNAF Performance Standardization Working Group: JANNAF Rocket Engine Performance Test Data Acquisition and Interpretation Manual. CPIA Publ. 245, April 1975.

64. Anon.: JANNAF Rocket Engine Performance Methodology Sample Cases. CPIA Publications 245 and 246 Supplement, April 1975.

65. Waldman, B. J.: Fluorine-Hydrogen Performance Evaluation, Phase II: Space-Storable Propellant Performance Demonstration and Analysis. Rinal Report, NASA CR-72542, Rocketdyne Div., North American Rockwell Corp., April 1969.

66. Harding, L. J.: A Digital Computer Program for Condensation in Expanding One-Component Flows. ARL 65-58, Aerospace Research Laboratories (WPAFB, OH), March 1965.

67. Pieper, J. L.: Performance Evaluation Methods for Liquid Propellant Rocket Thrust Chambers, Appendix A. CPIA Publ. 132, November 1966.

68. Pieper, J. L.: ICRPG Liquid Propellant Thrust Chamber Performance Evaluation Manual — Final Report, Oct. 15, 1967-Sept. 30, 1968. CPIA Publ. 178 (AD 843051), Sept. 30, 1968.

69. Hurty, W. C.; and Rubinstein, M. F.: Dynamics of Structures. Prentice-Hall, Inc. (Englewood Cliffs, NJ), 1964.

*Dossier for design criteria monograph "Liquid Rocket Engine Nozzles." Unpublished. Collected source material available for inspection at NASA Lewis Research Center, Cleveland, Ohio.

70. Papell, S. S.; and Trout, A. M.: Experimental Investigation of Air Film Cooling Applied to An Adiabatic Wall by Means of an Axially Discharging Slot. NASA TN D-9, August 1959.

*71. Garrett, A. J.: Recommended Method for Providing Access to Gas Side Wall Thermocouple Installations in New Thrust Chamber. IL 6124-2009, Rocketdyne Div., North American Aviation, Inc., unpublished, February 1966.

*72. Anon.: HT Micro-Miniature Thermocouples. Product Data 4336 — Thermocouples. Baldwin — Lima — Hamilton (Waltham, Mass.), December 1960.

---

*Dossier for design criteria monograph "Liquid Rocket Engine Nozzles." Unpublished. Collected source material available for inspection at NASA Lewis Research Center, Cleveland, Ohio.

NASA SPACE VEHICLE DESIGN CRITERIA MONOGRAPHS ISSUED TO DATE

ENVIRONMENT

SP-8005	Solar Electromagnetic Radiation, Revised May 1971
SP-8010	Models of Mars Atmosphere (1974), Revised December 1974
SP-8011	Models of Venus Atmosphere (1972), Revised September 1972
SP-8013	Meteoroid Environment Model—1969 (Near Earth to Lunar Surface), March 1969
SP-8017	Magnetic Fields—Earth and Extraterrestrial, March 1969
SP-8020	Surface Models of Mars (1975), Revised September 1975
SP-8021	Models of Earth's Atmosphere (90 to 2500 km), Revised March 1973
SP-8023	Lunar Surface Models, May 1969
SP-8037	Assessment and Control of Spacecraft Magnetic Fields, September 1970
SP-8038	Meteoroid Environment Model—1970 (Interplanetary and Planetary), October 1970
SP-8049	The Earth's Ionosphere, March 1971
SP-8067	Earth Albedo and Emitted Radiation, July 1971
SP-8069	The Planet Jupiter (1970), December 1971
SP-8084	Surface Atmospheric Extremes (Launch and Transportation Areas), Revised June 1974
SP-8085	The Planet Mercury (1971), March 1972
SP-8091	The Planet Saturn (1970), June 1972
SP-8092	Assessment and Control of Spacecraft Electromagnetic Interference, June 1972

SP-8103	The Planets Uranus, Neptune, and Pluto (1971), November 1972
SP-8105	Spacecraft Thermal Control, May 1973
SP-8111	Assessment and Control of Electrostatic Charges, May 1974
SP-8116	The Earth's Trapped Radiation Belts, March 1975
SP-8117	Gravity Fields of the Solar System, April 1975
SP-8118	Interplanetary Charged Particle Models (1974), March 1975

STRUCTURES

SP-8001	Buffeting During Atmospheric Ascent, Revised November 1970
SP-8002	Flight-Loads Measurements During Launch and Exit, December 1964
SP-8003	Flutter, Buzz, and Divergence, July 1964
SP-8004	Panel Flutter, Revised June 1972
SP-8006	Local Steady Aerodynamic Loads During Launch and Exit, May 1965
SP-8007	Buckling of Thin-Walled Circular Cylinders, Revised August 1968
SP-8008	Prelaunch Ground Wind Loads, November 1965
SP-8009	Propellant Slosh Loads, August 1968
SP-8012	Natural Vibration Modal Analysis, September 1968
SP-8014	Entry Thermal Protection, August 1968
SP-8019	Buckling of Thin-Walled Truncated Cones, September 1968
SP-8022	Staging Loads, February 1969
SP-8029	Aerodynamic and Rocket-Exhaust Heating During Launch and Ascent, May 1969
SP-8030	Transient Loads From Thrust Excitation, February 1969
SP-8031	Slosh Suppression, May 1969
SP-8032	Buckling of Thin-Walled Doubly Curved Shells, August 1969

108

SP-8035	Wind Loads During Ascent, June 1970
SP-8040	Fracture Control of Metallic Pressure Vessels, May 1970
SP-8042	Meteoroid Damage Assessment, May 1970
SP-8043	Design-Development Testing, May 1970
SP-8044	Qualification Testing, May 1970
SP-8045	Acceptance Testing, April 1970
SP-8046	Landing Impact Attenuation for Non-Surface-Planing Landers, April 1970
SP-8050	Structural Vibration Prediction, June 1970
SP-8053	Nuclear and Space Radiation Effects on Materials, June 1970
SP-8054	Space Radiation Protection, June 1970
SP-8055	Prevention of Coupled Structure-Propulsion Instability (Pogo), October 1970
SP-8056	Flight Separation Mechanisms, October 1970
SP-8057	Structural Design Criteria Applicable to a Space Shuttle, Revised March 1972
SP-8060	Compartment Venting, November 1970
SP-8061	Interaction with Umbilicals and Launch Stand, August 1970
SP-8062	Entry Gasdynamic Heating, January 1971
SP-8063	Lubrication, Friction, and Wear, June 1971
SP-8066	Deployable Aerodynamic Deceleration Systems, June 1971
SP-8068	Buckling Strength of Structural Plates, June 1971
SP-8072	Acoustic Loads Generated by the Propulsion System, June 1971
SP-8077	Transportation and Handling Loads, September 1971
SP-8079	Structural Interaction with Control Systems, November 1971

SP-8082	Stress-Corrosion Cracking in Metals, August 1971
SP-8083	Discontinuity Stresses in Metallic Pressure Vessels, November 1971
SP-8095	Preliminary Criteria for the Fracture Control of Space Shuttle Structures, June 1971
SP-8099	Combining Ascent Loads, May 1972
SP-8104	Structural Interaction With Transportation and Handling Systems, January 1973
SP-8108	Advanced Composite Structures, December 1974

GUIDANCE AND CONTROL

SP-8015	Guidance and Navigation for Entry Vehicles, November 1968
SP-8016	Effects of Structural Flexibility on Spacecraft Control Systems, April 1969
SP-8018	Spacecraft Magnetic Torques, March 1969
SP-8024	Spacecraft Gravitational Torques, May 1969
SP-8026	Spacecraft Star Trackers, July 1970
SP-8027	Spacecraft Radiation Torques, October 1969
SP-8028	Entry Vehicle Control, November 1969
SP-8033	Spacecraft Earth Horizon Sensors, December 1969
SP-8034	Spacecraft Mass Expulsion Torques, December 1969
SP-8036	Effects of Structural Flexibility on Launch Vehicle Control Systems, February 1970
SP-8047	Spacecraft Sun Sensors, June 1970
SP-8058	Spacecraft Aerodynamic Torques, January 1971
SP-8059	Spacecraft Attitude Control During Thrusting Maneuvers, February 1971
SP-8065	Tubular Spacecraft Booms (Extendible, Reel Stored), February 1971

SP-8070	Spaceborne Digital Computer Systems, March 1971
SP-8071	Passive Gravity-Gradient Libration Dampers, February 1971
SP-8074	Spacecraft Solar Cell Arrays, May 1971
SP-8078	Spaceborne Electronic Imaging Systems, June 1971
SP-8086	Space Vehicle Displays Design Criteria, March 1972
SP-8096	Space Vehicle Gyroscope Sensor Applications, October 1972
SP-8098	Effects of Structural Flexibility on Entry Vehicle Control Systems, June 1972
SP-8102	Space Vehicle Accelerometer Applications, December 1972

CHEMICAL PROPULSION

SP-8089	Liquid Rocket Engine Injectors, March 1976
SP-8087	Liquid Rocket Engine Fluid-Cooled Combustion Chambers, April 1972
SP-8113	Liquid Rocket Engine Combustion Stabilization Devices, November 1974
SP-8107	Turbopump Systems for Liquid Rocket Engines, August 1974
SP-8109	Liquid Rocket Engine Centrifugal Flow Turbopumps, December 1973
SP-8052	Liquid Rocket Engine Turbopump Inducers, May 1971
SP-8110	Liquid Rocket Engine Turbines, January 1974
SP-8081	Liquid Propellant Gas Generators, March 1972
SP-8048	Liquid Rocket Engine Turbopump Bearings, March 1971
SP-8101	Liquid Rocket Engine Turbopump Shafts and Couplings, September 1972
SP-8100	Liquid Rocket Engine Turbopump Gears, March 1974
SP-8088	Liquid Rocket Metal Tanks and Tank Components, May 1974
SP-8094	Liquid Rocket Valve Components, August 1973

111

SP-8097	Liquid Rocket Valve Assemblies, November 1973
SP-8090	Liquid Rocket Actuators and Operators, May 1973
SP-8112	Pressurization Systems for Liquid Rockets, October 1975
SP-8080	Liquid Rocket Pressure Regulators, Relief Valves, Check Valves, Burst Disks, and Explosive Valves, March 1973
SP-8064	Solid Propellant Selection and Characterization, June 1971
SP-8075	Solid Propellant Processing Factors in Rocket Motor Design, October 1971
SP-8076	Solid Propellant Grain Design and Internal Ballistics, March 1972
SP-8073	Solid Propellant Grain Structural Integrity Analysis, June 1973
SP-8039	Solid Rocket Motor Performance Analysis and Prediction, May 1971
SP-8051	Solid Rocket Motor Igniters, March 1971
SP-8025	Solid Rocket Motor Metal Cases, April 1970
SP-8115	Solid Rocket Motor Nozzles, June 1975
SP-8114	Solid Rocket Thrust Vector Control, December 1974
SP-8041	Captive-Fired Testing of Solid Rocket Motors, March 1971